Politecnico di Milano

Dipartimento di Matematica F. Brioschi

Dottorato di ricerca in Ingegneria Matematica - XIX Ciclo

Distortion-induced effects in nematic liquid crystals

Stefano Turzi

Supervisor: Prof. Paolo Biscari
Dipartimento di Matematica "F. Brioschi",
Politecnico di Milano, Italy

Ph.D. Coordinator: Prof. Filippo Gazzola

Contents

List of symbols

Symbol	Description	Page
$\mathscr{E}$	Euclidean space	3
$\mathcal{B}$	Region of $\mathscr{E}$ occupied by the liquid crystal	3
$\partial\mathcal{B}$	Reduced boundary of the region $\mathcal{B}$	
$\boldsymbol{\nu}$	Surface outer normal	
$\mathbb{S}^2$	Unit sphere of dimension 2	3
$\mathbb{RP}^2$	Real projective plane	3
$\mathbf{M}$	Second moment tensor	4
$\mathbf{n}$	Director field	4
$\mathbf{Q}$	Nematic tensor order parameter	5
s	Degree of orientation	7
β	Degree of biaxiality	7
$\mathrm{C}^k(A,B)$	Space of continuous mappings $A \to B$ having k continuous derivatives	8
$\mathcal{F}_{\mathrm{Fr}}$	Frank's energy functional	8
Ψ_{Fr}	Frank's free energy density	8
$\mathscr{L}(A,B)$	Space of linear and continuous mappings $A \to B$	8
$\mathscr{L}(A)$	$\mathscr{L}(A,A)$	8
$\mathcal{M}^n$	n-dimensional manifold	
$\mathrm{T}_p\mathcal{M}$	Tangent space to the manifold $\mathcal{M}$ at $p \in \mathcal{M}$	8
$\mathrm{d}_p f$	If $f : \mathcal{M} \to \mathcal{N}$ is a smooth map between manifolds, then $\mathrm{d}_p f : \mathrm{T}_p\mathcal{M} \to \mathrm{T}_{f(p)}\mathcal{N}$ is the tangent map at $p \in \mathcal{M}$	8
$\mathcal{D}_f$	Domain of definition of the function f	8
$O(3)$	Group of 3×3 orthogonal tensors	9
K_i	Frank's elastic constants	9
T	Temperature	10
$\nabla_{\mathrm{s}}\mathbf{n}$	Surface gradient	10
$\mathrm{div}_{\mathrm{s}}\,\mathbf{n}$	Surface divergence	10
$\mathbf{n}^{\perp}$	Linear space of vectors orthogonal to $\mathbf{n}$	14
$\mathbf{P}(\mathbf{n})$	Projection operator on $\mathbf{n}^{\perp}$	14
W	Anchoring strength	16
$\mathcal{F}_{\mathrm{w}}$	Anchoring energy functional	16
f_{w}	Anchoring energy density	16

$\mathrm{H}^1(A,B)$	Sobolev space of the L^2 mappings $A \subseteq \mathbb{R}^M \to B \subseteq \mathbb{R}^N$ with first weak derivatives in L^2	17
$\mathbf{D}$	Electric displacement	18
$\mathbf{E}$	Electric field	18
$\mathbf{M}$	Magnetization	18
$\mathbf{H}$	Magnetic field	18
$\varepsilon_{\|\|}$	Parallel dielectric constant	18
$\varepsilon_{\perp}$	Orthogonal dielectric constant	18
ε_a	Dielectric anisotropy	18
$\chi_{\|\|}$	Parallel magnetic susceptibility	18
$\chi_{\perp}$	Orthogonal magnetic susceptibility	18
χ_a	Diamagnetic anisotropy	18
Ψ	de Gennes' free energy density	23
Ψ_{LdG}	Landau-de Gennes' potential	25
s_{pr}	Preferred degree of orientation in the bulk, minimum of Ψ_{LdG} in the nematic phase	26
T^*	Supercooling temperature	25
T_{NI}	Nematic-isotropic transition temperature	27
T^+	Superheating temperature	27
Ψ_{el}	Elastic energy density	28
L_i	Elastic constants in de Gennes' theory	28
ξ	Nematic coherence length	36
ω	Measure of the depth of the potential well at s_{pr}	36
η	Boundary roughness wavelength	37
Δ	Boundary roughness amplitude	37
ε	Small parameter $\varepsilon = \xi/\eta$	39
m	Slope of the outer solution	42
ζ	Surface extrapolation length	56
$\{\mathbf{n}, \mathbf{e}_+, \mathbf{e}_-\}$	Eigenvectors of $\mathbf{Q}$	66
$\mathbf{G}$	$\nabla\mathbf{n} - (\nabla\mathbf{n})\mathbf{n} \otimes \mathbf{n}$	68
$\mathbf{S}$	$(\nabla\mathbf{n})\,(\nabla\mathbf{n})^T$	69
$\odot$	$(\mathbf{L} \odot \mathbf{u})\mathbf{a} = \mathbf{L}\mathbf{a} \otimes \mathbf{u}$ for any vector $\mathbf{a}$	70
$\omega^k_{\ i}$	Connection forms	76
θ^j	Dual frame	76
g	Metric tensor	76
d	Exterior derivative	77
$\wedge$	Exterior product	77
E, G	Coefficients (1,1) and (2,2) of the first fundamental form	80
κ_i	Principal curvatures	80

Preface

Many materials have complex properties intermediate between those of crystals and fluids. Among these are liquid crystals, with their well-established orientational order, polymers, foams and gels. Collectively these have come to be called *soft matter*.

Within the last few years, the physics of soft condensed matter has become a rapidly expanding branch of science. This is mainly due to the recognition that apparently disparate phenomena may be described by unified concepts. In fact, these materials generally consist of organic molecules that interact weakly; as a result, molecular order is easily perturbed and quite modest fields or boundary effects are sufficient to cause a quite massive reorganisation and to influence strongly their structure and macroscopic properties.

What distinguishes this area of study from other branches of contemporary physics, is that soft matter comprises almost all materials of our everyday life: consumer goods like toothpaste, shaving-foam, cleaning agents or mayonnaise, but also rubber, plastic, displays and cloth. Despite of its being close to our personal experience, the resulting phenomena present challenges to fundamental science and to mathematics itself. It will be sufficient to mention some major disciplines that are involved in establishing the theoretical basis of such materials: Continuum Mechanics, Statistical Mechanics, the Theory of Phase Transitions but also Mathematical Analysis, Calculus of Variations and Algebraic Topology, to name but a few.

For both historical, theoretical and technological reasons, liquid crystals play an important role in this picture. A nematic liquid crystal is a system of rod-like molecules whose centers of mass do not exhibit any positional order. The interaction between nearby molecules tries to line them up along a common direction and induces a partial ordering at mesoscopic scales. This effect competes against distortions induced by external mechanical actions, electric or magnetic fields, and disordering thermal effects. The average alignment of the molecules is represented by a unit vector, usually denoted by $\mathbf{n}$ and called the *director*.

This thesis is organized as follows. Chapter 1 gives a brief introduction to nematic liquid crystals. It is meant to provide a neat summary of the mathematical and physical tools that will be used in the remaining Chapters. The equilibrium configuration of a nematic liquid crystal bounded by a rough surface [19] is studied in Chapter 2.

The surface wrinkling induces a partial melting in the degree of orientation. This softened region penetrates the bulk up to a length scale which turns out to coincide with the characteristic wavelength of the corrugation. Within the boundary layer where the nematic degree of orientation decreases, the tilt angle steepens and gives rise to a nontrivial structure, which may be interpreted in terms of an effective weak anchoring potential. It is then possible to relate the effective surface extrapolation length to the microscopic anchoring parameters. We also analyze the crucial role played by the boundary conditions assumed on the degree of orientation. Quite different features emerge depending on whether they are Neumann- or Dirichlet-like. These features may be useful to ascertain experimentally how the degree of orientation interacts with an external boundary. Chapter 3 is devoted to the study of biaxiality [17]. Nematic liquid crystals possess three different phases: isotropic, uniaxial, and biaxial. The ground state of most nematics is either isotropic or uniaxial, depending on the external temperature. Nevertheless, biaxial domains have been frequently identified, especially close to defects or external surfaces. We show that any spatially varying director pattern may be a source of biaxiality. Indeed, in the Chapter we introduce the symmetric tensor $\mathbf{S} = (\nabla\mathbf{n})(\nabla\mathbf{n})^T$. The director $\mathbf{n}$ is an eigenvector of $\mathbf{S}$ with zero eigenvalue. It is then established that biaxiality arises naturally whenever the other two eigenvalues of $\mathbf{S}$ are distinct. The eigenvalue difference may be used as a measure of the expected biaxiality. Furthermore, the corresponding eigenvectors indicate the directions in which the order tensor $\mathbf{Q}$ is induced to break the uniaxial symmetry about the director $\mathbf{n}$. Finally, these general considerations are applied to some examples. In particular, when homeotropic anchoring is enforced on a curved surface, the order tensor becomes biaxial along the principal directions of the surface. The effect is triggered by the difference in surface principal curvatures.

Acknowledgments. Writing a dissertation cannot be done without the support, advice and encouragement of others, teachers, friends and colleagues. Among the many, I would like to use this opportunity to express my gratitude to a number of people who, in various ways, have helped me during these years.
First, I would like to thank my supervisor Prof. Paolo Biscari who has introduced me into the fascinating world of Soft Matter. Without his constant support and enlightening discussions the present thesis could have not been completed.
I am also grateful to Prof. Tim Sluckin for the invitation and hospitality at the University of Southampton. He showed me aspects of liquid crystals physics that I didn't know and probably still need to learn properly.

Next, I would like to thank Dr. Gaetano Napoli for the several fruitful days of work together. He has been an extraordinary and friendly collaborator all the time.
Finally, I owe special thanks to Elisa and Davide whose only presence and love has made these years the most emotionally intense period of my whole life. This work is dedicated to you.

1

Introduction to nematic liquid crystals

The first historical evidence of a liquid crystal happened in 1888 when an Austrian botanist named Friedrich Reinitzer observed that a material known as cholesteryl benzoate had two distinct melting points. Reinitzer increased the temperature of a solid sample and watched the crystal change into a hazy liquid. As he increased the temperature further, the material changed again into a clear, transparent liquid. Reinitzer discovered a new phase of matter - the liquid crystal phase. However, the term liquid crystal itself was coined by Otto Lehmann in the late 19th century and it has been widely used since then.

Roughly speaking, liquid crystals are intermediate states of matter that behave as liquids under some aspects (for instance they flow like incompressible fluids) and resemble crystals with regards to several features, especially optical.

Liquid crystal materials generally have several common characteristics. Among these are a rod-like easily polarizable molecular structure. The distinguishing characteristic of the liquid crystalline state is the tendency of the molecules to point along a common axis, called the director and traditionally denoted by the unit vector **n**. This is in contrast to molecules in the liquid phase, which have no intrinsic order.

Crystalline materials exhibit long range periodic order in three dimensions. In the solid state, molecules are typically arranged in lattice structures, are highly ordered and have little translational freedom. They possess positional and orientational order.

On the contrary, by definition, an isotropic liquid has no orientational nor positional order. Substances that are not as ordered as a solid, yet have some degree of alignment are properly called liquid crystals: systems with orientational order without complete positional order. The characteristic orientational order of the liquid crystal state is between the traditional solid and liquid phases. Among these common characteristics one can distinguish many different liquid crystal phases according to higher or lower orientational order. Moreover, most liquid crystal compounds exhibit more than one phase as temperature is varied.

The lowest ordered liquid crystal is the **nematic** liquid crystal whose molecules closely resemble rods of a typical dimension of 5 - 20 Å. Molecules have no posi-

tional order and are able to flow, but as a consequence of the interaction between neighbors, they tend to align parallel to one another, so as to induce a partial orientational order at the microscopic scale. As well, they posses a mirror symmetry with respect to a plane orthogonal to the axis. Stated differently, if we exchanged the "head" with the "tail" of a molecule, the configuration would be indistinguishable. There are two main reasons why this partial order may not appear: one is because the thermal motion prevails over molecular interactions (high temperature) and the other is because molecules are too separate apart so that they cannot interact (low concentration). So the appearance of a liquid crystal phase has to be viewed as delicate equilibrium between two opposite tendencies. At low temperatures the substance is solid and molecules are highly ordered. If the temperature is increased the melting point is reached, the solid liquefies and enters his liquid crystal phase. As the temperature is further increased, a critical value T_{NI} is reached which marks the exit from the liquid crystal phase and the entry in the **isotropic** phase where the molecules are randomly oriented.

In the present work we will be dealing uniquely with the nematic phase. However, for the sake of completeness we mention here other two important phases.

A special class of nematic liquid crystals is called **cholesteric** or chiral nematic. Cholesteric molecules resemble helical springs, which may be either right-handed or left-handed. From a physical standpoint, they much behave like nematics and even if the mirror symmetry of nematics is broken, nonetheless the molecular interaction depends only on the orientation and not on handedness. A second interesting feature of cholesterics, that distinguish them from nematics, is that the director $\mathbf{n}$ is naturally not uniform. Its structure is helical.

The **smectic** state is another distinct mesophase of liquid crystal substances. Molecules in this phase show a degree of translational order which is not present in the nematic. In the smectic state, the molecules maintain the general orientational order of nematics, but also their centers of mass tend to align themselves in layers or planes. Motion is restricted within these planes, and separate planes are observed to flow past each other. The increased order means that the smectic state is more "solid-like" than the nematic. Many compounds are observed to form more than one type of smectic phase. As many as 12 of these variations have been identified.

1.1 Order parameters

What is a description of the micro-structure of a liquid crystal? A full microscopic description which assigns a position and an orientation to every molecule, is by far the most complete. On the other hand, it is by far the most complicate and it requires a detailed knowledge of all microscopic interactions. Besides the practical

intractability of such a complex description for more than a few molecules, it is also superfluous in most circumstances, when only aggregate molecular behavior is important.

The molecular size of liquid crystals is typically on the scale of nanometers. By contrast, liquid crystal devices are usually on the micron scale. So another possible description is statistical. This choice is expected to be valid in the limit of the nearly molecular length scale, under the assumption that the elementary volumes contain a sufficiently high number of molecules. These arguments are typical of continuum theories, which can boast a long and glorious history and have been given precise mathematical definitions. Bodies consisting of liquid crystals are complex materials which cannot be framed in the theory of classical continuum mechanics since they are bodies with microstructure, for which parameters of a microscopic origin have mechanical meanings also on a macroscopic scale. These latter are often called **order parameters**.

Let $\mathscr{E}$ be a 3-dimensional euclidean space, i.e. a 3-dimensional Riemann manifold such that we can obtain an atlas with just one coordinate chart, a Cartesian coordinate system (x, y, z) which gives us a bijection between $\mathscr{E}$ and $\mathbb{R}^3$, and such that every tangent space $\mathrm{T}_p\mathscr{E}$, $p \in \mathscr{E}$ is isomorphic to $\mathbb{R}^3$. The inner product is the usual dot product in $\mathbb{R}^3$. Elements of $\mathscr{E}$ are called points, while elements of the tangent spaces are called vectors.

The region of $\mathscr{E}$ occupied by the liquid crystal will be denoted by $\mathcal{B}$.

Suppose to know the probability density function $f_p : \mathbb{S}^2 \to \mathbb{R}_+$ that describes at each point $p \in \mathcal{B}$ the probability distribution of the *orientation* of the molecules at p. The orientation of the molecular axis is described at each point in space by a point of the unit sphere $\mathbb{S}^2$ (or by a unit vector). Thus, if ω is any subset of $\mathbb{S}^2$, the probability of finding in p one molecule oriented within ω is given by

$$P\{\omega\} = \int_\omega f_p(\mathbf{l})\, \mathrm{d}a, \tag{1.1}$$

where a denotes the area measure on $\mathbb{S}^2$. Due to nematics mirror symmetry, the "head" and "tail" of a molecule can be changed without experiencing any change in the probability distribution, i.e. the two configurations have the same probability. Mathematically this is translated by the requirement that f_p is an *even* function:[1]

$$f_p(\mathbf{l}) = f_p(-\mathbf{l}) \qquad \text{for all } \mathbf{l} \in \mathbb{S}^2. \tag{1.2}$$

[1]The fact that $f_p(\mathbf{l}) = f_p(-\mathbf{l})$ tells us that opposite points of $\mathbb{S}^2$ can be identified, so that the domain of f_p can be restricted to the projective plane $\mathbb{RP}^2 \cong \mathbb{S}^2/\mathbb{Z}_2$, i.e. the sphere where any two antipodal points are identified. Thus $\mathbb{RP}^2$ seems to be the most appropriate manifold to set the theory. Though for historical reasons and since $\mathbb{S}^2$ is more familiar, we will stay on the side of tradition.

As a consequence, the first moments of the distribution function f_p are zero:

$$\mathbf{m} = \int_{\mathbb{S}^2} \mathbf{l}\, f_p(\mathbf{l})\, \mathrm{d}a = \mathbf{0}. \tag{1.3}$$

To obtain non trivial information we need to calculate the second moments, which are represented by the second-order tensor

$$\mathbf{M} = \int_{\mathbb{S}^2} (\mathbf{l} \otimes \mathbf{l})\, f_p(\mathbf{l})\, \mathrm{d}a. \tag{1.4}$$

It is straightforward to show that $\mathbf{M}$ is a *unit trace symmetric tensor*.

$$\operatorname{tr} \mathbf{M} = \int_{\mathbb{S}^2} \operatorname{tr} (\mathbf{l} \otimes \mathbf{l})\, f_p(\mathbf{l})\, \mathrm{d}a = \int_{\mathbb{S}^2} f_p(\mathbf{l})\, \mathrm{d}a = 1 \tag{1.5}$$

$$\mathbf{M}^T = \int_{\mathbb{S}^2} (\mathbf{l} \otimes \mathbf{l})^T\, f_p(\mathbf{l})\, \mathrm{d}a = \mathbf{M}. \tag{1.6}$$

So, by the spectral decomposition theorem, $\mathbf{M}$ can be diagonalised by means of an orthogonal tensor and its eigenvalues are regular. If λ_1, λ_2 and λ_3 are the eigenvalues with associated unit eigenvectors $(\mathbf{e}_1, \mathbf{e}_2, \mathbf{e}_3)$, then the spectral decomposition is

$$\mathbf{M} = \lambda_1 \mathbf{e}_1 \otimes \mathbf{e}_1 + \lambda_2 \mathbf{e}_2 \otimes \mathbf{e}_2 + \lambda_3 \mathbf{e}_3 \otimes \mathbf{e}_3. \tag{1.7}$$

$\mathbf{M}$ is positive semidefinite, in fact if λ is an eigenvalue of $\mathbf{M}$ and $\mathbf{e} \in \mathbb{S}^2$ is the respective unit eigenvector, we have

$$\lambda = \mathbf{e} \cdot \mathbf{M}\mathbf{e} = \int_{\mathbb{S}^2} (\mathbf{l} \cdot \mathbf{e})^2\, f_p(\mathbf{l})\, \mathrm{d}a \geq 0. \tag{1.8}$$

The eigenvalues of $\mathbf{M}$ then sum up to one, so that its spectrum is bounded by

$$\operatorname{sp} (\mathbf{M}) \subseteq [0, 1]. \tag{1.9}$$

Only one of the three cases may happen: (a) $\lambda_i = \frac{1}{3} \quad i = 1, 2, 3$, (b) one eigenvalue is greater than $\frac{1}{3}$ while the other two are not greater than $\frac{1}{3}$ and (c) one eigenvalue is smaller than $\frac{1}{3}$ while the other two are not less than $\frac{1}{3}$. In the following we will assume that in cases (b) and (c) the different eigenvalue is labeled with λ_1 and we will call the associated eigenvector $\mathbf{e}_1$ the *director* $\mathbf{n}$. Case (a) corresponds to the *isotropic* case, in fact when

$$f_p(\mathbf{l}) = \frac{1}{4\pi}, \tag{1.10}$$

it is $\lambda_1 = \lambda_2 = \lambda_3$. Since $\operatorname{tr} \mathbf{M} = 1$ then we have

$$\mathbf{M}_{\text{isotropic}} = \frac{1}{3}\mathbf{I}. \tag{1.11}$$

In liquid crystals literature, the order parameter is customary assumed to be the tensor

$$\mathbf{Q} = \mathbf{M} - \frac{1}{3}\mathbf{I}, \tag{1.12}$$

so that the isotropy phase corresponds to the case $\mathbf{Q} = \mathbf{0}$ as usual in phase transition theories. Note that the condition $\mathbf{Q} = \mathbf{0}$ is only necessary to have isotropic phase. It is possible to find probability distributions other than $f_p(\mathbf{l}) = \frac{1}{4\pi}$ having $\mathbf{Q} = \mathbf{0}$ [83]. These however are rather special cases, henceforth we will always assume the condition $\mathbf{Q} = \mathbf{0}$ as characteristic of the isotropic phase.[2] Clearly, $(\mathbf{n}, \mathbf{e}_2, \mathbf{e}_3)$ are too eigenvectors of $\mathbf{Q}$ with shifted eigenvalues,

$$\mathrm{sp}\,(\mathbf{Q}) \subseteq \left[-\frac{1}{3}, \frac{2}{3}\right], \qquad \mathrm{tr}\,\mathbf{Q} = 0. \tag{1.13}$$

1.1.1 Uniaxial and biaxial states

If $\lambda_1 \neq \lambda_2 = \lambda_3$ in (1.7), we say that the liquid crystal is **uniaxial** and it is common to write $\mathbf{Q}$ as

$$\mathbf{Q} = s\left(\mathbf{n} \otimes \mathbf{n} - \frac{1}{3}\mathbf{I}\right), \tag{1.14}$$

where the director $\mathbf{n}$ is the unit eigenvector of $\mathbf{M}$ associated to the eigenvalue λ_1. The scalar s is the **degree of orientation** (or degree of order). Since by (1.14), $\frac{2}{3}s$ is an eigenvalue of $\mathbf{Q}$; s takes its values in

$$s \in \left[-\frac{1}{2}, 1\right]. \tag{1.15}$$

When $s = 1$, $\mathbf{M} = \mathbf{n} \otimes \mathbf{n}$ and so all the molecules are aligned along $\mathbf{n}$. When $s = 0$ the distribution is isotropic and when $s = -\frac{1}{2}$, $\mathbf{M} = \frac{1}{2}(\mathbf{I} - \mathbf{n} \otimes \mathbf{n})$ which is proportional to the projection operator on the plane orthogonal to $\mathbf{n}$ so that the distribution is *planar isotropic*. Typical values for s range between 0.3 and 0.9, with the exact value a function of temperature (see §1.4.2).

If $\lambda_1 \neq \lambda_2 \neq \lambda_3 \neq \lambda_1$ in (1.7), we say that the liquid crystal is **biaxial** and we can write the general expression for $\mathbf{Q}$ as [74, 68]

$$\mathbf{Q} = s_1\left(\mathbf{n} \otimes \mathbf{n} - \frac{1}{3}\mathbf{I}\right) + s_2\left(\mathbf{e}_2 \otimes \mathbf{e}_2 - \mathbf{e}_3 \otimes \mathbf{e}_3\right), \tag{1.16}$$

[2] Such distributions share at least the second moments with the uniform distribution, so that they can be considered "isotropic" at least to the second moment.

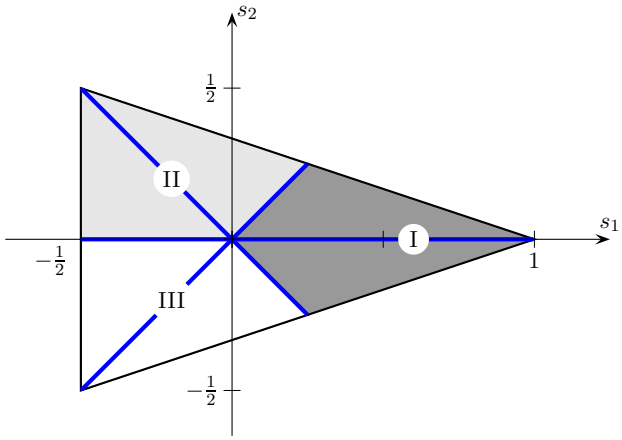

Figure 1.1: (s_1, s_2) domain. Regions I, II, and III show the values of (s_1, s_2) for which the maximum positive eigenvalues are respectively μ_1, μ_2 and μ_3. Molecules exhibit a preferred direction along the associated eigenvector. Thick lines represent the uniaxial states.

whose eigenvalues are: $\mu_1 = \frac{2}{3}s_1$, $\mu_2 = s_2 - \frac{1}{3}s_1$ and $\mu_3 = -s_2 - \frac{1}{3}s_1$. Using the bounds on the eigenvalues of $\mathbf{Q}$, one finds that the admissible values for (s_1, s_2) are

$$-\frac{1}{2} \leq s_1 \leq 1\,, \quad -\frac{1-s_1}{3} \leq s_2 \leq \frac{1-s_1}{3}. \tag{1.17}$$

This admissible domain is depicted in Figure 1.1. The parameter s_2 ranges in $\left[-\frac{1}{2}, \frac{1}{2}\right]$, but not all the values of $(s_1, s_2) \in \left[-\frac{1}{2}, 1\right] \times \left[-\frac{1}{2}, \frac{1}{2}\right]$ are allowed.

When $s_2 = 0$, (1.16) reduces to (1.14) and the liquid crystal is uniaxial, so that the scalar s_2 can be interpreted as the *biaxial amplitude*. Note, however, that also when $s_2 = \pm s_1$ two of the eigenvalues are equal and the liquid crystal is uniaxial. Bold lines in Figure 1.1 represent uniaxial states. The representation given by (1.16) is therefore more expressive when μ_1 is the maximum *positive* eigenvalue. In this case, in fact, s_1 and s_2 can be rightly interpreted as a degree of order and a degree of biaxiality of the liquid crystal. This is shown by the gray area labeled with I in Figure 1.1 where the values of (s_1, s_2) are such that μ_1 is the maximum positive eigenvalue and the molecules are mostly oriented along $\mathbf{n}$. Likewise, in regions II and III the molecules are mostly directed with $\mathbf{e}_2$ and $\mathbf{e}_3$ respectively. The horizontal line, in particular, represent the uniaxial states with director $\mathbf{n}$.

We remark that the description given by (1.16) is particularly simple and meaningful in the case of a "nearly uniaxial state" all within the liquid crystal, where s_2 is small (so that $\mu_1 > \mu_2$ and $\mu_1 > \mu_3$).

In the general case, one finds in literature the expressions for the **degree of order**

s and the **degree of biaxiality** β as functions of the eigenvalues of $\mathbf{Q}$ [12, 13, 14]

$$s = \left(\frac{27}{2}\mu_1\mu_2\mu_3\right)^{1/3} \tag{1.18}$$

$$\beta = \left(6\sqrt{3}\,|(\mu_1-\mu_2)(\mu_2-\mu_3)(\mu_3-\mu_1)|\right)^{1/3}. \tag{1.19}$$

s takes values in $\left[-\frac{1}{2},1\right]$ and it is consistent with the formula (1.14) when two eigenvalues are equal. β ranges in the interval $[0,1]$ and it is clearly zero whenever two eigenvalues are equal (uniaxial states). Its expression (1.19) is normalized so that a state with maximum biaxiality would correspond to $\beta = 1$.

Remark 1.1. Using notation of (1.16), one can write s and β in terms of s_1 and s_2 as follows

$$s = \left[s_1\left(s_1^2 - 9s_2^2\right)\right]^{1/3} \tag{1.20}$$

$$\beta = \left(12\sqrt{3}\,|s_2(s_1+s_2)(s_1-s_2)|\right)^{1/3}. \tag{1.21}$$

Equivalently, it is often found the definition of the degree of biaxiality in terms of $\operatorname{tr}\mathbf{Q}^2$ and $\operatorname{tr}\mathbf{Q}^3$ [51, 53, 52]

$$\beta^2 = 1 - 6\frac{\left(\operatorname{tr}\mathbf{Q}^3\right)^2}{\left(\operatorname{tr}\mathbf{Q}^2\right)^3} \tag{1.22}$$

Remark 1.2. Every point $p \in \mathbb{S}^2$ can be identified by a unit vector $\mathbf{l} \in \mathbb{R}^3$. Choosing a orthonormal frame of reference $(\mathbf{e}_1, \mathbf{e}_2, \mathbf{e}_3)$ at the point $O \in \mathscr{E}$, a unit vector $\mathbf{l}$ can be represented in spherical coordinates,

$$\mathbf{l} = \sin\vartheta\cos\varphi\,\mathbf{e}_1 + \sin\vartheta\sin\varphi\,\mathbf{e}_2 + \cos\vartheta\,\mathbf{e}_3. \tag{1.23}$$

Explicitly, $\mathbf{Q}$ is

$$\mathbf{Q} = \begin{pmatrix} <\sin^2\vartheta\,\cos^2\varphi - \frac{1}{3}> & <\sin^2\vartheta\,\sin\varphi\cos\varphi> & <\sin\vartheta\cos\vartheta\,\cos\varphi> \\ <\sin^2\vartheta\,\sin\varphi\cos\varphi> & <\sin^2\vartheta\,\sin^2\varphi - \frac{1}{3}> & <\sin\vartheta\cos\vartheta\,\sin\varphi> \\ <\sin\vartheta\cos\vartheta\,\cos\varphi> & <\sin\vartheta\cos\vartheta\,\sin\varphi> & <\cos^2\vartheta - \frac{1}{3}> \end{pmatrix} \tag{1.24}$$

where we have denoted with the angle brackets $<>$ the ensemble average with respect to the probability distribution $f(\vartheta,\varphi)$

$$<g(\vartheta,\varphi)> := \int_0^{2\pi} \mathrm{d}\varphi \int_0^{\pi} f_p(\vartheta,\varphi)g(\vartheta,\varphi)\,\sin\vartheta\mathrm{d}\vartheta. \tag{1.25}$$

If we use the orthonormal frame given by the eigenvectors of $\mathbf{Q}$, with the director $\mathbf{n} \equiv \mathbf{e}_3$, then ϑ measures the angle between the molecules at O and the director. With this choice of the axes, $\mathbf{Q}$ is diagonal, so that we can compare the diagonal elements of (1.24) with the expression (1.16) and gather direct expressions of s_1 and s_2

$$s_1 = \frac{1}{2} <3\cos^2\vartheta - 1> \qquad\qquad s_2 = \frac{1}{2} <\sin^2\vartheta\cos 2\varphi> \tag{1.26}$$

1.2 Frank's classical theory

We make the assumption that the equilibrium configurations of the liquid crystal attain the minima of a free energy functional. In the classical theory the degree of orientation is regarded as a prescribed positive constant and the liquid crystal is assumed to be uniaxial. Posing $s = \text{constant} > 0$ and $\beta = 0$, the order parameter may be described only through the director $\mathbf{n}$. Let $\mathcal{B}$ the regular region of the euclidean space $\mathscr{E}$ occupied by the liquid crystal. Then the orientation of the director is described by a mapping:

$$\mathbf{n} : \mathcal{B} \to \mathbb{S}^2 \tag{1.27}$$

which is assumed for the moment to be at least of class $\mathrm{C}^1\left(\mathcal{B}, \mathbb{S}^2\right)$.

1.2.1 Bulk free energy

The classical theory takes the bulk free energy of liquid crystals as given by the functional

$$\mathcal{F}_{\mathrm{fr}}[\mathbf{n}] = \int_{\mathcal{B}} \Psi(\mathbf{n}, \nabla\mathbf{n}) \mathrm{d}v \tag{1.28}$$

The free energy density $\Psi(\mathbf{n}, \nabla\mathbf{n})$ is customarily assumed to depend only upon $\mathbf{n}$ and its first gradient $\nabla\mathbf{n}$. Since $\mathbf{n}\cdot\mathbf{n} = 1$, $\nabla\mathbf{n}$ cannot be an arbitrary element of $\mathscr{L}\left(\mathbb{R}^3\right)$, where we have denoted with $\mathscr{L}\left(\mathbb{R}^3\right)$ the space of the linear mappings $\mathbb{R}^3 \to \mathbb{R}^3$, but must satisfy

$$(\nabla\mathbf{n})^T \mathbf{n} = \mathbf{0}. \tag{1.29}$$

Stated differently, using a more geometric language, $\nabla\mathbf{n}$ is a differential mapping between tangent spaces

$$\nabla\mathbf{n}(p) = \mathrm{d}_p\mathbf{n} : \mathrm{T}_p\mathcal{B} \to \mathrm{T}_{\mathbf{n}(p)}\mathbb{S}^2 \tag{1.30}$$

where we have denoted with $\mathrm{T}_p\mathcal{B} \equiv \mathrm{T}_p\mathscr{E} \cong \mathbb{R}^3$ the tangent space of $\mathcal{B}$ at $p \in \mathcal{B}$ and with $\mathrm{T}_{\mathbf{n}(p)}\mathbb{S}^2$ the tangent space of the unit sphere in $\mathbf{n}(p)$. Using the fact that $\mathrm{T}_{\mathbf{n}}\mathbb{S}^2 = \mathbf{n}^\perp$, the orthogonal complement of $\mathbf{n}$, one has that for all $\mathbf{v} \in \mathbb{R}^3$, $(\nabla\mathbf{n})\mathbf{v}$ is orthogonal to $\mathbf{n}$,

$$(\nabla\mathbf{n})\mathbf{v}\cdot\mathbf{n} = \mathbf{v}\cdot(\nabla\mathbf{n})^T\mathbf{n} = \mathbf{0} \qquad \forall\mathbf{v} \in \mathbb{R}^3, \tag{1.31}$$

so that we get to the same conclusion as before.
Therefore the domain of the energy density Ψ is the set

$$\mathcal{D}_\Psi = \left\{(\mathbf{n}, \mathbf{N}) : \mathbf{n} \in \mathbb{S}^2, \mathbf{N} \in \mathscr{L}\left(\mathbb{R}^3\right), \mathbf{N}^T\mathbf{n} = \mathbf{0}\right\}. \tag{1.32}$$

The physical insight of the problem suggests a list of requirements that Ψ must obey [83]:

(i) **frame-indifference**: Ψ must be the same in any two frames, i.e. independently from the observer, therefore it must be indifferent to rigid rotations

(ii) **material-symmetry**: when $\mathcal{B}$ suffers a mirror reflection, the energy density must remain unaffected.

(iii) **evenness**: Ψ must be indifferent to the change $\mathbf{n} \to -\mathbf{n}$

(iv) **positive definiteness**

The mathematical translations of these requirements are the hypothesis of the following theorem, due to Frank, which provides an explicit form for the energy density [43].

Theorem 1.3. Assume that $\Psi : \mathcal{D}_\Psi \to \mathbb{R}$ satisfies the following conditions, for every $\mathbf{n} : \mathcal{B} \to \mathbb{S}^2$:

(a) $\Psi\left(\mathbf{Rn}, \mathbf{R}\nabla\mathbf{n}\mathbf{R}^T\right) = \Psi\left(\mathbf{n}, \nabla\mathbf{n}\right), \qquad \forall \mathbf{R} \in O(3)$

(b) $\Psi\left(-\mathbf{n}, -\nabla\mathbf{n}\right) = \Psi\left(\mathbf{n}, \nabla\mathbf{n}\right)$

(c) $\Psi\left(\mathbf{n}, \nabla\mathbf{n}\right) \geq 0$ and $\Psi\left(\mathbf{n}, \nabla\mathbf{n}\right) = 0$ if and only if $\mathbf{n}$ is constant.

Assume moreover that $\Psi\left(\mathbf{n}, \nabla\mathbf{n}\right)$ depends at most quadratically on $\nabla\mathbf{n}$.
Then the free energy density has the form

$$\begin{aligned}\Psi_{\mathrm{Fr}}\left(\mathbf{n}, \nabla\mathbf{n}\right) &= K_1 \left(\operatorname{div}\mathbf{n}\right)^2 + K_2 \left(\mathbf{n} \cdot \operatorname{curl}\mathbf{n}\right)^2 + K_3 \left|\mathbf{n} \wedge \operatorname{curl}\mathbf{n}\right|^2 \\ &\quad + K_{24}\left(\operatorname{tr}\nabla\mathbf{n}^2 - \left(\operatorname{div}\mathbf{n}\right)^2\right)\end{aligned} \tag{1.33}$$

K_1, K_2, K_3 and K_{24} are called the **splay**, **bend**, **twist** and **saddle-splay moduli**, respectively. Using a tensor notation, equation (1.33) can be rewritten

$$\begin{aligned}\Psi_{\mathrm{Fr}}\left(\mathbf{n}, \mathbf{N}\right) &= K_1 \left(\operatorname{tr}\mathbf{N}\right)^2 + K_2 \left(\mathbf{W}(\mathbf{n}) \cdot \mathbf{N}\right)^2 + K_3 \left|\mathbf{N}\mathbf{n}\right|^2 \\ &\quad + K_{24}\left(\operatorname{tr}\mathbf{N}^2 - \left(\operatorname{tr}\mathbf{N}\right)^2\right)\end{aligned} \tag{1.34}$$

where we have set $\nabla\mathbf{n} = \mathbf{N}$ and we have made use of the relations (see [83] for details)

$$\operatorname{curl}\mathbf{n} \wedge \mathbf{n} = \left(\nabla\mathbf{n}\right)\mathbf{n} \tag{1.35}$$

$$\operatorname{div}\mathbf{n} = \operatorname{tr}\nabla\mathbf{n} \tag{1.36}$$

$$\mathbf{n} \cdot \operatorname{curl}\mathbf{n} = \mathbf{W}(\mathbf{n}) \cdot \nabla\mathbf{n}. \tag{1.37}$$

We remind that $\mathbf{W}(\mathbf{n})$ is the skew second order tensor associated with $\mathbf{n}$ so that $\mathbf{W}(\mathbf{n})\mathbf{n} = \mathbf{0}$ and for all $\mathbf{v} \in \mathbb{R}^3$, $\mathbf{W}(\mathbf{n})\mathbf{v} = \mathbf{n} \wedge \mathbf{v}$. In such a case $\mathbf{n}$ is called the axial vector of $\mathbf{W}$. The inner product between tensors is defined such that $\mathbf{A} \cdot \mathbf{B} = \operatorname{tr}\left(\mathbf{A}^T\mathbf{B}\right)$.

It must also be emphasized that the K_i values depend on the temperature T and decrease rather strongly when T increases but their ratio is nearly independent of T.

In many cases the full form (1.33) is too complex to be of practical use, either because the relative values of the elastic constants K_i are unknown, or because the equilibrium equations are extremely difficult to solve. In such cases, one may resort to the *one-constant approximation*; this amount to assuming

$$K_1 = K_2 = K_3 = K_{24} = K. \tag{1.38}$$

After some calculus, one can show that the free energy takes the form

$$\Psi_{\mathrm{Fr}}(\mathbf{n}, \nabla\mathbf{n}) = K|\nabla\mathbf{n}|^2. \tag{1.39}$$

Even if the free energy density (1.39) does not provide very accurate solutions, nevertheless its simpler form makes it a valuable tool to reach a qualitative insight into distortions in nematics. Hereafter we will always make use of the one-constant approximation and take the equation (1.39) as the expression of the free energy density in the classical theory of nematic liquid crystals.

Remark 1.4. The function multiplying K_{24} is a null-lagrangian, that is a free energy density which does not contribute to the equilibrium equations of the free energy functional (1.33). Indeed it can be shown that

$$\Psi_{24}(\mathbf{n}, \nabla\mathbf{n}) = \operatorname{tr}\nabla\mathbf{n}^2 - (\operatorname{div}\mathbf{n})^2 = \operatorname{div}(\mathbf{v}), \tag{1.40}$$

where $\mathbf{v}$ is the vector field defined by

$$\mathbf{v} = (\nabla\mathbf{n})\mathbf{n} - (\operatorname{div}\mathbf{n})\mathbf{n}. \tag{1.41}$$

Let $\boldsymbol{\nu}$ and $\partial\mathcal{B}$ be respectively the unit outer normal and the boundary of $\mathcal{B}$ and let $\nabla_{\mathrm{s}}\mathbf{n}$ be the surface gradient of $\mathbf{n}$ on $\partial\mathcal{B}$, defined by

$$\nabla_{\mathrm{s}}\mathbf{n} = \nabla\mathbf{n}\,(\mathbf{I} - \boldsymbol{\nu}\otimes\boldsymbol{\nu})\,. \tag{1.42}$$

Then it follows that

$$(\nabla_{\mathrm{s}}\mathbf{n})\mathbf{n}\cdot\boldsymbol{\nu} = (\nabla\mathbf{n})\mathbf{n}\cdot\boldsymbol{\nu} - (\mathbf{n}\cdot\boldsymbol{\nu})(\nabla\mathbf{n})\boldsymbol{\nu}\cdot\boldsymbol{\nu}, \tag{1.43}$$

$$(\operatorname{tr}\nabla_{\mathrm{s}}\mathbf{n})\mathbf{n}\cdot\boldsymbol{\nu} = (\operatorname{tr}\nabla\mathbf{n})(\mathbf{n}\cdot\boldsymbol{\nu}) - (\mathbf{n}\cdot\boldsymbol{\nu})(\nabla\mathbf{n})\boldsymbol{\nu}\cdot\boldsymbol{\nu}, \tag{1.44}$$

and so

$$((\nabla_{\mathrm{s}}\mathbf{n})\mathbf{n} - (\operatorname{div}_{\mathrm{s}}\mathbf{n})\mathbf{n})\cdot\boldsymbol{\nu} = ((\nabla\mathbf{n})\mathbf{n} - (\operatorname{div}\mathbf{n})\mathbf{n})\cdot\boldsymbol{\nu} \tag{1.45}$$

where $\operatorname{div}_{\mathrm{s}}\mathbf{n}$ is defined such that

$$\operatorname{div}_{\mathrm{s}}\mathbf{n} = \operatorname{tr}\nabla_{\mathrm{s}}\mathbf{n} = \operatorname{tr}\left(\nabla\mathbf{n}\,(\mathbf{I} - \boldsymbol{\nu}\otimes\boldsymbol{\nu})\right). \tag{1.46}$$

Then, by the divergence theorem,

$$\int_{\mathcal{B}} \left(\operatorname{tr} \nabla \mathbf{n}^2 - (\operatorname{div} \mathbf{n})^2 \right) \mathrm{d}v = \int_{\partial \mathcal{B}} \left((\nabla \mathbf{n})\mathbf{n} - (\operatorname{div} \mathbf{n})\mathbf{n} \right) \cdot \boldsymbol{\nu} \, \mathrm{d}a$$
$$= \int_{\partial \mathcal{B}} \left((\nabla_{\mathrm{s}} \mathbf{n})\mathbf{n} - (\operatorname{div}_{\mathrm{s}} \mathbf{n})\mathbf{n} \right) \cdot \boldsymbol{\nu} \, \mathrm{d}a. \tag{1.47}$$

Thus Ψ_{24} gives rise to a surface energy that does not contribute to the equilibrium equations for the functional (1.33), but it generally enters the boundary conditions. However, in the special case where Dirichlet conditions are assumed, the field $\mathbf{n}$ is prescribed at the boundary so that also the surface derivatives of $\mathbf{n}$ are known on $\partial\mathcal{B}$ and expression (1.47) is determined. Therefore, when $\mathbf{n}$ is subject to strong anchoring conditions the surface contribution of Ψ_{24} is the same for all admissible orientation fields.

Ericksen has given a set of conditions that the Frank's constants must satisfy to render Ψ_{Fr} positive definite [35].

Theorem 1.5. The function Ψ_{Fr} in (1.34) satisfies

$$\Psi_{\mathrm{Fr}}(\mathbf{n}, \mathbf{N}) \geq 0 \tag{1.48}$$

for any given $\mathbf{n} \in \mathbb{S}^2$ and for all $\mathbf{N} \in \mathscr{L}(\mathbb{R}^3)$ if, and only if,

$$2K_1 \geq K_{24}, \quad K_2 \geq |K_2 - K_{24}|, \quad K_3 \geq 0\,. \tag{1.49}$$

1.2.2 Splay, bend and twist fields

The constants K_1, K_2, K_3 are directly associated with three basic types of deformations. It is in fact possible to generate deformations that are pure splay, pure bend and pure twist using which the values of the material constants K_i $(i = 1, 2, 3)$ can be experimentally determined [32].
Consider a system of cylindrical coordinates (ρ, ϑ, z) and the coordinate orthonormal base $(\mathbf{e}_\rho, \mathbf{e}_\vartheta, \mathbf{e}_z)$. Let $\mathbf{n}_s$ be the **splay field** defined by (see Figure 1.2(a))

$$\mathbf{n}_s = \mathbf{e}_\rho. \tag{1.50}$$

It can be shown that

$$\nabla \mathbf{n}_s = \frac{1}{\rho} \mathbf{e}_\vartheta \otimes \mathbf{e}_\vartheta, \tag{1.51}$$

whence it follows that

$$\operatorname{div} \mathbf{n}_s = \frac{1}{\rho}, \qquad \operatorname{curl} \mathbf{n}_s = \mathbf{0}, \qquad \operatorname{tr} (\nabla \mathbf{n}_s)^2 = \frac{1}{\rho^2}. \tag{1.52}$$

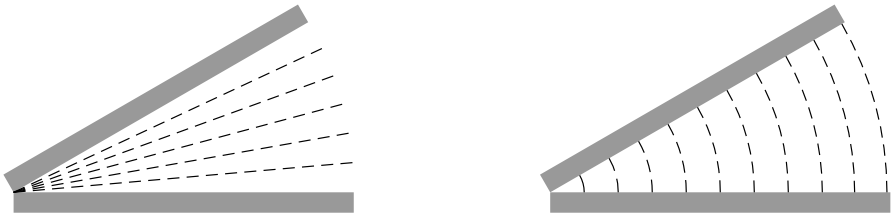

(a) (b)

Figure 1.2: (a) Splay field ($\operatorname{div}\mathbf{n} \neq 0$). (b) Bend field ($\operatorname{curl}\mathbf{n} \perp \mathbf{n}$).

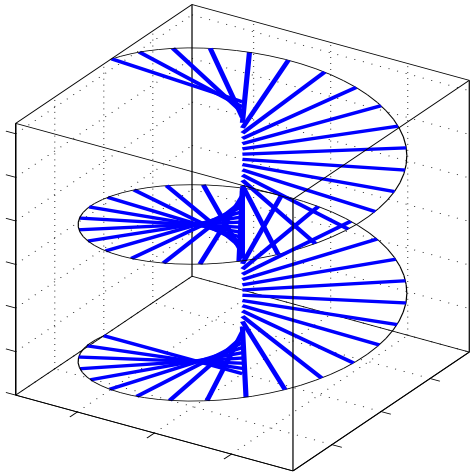

Figure 1.3: Twist field ($\operatorname{curl}\mathbf{n} \,||\, \mathbf{n}$).

The Frank's elastic energy depends only on K_1: $\Psi_{\mathrm{Fr}}(\mathbf{n}, \nabla\mathbf{n}) = K_1 \frac{1}{\rho^2}$.

In the same cylindrical coordinate system, define the **bend field** $\mathbf{n}_b$ by (see Figure 1.2(b))

$$\mathbf{n}_b = \mathbf{e}_\vartheta. \tag{1.53}$$

We have

$$\nabla\mathbf{n}_b = -\frac{1}{\rho}\mathbf{e}_\rho \otimes \mathbf{e}_\vartheta, \tag{1.54}$$

whence

$$\operatorname{div}\mathbf{n}_b = 0\,, \quad \operatorname{curl}\mathbf{n}_b = \frac{1}{\rho}\mathbf{e}_z\,, \quad (\nabla\mathbf{n}_b)\,\mathbf{n}_b = -\frac{1}{\rho}\mathbf{e}_\rho\,, \quad (\nabla\mathbf{n}_b)^2 = \mathbf{0}\,. \tag{1.55}$$

Therefore, the Frank's elastic energy depends only on K_3: $\Psi_{\mathrm{Fr}}(\mathbf{n}, \nabla\mathbf{n}) = K_3 \frac{1}{\rho^2}$.

K_2 enters into play when we consider the **twist field**. We take now a system of Cartesian coordinates (x, y, z) and the coordinate orthonormal base $(\mathbf{i}, \mathbf{j}, \mathbf{k})$. $\mathbf{n}_t$ is

defined by (see Figure 1.3)

$$\mathbf{n}_t \;=\; \cos(tz)\,\mathbf{i} + \sin(tz)\,\mathbf{j} \tag{1.56}$$

which follows an helical pattern and the scalar t is also referred to as the twist. After some calculus, we yield

$$\operatorname{div}\mathbf{n}_t \;=\; 0\,, \qquad \operatorname{curl}\mathbf{n}_t \;=\; -t\mathbf{n}_t\,, \qquad (\nabla\mathbf{n}_b)^2 \;=\; \mathbf{0}\,. \tag{1.57}$$

and $\Psi_{\mathrm{Fr}}(\mathbf{n}, \nabla\mathbf{n}) \;=\; K_2\, t^2$ for the bulk free energy.

Remark 1.6. It must be noted that the splay and bend fields are discontinuous in $\rho = 0$. We say that the z axis is a defect for these fields. Moreover an integration of the energy density over a cylinder enclosing a portion of the z axis yields an infinite result. This has been the main motivating reason for the search of a new theory able to handle the energetics of defects.

1.2.3 Equilibrium equations

In this Section we derive the general Euler-Lagrange equations for the energy functional (1.28). Therefore we set the first differential of $\mathcal{F}_{\mathrm{fr}}$ equal to zero. Proceeding in a customary way, we get

$$\begin{aligned}
\mathrm{d}\mathcal{F}_{\mathrm{fr}}[\mathbf{n}]\mathbf{u} \;&=\; \frac{\partial}{\partial\varepsilon}\int_{\mathcal{B}} \Psi(\mathbf{n}+\varepsilon\mathbf{u}, \nabla\mathbf{n}+\varepsilon\nabla\mathbf{u})\mathrm{d}v\Big|_{\varepsilon=0} \\
&=\; \int_{\mathcal{B}} \left(\frac{\partial\Psi}{\partial\mathbf{n}}\cdot\mathbf{u} + \frac{\partial\Psi}{\partial\nabla\mathbf{n}}\cdot\nabla\mathbf{u}\right)\mathrm{d}v \\
&=\; \int_{\mathcal{B}} \left(\frac{\partial\Psi}{\partial\mathbf{n}} - \operatorname{div}\frac{\partial\Psi}{\partial\nabla\mathbf{n}}\right)\cdot\mathbf{u}\,\mathrm{d}v + \int_{\mathcal{B}} \operatorname{div}\left(\left(\frac{\partial\Psi}{\partial\nabla\mathbf{n}}\right)^T\mathbf{u}\right)\mathrm{d}v \\
&=\; \int_{\mathcal{B}} \left(\frac{\partial\Psi}{\partial\mathbf{n}} - \operatorname{div}\frac{\partial\Psi}{\partial\nabla\mathbf{n}}\right)\cdot\mathbf{u}\,\mathrm{d}v + \int_{\partial\mathcal{B}} \frac{\partial\Psi}{\partial\nabla\mathbf{n}}\boldsymbol{\nu}\cdot\mathbf{u}\,\mathrm{d}a.
\end{aligned} \tag{1.58}$$

The divergence of a tensor is defined such that for every tensor $\mathbf{L}$ and for all constant vectors $\mathbf{a}$

$$\operatorname{div}\left(\mathbf{L}^T\mathbf{a}\right) \;=\; \mathbf{a}\cdot\operatorname{div}\mathbf{L}. \tag{1.59}$$

In (1.58) we have used the identity

$$\operatorname{div}\left(\mathbf{L}^T\mathbf{u}\right) \;=\; \mathbf{L}\cdot\nabla\mathbf{u} + \operatorname{div}\mathbf{L}\cdot\mathbf{u}. \tag{1.60}$$

We cannot immediately deduce the Euler-Lagrange equations from (1.58) since not all the variations $\mathbf{u}$ are admissible. In fact Ψ is defined when $\mathbf{n} \in \mathbb{S}^2$, then its differential must be a linear map taking values in $\mathrm{T}_{\mathbf{n}}\mathbb{S}^2$ with respect to the first

argument. Stated directly, the allowed variations are those for which the "varied vector field" $\mathbf{n}+\varepsilon\mathbf{u}$ is still an element (at the first order) of $\mathbb{S}^2$ as $\varepsilon \to 0$. From the requirement that $(\mathbf{n}+\varepsilon\mathbf{u})\cdot(\mathbf{n}+\varepsilon\mathbf{u}) = 1$ at the first order we get the condition $\mathbf{u}\cdot\mathbf{n} = 0$, so that $\mathbf{u} \in \mathrm{T}_{\mathbf{n}}\mathbb{S}^2 = \mathbf{n}^{\perp}$. Introducing the projection operator on the tangent space , we can thus write an arbitrary $\mathbf{u}$ as

$$\mathbf{u} = (\mathbf{I} - \mathbf{n}\otimes\mathbf{n})\,\mathbf{w} = \mathbf{P}(\mathbf{n})\mathbf{w} \tag{1.61}$$

for a suitable $\mathbf{w} \in \mathbb{R}^3$. Using the symmetry of $\mathbf{P}(\mathbf{n})$, equation (1.58) then becomes

$$\mathrm{d}\mathcal{F}_{\mathrm{fr}}[\mathbf{n}]\mathbf{u} = \int_{\mathcal{B}} \mathbf{P}(\mathbf{n})\left(\frac{\partial\Psi}{\partial\mathbf{n}} - \operatorname{div}\frac{\partial\Psi}{\partial\nabla\mathbf{n}}\right)\cdot\mathbf{w}\,\mathrm{d}v + \int_{\partial\mathcal{B}} \frac{\partial\Psi}{\partial\nabla\mathbf{n}}\boldsymbol{\nu}\cdot\mathbf{u}\,\mathrm{d}a. \tag{1.62}$$

Equilibrium configurations must render this expression zero for all $\mathbf{w} \in \mathbb{R}^3$, therefore we gather from the first integral the bulk equilibrium equations

$$\mathbf{P}(\mathbf{n})\left(\frac{\partial\Psi}{\partial\mathbf{n}} - \operatorname{div}\frac{\partial\Psi}{\partial\nabla\mathbf{n}}\right) = \mathbf{0}. \tag{1.63}$$

However, in practice, the equilibrium equations are rarely used in this general form; it is often more convenient to express the unit vector $\mathbf{n}$ in terms of suitably chosen polar angles and to write that $\mathcal{F}_{\mathrm{fr}}$ is a minimum with respect to all variations in these angles.

1.2.4 Anchoring

The second term in (1.62) gives an equation that must be satisfied at the boundary and whose form depends strongly on the assumed boundary conditions. It can be further simplified by means of the following lemma.

Lemma 1.7. Be $\Psi : \mathcal{D}_\Psi \to \mathbb{R} : (\mathbf{n},\mathbf{N}) \mapsto \Psi(\mathbf{n},\mathbf{N})$ a smooth map. Then

$$\mathbf{P}(\mathbf{n})\frac{\partial\Psi}{\partial\mathbf{n}} = \frac{\partial\Psi}{\partial\mathbf{n}} \tag{1.64}$$

$$\mathbf{P}(\mathbf{n})\frac{\partial\Psi}{\partial\mathbf{N}} = \frac{\partial\Psi}{\partial\mathbf{N}} \tag{1.65}$$

Proof. The proof is just a matter of properly understand how the differential of Ψ is defined. Let's denote with $\mathcal{L}_{\mathbf{n}}$ the space of linear mappings between $\mathbb{R}^3$ and $\mathrm{T}_{\mathbf{n}}\mathbb{S}^2 = \mathbf{n}^{\perp}$. Clearly, by definition, if $\mathbf{N} \in \mathcal{L}_{\mathbf{n}}$ then $\mathbf{N}^T\mathbf{n} = \mathbf{0}$. The differential of Ψ is a map

$$\mathrm{d}_{(\mathbf{n},\mathbf{N})}\Psi : \mathrm{T}_{\mathbf{n}}\mathbb{S}^2 \times \mathcal{L}_{\mathbf{n}} \to \mathbb{R}, \tag{1.66}$$

whose general expression is

$$\mathrm{d}_{(\mathbf{n},\mathbf{N})}\Psi(\mathbf{h},\mathbf{H}) = \langle \boldsymbol{a},\mathbf{h}\rangle + \langle \boldsymbol{A},\mathbf{H}\rangle, \tag{1.67}$$

where the angle brackets represent duality between linear spaces and $\boldsymbol{a}$ and $\boldsymbol{A}$ are elements of the dual spaces. In particular $\boldsymbol{a} \in \left(\mathrm{T}_{\mathbf{n}}\mathbb{S}^2\right)^*$. By the representation theorem of linear spaces (i.e. the fact that a finite dimensional linear space $\mathscr{V}$ is isomorphic to its dual $\mathscr{V}^*$, the isomorphism being induced by the inner product in $\mathscr{V}$), there exist unique elements $\frac{\partial \Psi}{\partial \mathbf{n}} \in \mathrm{T}_{\mathbf{n}}\mathbb{S}^2$ and $\frac{\partial \Psi}{\partial \mathbf{N}} \in \mathcal{L}_{\mathbf{n}}$ so that

$$\mathrm{d}_{(\mathbf{n},\mathbf{N})}\Psi(\mathbf{h},\mathbf{H}) = \frac{\partial \Psi}{\partial \mathbf{n}} \cdot \mathbf{h} + \frac{\partial \Psi}{\partial \mathbf{N}} \cdot \mathbf{H} \tag{1.68}$$

where, as usual in continuum mechanics, we have used the same symbol (the dot product) for two conceptually different inner products (the first is the usual scalar product between vectors while the second acts on double tensors). Then (1.64) is an immediate consequence of $\frac{\partial \Psi}{\partial \mathbf{n}} \in \mathrm{T}_{\mathbf{n}}\mathbb{S}^2$.
Moreover, since $\frac{\partial \Psi}{\partial \mathbf{N}} \in \mathcal{L}_{\mathbf{n}}$ we have for all vectors $\mathbf{w} \in \mathbb{R}^3$

$$\frac{\partial \Psi}{\partial \mathbf{N}} \mathbf{w} \cdot \mathbf{n} = \mathbf{0}, \tag{1.69}$$

and equation (1.65) follows. □

By the use of equation (1.65), the surface integral then yields, for all variations $\mathbf{w} \in \mathbb{R}^3$

$$\int_{\partial \mathcal{B}} \frac{\partial \Psi}{\partial \nabla \mathbf{n}} \boldsymbol{\nu} \cdot \mathbf{w} \, \mathrm{d}a = \mathbf{0} \tag{1.70}$$

The easiest case is when *Dirichlet conditions* are assumed on $\partial\mathcal{B}$, so that the value of $\mathbf{n}$ is prescribed on the border of the domain. Then $\mathbf{w}$ must vanish identically on $\partial\mathcal{B}$ and so no surface energy contributions come from the integral in (1.70). This is known as **strong anchoring** condition. In this case the molecules are constrained to hold a prescribed orientation at the limiting surfaces and are said to be subject to strong anchoring forces. These forces are due partly to the detailed form of the interparticle potentials near the boundary of the sample, and partly to the ways of preparing the surface on a mesoscopic length scale. For instance, when a glass surface is rubbed in one direction, the nematic molecules tend to line up along this direction. A clear microscopic explanation of this effect is still lacking. Berreman [11] gives an explanation on the basis of the additional elastic energy that would occur in a nematic liquid crystal if the molecules were not parallel to the grooves. Likewise, energy considerations would explain a tendency for the molecules to line up *normal* to the surface when it is rubbed in *both* dimensions.
In recent years several alternative methods of alignment have been proposed, for example, photoalignment by means of a polarized laser beam [45], atomic force microscope treated surfaces [72] or alignment with atomic beams [24].
When no conditions are assumed at the boundary, the second integral must vanish for all the possible variations and can be treated in precisely the same way as the

first. This leads to the *natural (or Neumann) boundary conditions* and corresponds to the fact that the limiting surface exerts **no anchoring** on the liquid crystal. The equations that give such condition are

$$\left.\frac{\partial \Psi}{\partial \nabla \mathbf{n}}\boldsymbol{\nu}\right|_{\partial\mathcal{B}} = \mathbf{0}. \tag{1.71}$$

An intermediate and more realistic condition between the strong anchoring and the total lack of anchoring, is provided by the **weak anchoring** condition. In such case, molecules close to the boundary have a preferred direction imposed by the limiting surface (for instance, by means of mechanical or chemical treatment) but can deviate from this prescribed direction at the cost of some surface energy. Weak anchoring forces does not provide a boundary condition, but add a surface term to the energy functional (1.28)

$$\mathcal{F}_{\mathrm{w}}[\mathbf{n}] = W\int_{\partial\mathcal{B}} f_{\mathrm{w}}(\mathbf{n})\,\mathrm{d}a, \tag{1.72}$$

which is called **anchoring energy**. The function $f_{\mathrm{w}}(\mathbf{n})$ must attain a minimum for a particular $\mathbf{n}_0 \in \mathbb{S}^2$ whose direction is called the **easy axis**. W is the *anchoring strength*.

We note that the same arguments found in the proof of Lemma 1.7 hold for $\frac{\partial f_{\mathrm{w}}}{\partial \mathbf{n}}$ and therefore one can show that $\frac{\partial f_{\mathrm{w}}}{\partial \mathbf{n}} = \mathbf{P}(\mathbf{n})\frac{\partial f_{\mathrm{w}}}{\partial \mathbf{n}}$. Performing the first variation of $\mathcal{F}_{\mathrm{w}}[\mathbf{n}]$ yields the term

$$\mathrm{d}\mathcal{F}_{\mathrm{w}}[\mathbf{n}]\mathbf{u} = W\int_{\partial\mathcal{B}} \frac{\partial f_{\mathrm{w}}}{\partial \mathbf{n}}\cdot\mathbf{u}\,\mathrm{d}a = W\int_{\partial\mathcal{B}} \mathbf{P}(\mathbf{n})\frac{\partial f_{\mathrm{w}}}{\partial \mathbf{n}}\cdot\mathbf{w}\,\mathrm{d}a = W\int_{\partial\mathcal{B}} \frac{\partial f_{\mathrm{w}}}{\partial \mathbf{n}}\cdot\mathbf{w}\,\mathrm{d}a, \tag{1.73}$$

where $\mathbf{u}$ is an arbitrary vector belonging to the orthogonal space $\mathbf{n}^{\perp}$ and $\mathbf{w} \in \mathbb{R}^3$ is such that $\mathbf{u} = \mathbf{P}(\mathbf{n})\mathbf{w}$.

Joining the latter expression to the boundary term in equation (1.62), we obtain the equation that must be satisfied at the boundary

$$\frac{\partial \Psi}{\partial \nabla \mathbf{n}}\boldsymbol{\nu} + W\frac{\partial f_w}{\partial \mathbf{n}} = 0 \quad \text{on } \partial\mathcal{B}. \tag{1.74}$$

The most commonly used expression for the surface free energy is of the form proposed by Rapini and Papoular [69]

$$\mathcal{F}_{\mathrm{w}}[\mathbf{n}] = W\int_{\partial\mathcal{B}} (\mathbf{n}\cdot\boldsymbol{\nu})^2\,\mathrm{d}a, \tag{1.75}$$

where the anchoring strength W is assumed constant throughout the limiting surface. When $W > 0$, $\mathcal{F}_{\mathrm{w}}$ is minimum when $\mathbf{n}\perp\boldsymbol{\nu}$, so the easy axis is tangent to the boundary and we speak of *degenerate planar weak condition*. When $W < 0$ the minimum of $\mathcal{F}_{\mathrm{w}}$ is attained when $\mathbf{n}||\boldsymbol{\nu}$, the easy axis is along the normal vector $\boldsymbol{\nu}$

and this situation is referred to as *hometropic weak anchoring*.
A straightforward generalization of the above formula is obtained when two different coefficients are introduced: the azimuthal anchoring strength W_φ related to director deviation in the tangent plane to the limiting surface and the zenithal (or polar) anchoring strength W_ϑ related to the director deviations in the direction perpendicular to the liquid crystal-substrate boundary.

Remark 1.8. In principle, there is no reason why $f_{\rm w}(\mathbf{n})$ should depend only on the director $\mathbf{n}$. In the more general framework of the new theory, the anchoring energy can depend on the whole tensor $\mathbf{Q}$ and in particular on the surface order parameter s. A possible generalization [65, 8] is

$$f_{\rm w}(\mathbf{Q}) \,=\, W\,{\rm tr}\,(\mathbf{Q}-\mathbf{Q}_0)^2\,, \tag{1.76}$$

where $\mathbf{Q}_0$ is the order parameter preferred at the surface.
In the uniaxial case where $\mathbf{Q}_0$ is written as in (1.14), it comprises an easy axis $\mathbf{n}_0$ and a preferred surface ordering s_0. Explicitly,

$$f_{\rm w}(s,\mathbf{n}) \,=\, \frac{2}{3}W\Big(s^2+s_0^2+ss_0\left(1-3(\mathbf{n}\cdot\mathbf{n}_0)^2\right)\Big). \tag{1.77}$$

Expression (1.77) looks like the Rapini-Papoular expression if s is constant. Note that when $\mathbf{n}||\mathbf{n}_0$, equation (1.77) has a minimum in $s=s_0$ as expected.

1.2.5 Existence of minimizers

Throughout this Section we assume that the region $\mathcal{B}$ occupied by a nematic liquid crystal has a smooth boundary. We consider the existence of minimizers for the Frank's energy functional (1.33), when strong anchoring conditions are assumed at the boundary [48, 49] (mathematically this amounts to using Dirichlet conditions on $\partial\mathcal{B}$).
Let $\mathrm{H}^1\left(\mathcal{B},\mathbb{R}^3\right)$ the Sobolev space of the L^2-mappings with first weak derivatives in L^2, and consider the closed subset

$$\mathrm{H}^1\left(\mathcal{B},\mathbb{S}^2\right) \,=\, \left\{\mathbf{n}\in\mathrm{H}^1\left(\mathcal{B},\mathbb{R}^3\right)\,:\,|\mathbf{n}|=1\right\}. \tag{1.78}$$

Under the assumption of strong anchoring conditions, $\mathbf{n}$ is prescribed at the boundary

$$\mathbf{n}|_{\partial\mathcal{B}} \,=\, \mathbf{n}_0; \tag{1.79}$$

the class of admissible functions is

$$\mathscr{A}(\mathbf{n}_0) \,=\, \left\{\mathbf{n}\in\mathrm{H}^1\left(\mathcal{B},\mathbb{S}^2\right)\,:\,\mathbf{n}_0 \text{ is the trace of } \mathbf{n} \text{ on } \partial\mathcal{B}\right\}^{3}. \tag{1.80}$$

[3] We don't want to go into the mathematical details of properly defining the trace operators. It is sufficient to say that $\mathbf{n}_0$ can be assumed to stand in another Sobolev space, usually denoted with $\mathrm{H}^{1/2}(\partial\mathcal{B},\mathbb{S}^2)$.

The following theorem guarantees that there is always a minimum for $\mathcal{F}$ in $\mathscr{A}$ [83].

Theorem 1.9. For any given $\mathbf{n}_0 : \partial\mathcal{B} \to \mathbb{S}^2$ there is a mapping $\widehat{\mathbf{n}} \in \mathscr{A}(\mathbf{n}_0)$ where $\mathcal{F}$ attains its minimum:

$$\mathcal{F}[\widehat{\mathbf{n}}] \;=\; \min\left\{\mathcal{F}[\mathbf{n}] \;:\; \mathbf{n} \in \mathscr{A}(\mathbf{n}_0)\right\}. \tag{1.81}$$

1.3 Freedericksz transition

The tensor order parameter $\mathbf{Q}$ of the nematic phase is a microscopic articulation of its anisotropy. The macroscopic analogue involves the electric or magnetic *susceptibility*. In an isotropic and linear medium, the electric displacement $\mathbf{D}$ and the magnetic moment density (or magnetization) $\mathbf{M}$ are directly respectively proportional to the electric and magnetic fields inducing them: $\mathbf{D} = \varepsilon\mathbf{E}$ and $\mathbf{M} = \chi\mathbf{H}$, where ε is the dielectric constant and χ is the magnetic susceptibility.

In the case of a uniaxial nematic fluid the material constants ε and χ are no longer scalars. They too are tensors, with the same eigenvectors as the order parameter

$$\boldsymbol{\varepsilon} = \varepsilon_{||}\,\mathbf{n}\otimes\mathbf{n} + \varepsilon_{\perp}\,(\mathbf{I} - \mathbf{n}\otimes\mathbf{n}) = \varepsilon_{\perp}\mathbf{I} + \varepsilon_a\mathbf{n}\otimes\mathbf{n} \tag{1.82}$$

$$\boldsymbol{\chi} = \chi_{||}\,\mathbf{n}\otimes\mathbf{n} + \chi_{\perp}\,(\mathbf{I} - \mathbf{n}\otimes\mathbf{n}) = \chi_{\perp}\mathbf{I} + \chi_a\mathbf{n}\otimes\mathbf{n}, \tag{1.83}$$

where $\varepsilon_{||}$ and $\chi_{||}$ are exhibited by the material when the electric and magnetic fields are applied parallel to the director $\mathbf{n}$, $\varepsilon_{\perp}$ and $\chi_{\perp}$ are relative to fields lying in the plane orthogonal to $\mathbf{n}$, $\varepsilon_a = \varepsilon_{||} - \varepsilon_{\perp}$ is the **dielectric anisotropy** and $\chi_a = \chi_{||} - \chi_{\perp}$ is the **diamagnetic anisotropy**. The electric displacement $\mathbf{D}$ and the magnetization $\mathbf{M}$ become

$$\mathbf{D} = \boldsymbol{\varepsilon}\mathbf{E} \;=\; \varepsilon_{\perp}\mathbf{E} + \varepsilon_a\,(\mathbf{E}\cdot\mathbf{n})\,\mathbf{n} \tag{1.84}$$

$$\mathbf{M} = \boldsymbol{\chi}\mathbf{H} \;=\; \chi_{\perp}\mathbf{H} + \chi_a\,(\mathbf{H}\cdot\mathbf{n})\,\mathbf{n}. \tag{1.85}$$

$\mathbf{E}$ and $\mathbf{H}$ represent the fields suffered by the liquid crystal; it is taken to be equal to the field created from outside the material. In other words, we assume that $\mathbf{E}$ and $\mathbf{H}$ are strong enough not to get distorted within the liquid crystal (see [33, 75, 63] for discussions not employing this assumption).
The free energy density associated with the fields (expressed in c.g.s. units) are

$$\Psi_e \;=\; -\frac{1}{8\pi}\mathbf{D}\cdot\mathbf{E} \;=\; -\frac{1}{8\pi}\left(\varepsilon_{\perp}\,|\mathbf{E}|^2 + \varepsilon_a\,(\mathbf{E}\cdot\mathbf{n})^2\right) \tag{1.86}$$

$$\Psi_m \;=\; -\frac{1}{2}\mathbf{M}\cdot\mathbf{H} \;=\; -\frac{1}{2}\left(\chi_{\perp}\,|\mathbf{H}|^2 + \chi_a\,(\mathbf{H}\cdot\mathbf{n})^2\right). \tag{1.87}$$

In (1.86) and (1.87), the terms independent of the nematic director $\mathbf{n}$ do not affect the minimum of the energy, they are simply constants since the electric and magnetic fields are assumed to be imposed from the outside and can be omitted for the purposes of the present discussion. Since in nematics it is found that $\chi_a > 0$, a glance at equation (1.87) tells that Ψ_m is minimized when the director $\mathbf{n}$ is parallel to the magnetic field $\mathbf{H}$. The effective molecular orientation will be the result of the competing energy contributions of the boundary surface potential, the elastic distortion and the magnetic (or electric) external field. Whereas for the electric field, Ψ_e is minimized by $\mathbf{E}||\mathbf{n}$ if $\varepsilon_a > 0$ and by $\mathbf{E}\perp\mathbf{n}$ if $\varepsilon_a < 0$. So, in particular, when the dielectric anisotropy is negative and in absence of other distorting causes, an electric field tends to align the molecules perpendicularly to its direction.

1.3.1 Instability and pitchfork bifurcation

We will limit ourselves to a rather simple example, for a more complete treatment see [33, 81, 75, 83, 63]. In a Cartesian coordinate system $(O; x, y, z)$ with unit vectors $(\mathbf{i}, \mathbf{j}, \mathbf{k})$, let's consider a nematic liquid crystal confined between two parallel plates placed at $z = -d/2$ and $z = d/2$, subject to strong anchoring at the external surfaces. The director at the boundary is assumed to lie in the boundary planes along the x-axis. So, in the absence of any external action, the nematic is in homogeneous planar alignment $\mathbf{n} = (1, 0, 0)$. A homogeneous magnetic field $\mathbf{H}$ is applied orthogonally to the delimiting plates and tends to align the molecules along the z-axis (a completely analogous treatment would hold if we chose an electric field $\mathbf{E}$). There is then a competition between the aligning forces at the surface, favouring $\mathbf{n}||\mathbf{i}$ and in the bulk, favouring $\mathbf{n}||\mathbf{k}$. The elastic forces then take into account the fact that the nematic is not willing to exhibit inhomogeneity. At low magnetic fields, the aligning force is weak and the elastic bend price is too high to alter the uniform surface-induced alignment. At high fields, the liquid crystal aligns parallel to the field except in thin boundary layers close to the surface. This transition is known as **Freedericksz transition** and occurs at a critical value of the magnetic field (*Freedericksz threshold*) where the director just begins to turn toward the magnetic field.

We assume plane deformations of the director field. In that case, the following representation of the director is possible $\mathbf{n} = (\cos\vartheta, 0, \sin\vartheta)$. The angle ϑ is determined by the director $\mathbf{n}$ and the $x-$axis and it will be a function of z coordinate only. The

magnetic field is $\mathbf{H} = H\mathbf{k}$. Within these hypotheses, the free energy density is

$$\begin{aligned}\Psi \;=\; \Psi_{\mathrm{Fr}} + \Psi_m \;&=\; K|\nabla\mathbf{n}|^2 - \frac{1}{2}\chi_a\left(\mathbf{H}\cdot\mathbf{n}\right)^2 \\ &=\; K\left(\frac{\mathrm{d}\vartheta}{\mathrm{d}z}\right)^2 - \frac{1}{2}\chi_a H^2\left(\sin\vartheta\right)^2. \end{aligned} \tag{1.88}$$

By introducing the scaled variable $\bar{z} = z/d$ and defining

$$\lambda = \frac{\chi_a}{2K}(Hd)^2 \tag{1.89}$$

the equilibrium solutions are given by the minima of the functional

$$\mathcal{F} = \int_{-1/2}^{1/2}\left(\vartheta'^2 - \lambda\left(\sin\vartheta\right)^2\right)\mathrm{d}\bar{z}. \tag{1.90}$$

where the prime denotes differentiation with respect to the scaled variable $\bar{z}$. In the case of strong anchoring, boundary conditions are

$$\vartheta|_{\bar{z}=\pm 1/2} \;=\; 0, \tag{1.91}$$

so that the trivial solution $\vartheta(\bar{z}) \equiv 0$ is always a stationary point of the functional (1.90). When the Freedericksz transition is reached, a *pitchfork bifurcation* occurs in the solution: below the transition, at low fields, only the trivial $\vartheta(\bar{z}) \equiv 0$ solution is allowed, whereas above the transition two other symmetric non-trivial solutions appear. We are interested in the determination of the critical value λ_{cr} at which the Freedericksz transition happens. A technique presented in [64] and reported in Appendix A will be hereafter applied. Assume that λ is incremented by a small amount above a value $\lambda_0 \leq \lambda_{cr}$ (which will be later set equal to the critical value λ_{cr})

$$\lambda \;=\; \lambda_0\left(1+\varepsilon^2\right), \tag{1.92}$$

where ε simply represent a small quantity. The minimum of (1.90) can be expanded in terms of ε. Retaining only the first term, and considering that the zero-th order solution is the trivial one, we can write $\vartheta(\bar{z}) = \varepsilon\vartheta_1(\bar{z})$. Next, we consider the expansion of the functional (1.90) up to the $\mathcal{O}\left(\varepsilon^4\right)$ term

$$\mathcal{F} = \varepsilon^2\int_{-1/2}^{1/2}\left(\vartheta_1'^2 - \lambda_0\vartheta_1^2\right)\mathrm{d}\bar{z} \;+\; \varepsilon^4\,\lambda_0\int_{-1/2}^{1/2}\left(\frac{1}{3}\vartheta_1^4 - \vartheta_1^2\right)\mathrm{d}\bar{z} \;+\; o(\varepsilon^4). \tag{1.93}$$

The $\mathcal{O}\left(\varepsilon^2\right)$ term provides an equation for $\vartheta_1(\bar{z})$: $\vartheta_1'' + \lambda_0\,\vartheta_1 = 0$. Taking into account the boundary conditions, one finds that the only non-trivial solutions are of the type $\vartheta_1(\bar{z}) = A_1\,\cos(\sqrt{\lambda_0}\,\bar{z})$, where λ_0 must satisfy the condition

$$\sin\sqrt{\lambda_0} \;=\; 0. \tag{1.94}$$

Therefore the critical value of λ is the lowest non-null solution of equation (1.94). A corresponding critical value H_{cr} for the applied magnetic field is gathered:

$$\lambda_{cr} = \pi^2, \qquad H_{cr} = \sqrt{\frac{2K}{\chi_a}}\frac{\pi}{d}. \tag{1.95}$$

The value of A_1 can be determined by using the $\mathcal{O}\left(\varepsilon^4\right)$ term in (1.90). Taking into account the expression found for $\vartheta_1(\bar{z})$ and performing the integration, the $\mathcal{O}\left(\varepsilon^4\right)$ term of the functional is

$$\varepsilon^4 \frac{\pi^2}{8} A_1^2 \left(A_1^2 - 4\right). \tag{1.96}$$

Minimization of the energy functional is then possible up to this term by means of a minimization of (1.96) with respect to A_1. Imposing the derivative of (1.96) with respect to A_1 equal to zero, it is easily obtained a third order polynomial equation in A_1 whose non-null solutions are $A_1 = \pm\sqrt{2}$. We can conclude that there are two possible opposite solution just above the critical value λ_{cr} depending on the sign of the coefficient A_1

$$\vartheta_1(\bar{z}) = \pm\sqrt{2}\cos(\pi\bar{z}). \tag{1.97}$$

They correspond to the fact that the transition can be induced by magnetic fields in both positive or negative direction of the x-axis.
The double sign is due to the fact that the liquid crystal molecules can arrange themselves into two symmetric configurations having the same total energy, one tilted in a clockwise direction and the other tilted by the same angle in a counterclockwise direction. It has to be noted that in addition to these solutions there is the trivial solution $A_1 = 0$ which corresponds to the case $\vartheta(x) \equiv 0$ that is unstable since represents a relative maximum of the free energy functional.

1.3.2 Applications in LCD technology

The most common application of liquid crystal technology is in liquid crystal displays (LCDs). From the watch or pocket calculator to an advanced VGA computer screen, this type of display has evolved into an important and versatile interface.

In general, LCDs use much less power than their cathode-ray tube (CRT) counterparts. Many LCDs are reflective, meaning that they use only ambient light to illuminate the display. Even displays that do require an external light source (i.e. computer displays) consume much less power than CRT devices.

We will restrict this discussion to traditional nematic LCDs since the major technological advances have been developed for this group of devices.

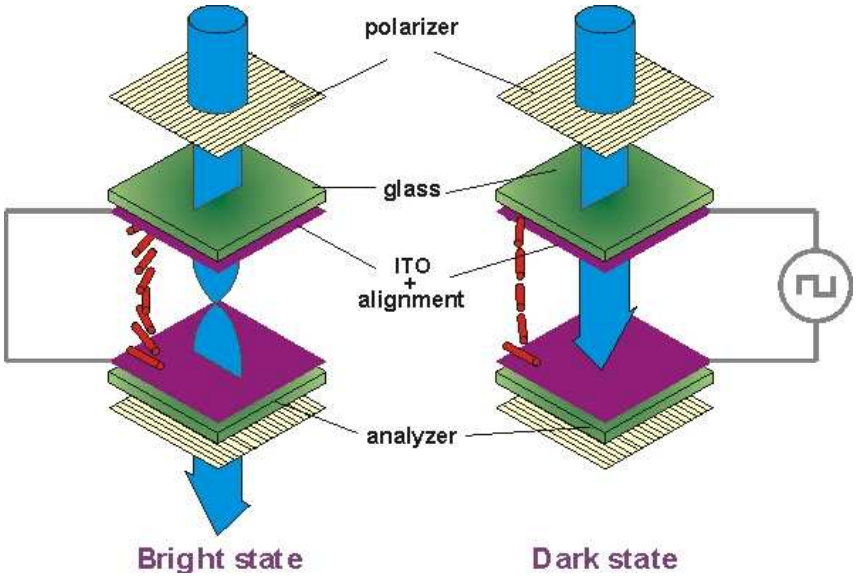

Figure 1.4: Schematic of a twist nematic cell (TNC).

A liquid crystal display consists of an array of tiny segments (called pixels) that can be manipulated independently. This basic idea is common to all displays. Each pixel is composed by a cell filled with a liquid crystal.

The most common cell used in nowadays technology is the **twist nematic** (TN) cell. It consists typically of a liquid crystal placed between two sheets of glass which are rubbed to control the alignment of the molecules. The molecules follow the alignment of the grooves: if the grooves are parallel to each other so are the liquid crystal molecules. The grooves on one sheet of glass are twisted by 90 degrees with respect to the grooves on the other sheet of glass. The boundary conditions thus impose that the molecules twist in between the sheets of glass. The optical properties of the liquid crystal are governed by the tensor $\mathbf{M} = \mathbf{Q} + \frac{1}{3}\mathbf{I}$, so that $\mathbf{M}$ has not only a microscopic meaning, but reflects the macroscopic anisotropy of the material. In particular the *Fresnel ellipsoid* [83, 23, 47], which determines the optical response of birefringent materials, is closely linked to $\mathbf{M}$.

It is then no surprise that a distorted field $\mathbf{n}$, like the one in a TN display, manipulates the polarized light entering the cell. When light enters the TN cell, the polarization state twists with the director of the liquid crystal material. Crossed polarizers are attached to the top and bottom of the display. As light enters the cell, its polarization rotates with the molecules. When the light reaches the bottom of the cell, its polarization vector has rotated by 90 degrees, and now can pass through the second polarizer.

When an electric field of sufficient magnitude (above the critical value) is applied to a sample, the molecules undergo a Freederickzs transition, typically aligning their direction to the electric field. Note that in this state, the twist is destroyed. The director of the bulk liquid crystal is parallel to the field and no longer twisted. When polarized light enters a cell in such a configuration, it is not twisted, and is canceled by the second polarizer. Regions where an electric field is applied appear dark against a bright background. By properly adjusting the level of the voltage almost any gray level of transmission can be achieved.

1.4 de Gennes' theory

When s_1 and s_2 in equation (1.16) are not constants throughout the region $\mathcal{B}$ occupied by the liquid crystal, the microstate is described by s_1, s_2 and the orthonormal frame of eigenvectors $(\mathbf{n}, \mathbf{e}_2, \mathbf{e}_3)$ which amount to give 5 scalars at each point in space. As described in §1.1.1, qualitatively the degree of orientation s measures on the macroscopic scale the degree of microscopic order; it may vary in space and ranges in the interval $\left[-\frac{1}{2}, 1\right]$. When s vanishes the molecular orientation is completely disordered: the liquid crystal becomes an isotropic fluid on the macroscopic scale. In the isotropic phase $\mathbf{n}$ has no definite meaning, since the molecules have no preferred direction. Therefore $\mathbf{n}$ is well defined only where $s \neq 0$.
If we define the **singular set** as the set of points of $\mathcal{B}$ where $s = 0$,

$$\mathscr{S} \;=\; \{p \in \mathcal{B} \;:\; s(p) = 0\}\,, \tag{1.98}$$

then $\mathbf{n}$ is allowed to have discontinuities in $\mathscr{S}$ (while $\mathbf{Q}$ is still continuous). Thus within the new theory, defects of liquid crystals are to be interpreted as transitions to the isotropic phase which happen to be confined in space. The theory that we employ in this and the following chapters has been strongly motivated by the desire of a comprehensive treatment of defects. While point defects are described fairly well within the classical theory, this is not the case for both line and plane defects: these latter need to be approximated by regular fields in order to keep Frank's energy finite.
Equilibrium states of nematics are now given by stationary points of the free-energy functional whose density, in the absence of external fields, comprises the elastic term, due to the spatial variation of $\mathbf{Q}$, and the Landau-de Gennes potential, that accounts for the thermal contribution to the energy

$$\Psi(\mathbf{Q}, \nabla\mathbf{Q}) \;=\; \Psi_{\mathrm{el}}(\mathbf{Q}, \nabla\mathbf{Q}) + \Psi_{\mathrm{LdG}}(\mathbf{Q}). \tag{1.99}$$

1.4.1 Defects

Even if we do not deal with defects in the present thesis, we want to mention them as their study has played an important role in the developing of the new theory of liquid crystals. In the classical theory we restricted our attention to distortions of the nematic arrangement that involved continuous variations of the director $\mathbf{n}$. But there are other important physical situations where $\mathbf{n}$ is not a smooth function of position at all points. We have seen, for instance, that the simple splay and bend fields, defined in §1.2.2 are discontinuous in $\rho = 0$ (see Remark 1.6).

Defects in uniaxial nematics are classically described in terms of the spatial distribution on the director. Where the mapping $\mathbf{n} : \mathcal{B} \to \mathbb{S}^2$ is singular we say that there is a defect. For three-dimensional nematics, the singular regions may be either zero-dimensional (points), one-dimensional (lines) or two-dimensional (plane). The defect is then called *topologically stable* whenever there is no continuous deformation of the director field that yields the uniform state $\mathbf{n} =$constant.

It must be noted however that even topologically unstable defects can exist in nature in the case that they are *energetically stable*. This means that they attain the minimum of the energy functional and every other admissible configuration (though possibly non-singular) have higher free energy.

To each defect can be associated a *winding number* which is a number describing the topological charge of the defect. We describe an intuitive way to calculate this number in the easy case of a line defect. Imagine to surround the line defect by a circular loop γ in $\mathcal{B}$; the only requirement is that γ does not approach the singular region too closely and the mapping $\mathbf{n} : \mathcal{B} \to \mathbb{S}^2$ restricted to γ is everywhere continuous. Since in nematics $\mathbf{n}$ and $-\mathbf{n}$ are indistinguishable, the proper order parameter space is the projective plane $\mathbb{RP}^2 = \mathbb{S}^2/\mathbb{Z}_2$ i.e. the two dimensional sphere where antipodal points are identified. Then $\mathbf{n}$ maps γ on some closed curve φ in the space $\mathbb{RP}^2$. The curve φ can be of two types: (a) a contour that starts and ends at the same point of $\mathbb{S}^2$ and (b) a contour that connects two diametrically opposite points of $\mathbb{S}^2$. Loops (a) are also loops for the sphere $\mathbb{S}^2$ itself and because $\mathbb{S}^2$ is simply connected, φ can be contracted to a single point. Since the field corresponding to a single point is the uniform field $\mathbf{n} =$constant, then the field $\mathbf{n}$ can be continuously deformed to a uniform state and the defect is not topologically stable. By contrast, loops (b) cannot be contracted: under any continuous deformations their ends must remain diametrically opposite on the sphere. Thus the corresponding line defects are topologically stable.

The winding number associated with line defects can be defined as the number of times that φ rounds on the sphere when the defect is orbited once (i.e. when moving in $\mathcal{B}$ along γ). It can be showed that this number is independent on the particular

chosen curve γ and depends only on the nature of the defect. From the discussion above, it is clear that defects (a) have a *integer* winding number, while defects (b) have *half-integer* winding number.

Analogous considerations hold for point defects, where one has to take into account the mapping of closed surfaces surrounding the defect.

The preceding arguments can be given a precise mathematical meaning in the frame of algebraic topology by using the homotopy theory (see [60, 15]) and the topological degree of a map, but due to the introductory level of this paragraph we will not purse this argument any further.

1.4.2 Landau-de Gennes' thermodynamic potential

The Landau-de Gennes potential Ψ_{LdG} in (1.99) takes into account the material tendency to spontaneously arrange in ordered or disordered states and must incorporate the effects of temperature. Following the work of Landau [56], de Gennes has proposed the following phenomenological expression for Ψ_{LdG} [32], which can be constructed independently of the detailed nature of the interactions and of molecular structure,

$$\Psi_{\mathrm{LdG}}(\mathbf{Q}) \;=\; A\,\mathrm{tr}\,\mathbf{Q}^2 - B\,\mathrm{tr}\,\mathbf{Q}^3 + C\,\mathrm{tr}\,\mathbf{Q}^4. \tag{1.100}$$

The equation (1.100) has been found considering an expansions in powers of $\mathbf{Q}$ up to the fourth order and retaining only those terms that are invariants by rotations (i.e. frame indifference condition). The first order term is absent since $\mathrm{tr}\,\mathbf{Q} = 0$. We have no *a priori* knowledge of the coefficients, but in agreement with molecular theories it is usually assumed that $A = a(T - T^*)$ and a,B and C are *positive* material constants essentially independent of temperature. Coefficients are chosen such that the minimizer of Ψ_{LdG} alone is a *uniaxial* order tensor. T is the temperature and T^* is the nematic *supercooling temperature*. For $T > T^*$ the potential Ψ_{LdG} attains a local minimum at the isotropic phase, whereas for $T < T^*$ this local minimum ceases to exist and only the nematic phase is possible. The parameter B is usually much smaller that both $|A|$ and C.

Remark 1.10. It is often found in literature, the expression

$$\Psi_{\mathrm{LdG}}(\mathbf{Q}) \;=\; a(T - T^*)\,\mathrm{tr}\,\mathbf{Q}^2 - b\,\mathrm{tr}\,\mathbf{Q}^3 + c\left(\mathrm{tr}\,\mathbf{Q}^2\right)^2. \tag{1.101}$$

which we show to be equivalent to our expression (1.100).
Let's denote with μ_1,μ_2 and μ_3 the eigenvalues of $\mathbf{Q}$. By virtue of the Cayley-Hamilton

theorem, there are only three independent invariants of $\mathbf{Q}$:

$$\operatorname{tr}\mathbf{Q} = \mu_1 + \mu_2 + \mu_3 \tag{1.102}$$

$$\mathrm{II}_{\mathbf{Q}} = \mu_1\mu_2 + \mu_2\mu_3 + \mu_3\mu_1 \tag{1.103}$$

$$\det\mathbf{Q} = \mu_1\mu_2\mu_3. \tag{1.104}$$

Then we must have that exist coefficients for which the following relations hold

$$\operatorname{tr}\mathbf{Q}^2 = A_1\left(\operatorname{tr}\mathbf{Q}\right)^2 + B_1\mathrm{II}_{\mathbf{Q}} \tag{1.105}$$

$$\operatorname{tr}\mathbf{Q}^3 = A_2\left(\operatorname{tr}\mathbf{Q}\right)^3 + B_2\operatorname{tr}\mathbf{Q}\,\mathrm{II}_{\mathbf{Q}} + C_2\det\mathbf{Q} \tag{1.106}$$

$$\operatorname{tr}\mathbf{Q}^4 = A_3\left(\operatorname{tr}\mathbf{Q}\right)^4 + B_3\left(\operatorname{tr}\mathbf{Q}\right)^2\mathrm{II}_{\mathbf{Q}} + C_3\operatorname{tr}\mathbf{Q}\,\det\mathbf{Q} + D_3\left(\mathrm{II}_{\mathbf{Q}}\right)^2. \tag{1.107}$$

Since in our case $\operatorname{tr}\mathbf{Q} = 0$, the first and third of the above expressions yields

$$\operatorname{tr}\mathbf{Q}^4 = \alpha\left(\operatorname{tr}\mathbf{Q}^2\right)^2, \tag{1.108}$$

performing an explicit calculation gives $\alpha = \frac{1}{2}$.

Let us study the explicit form of (1.100) in the uniaxial case, where $\mathbf{Q}$ can be represented by

$$\mathbf{Q} = s\left(\mathbf{n}\otimes\mathbf{n} - \frac{1}{3}\mathbf{I}\right). \tag{1.109}$$

The potential (1.100) is

$$\Psi_{\mathrm{LdG}}(s) = \frac{2}{9}\left(Cs^4 - Bs^3 + 3As^2\right), \tag{1.110}$$

whose stationary points are $\left(\Delta = 9B^2 - 96AC\right)$

$$s = 0, \qquad s = s_\pm = \frac{3B \pm \sqrt{\Delta}}{8C}. \tag{1.111}$$

The following cases can happen

- ⋆ $A < 0$ (i.e. $T < T^*$): only the liquid crystal phase is possible. Note that when T is well below T^* the liquid freezes and the liquid crystal phase ceases to exist: our description is no longer valid. $s_+ > 0$ is the absolute minimum for Ψ_{LdG} and it represents the *preferred degree of orientation* s_{pr}.
- ⋆ $A = 0$ (i.e. $T = T^*$): $s = 0$ is an inflection point and the absolute minimum is still $s_{\mathrm{pr}} = s_+$. T^* is the *supercooling temperature*.
- ⋆ $0 < A < \frac{B^2}{12C}$ $\left(\text{i.e. } T^* < T < T^* + \frac{B^2}{12aC} = T_{NI}\right)$: Ψ_{LdG} possesses two minima: one at $s = 0$ and the other at $s = s_+$. The latter is still the absolute ($s_{\mathrm{pr}} = s_+$), so that the liquid crystal phase is **stable**, while the isotropic phase is **metastable**.

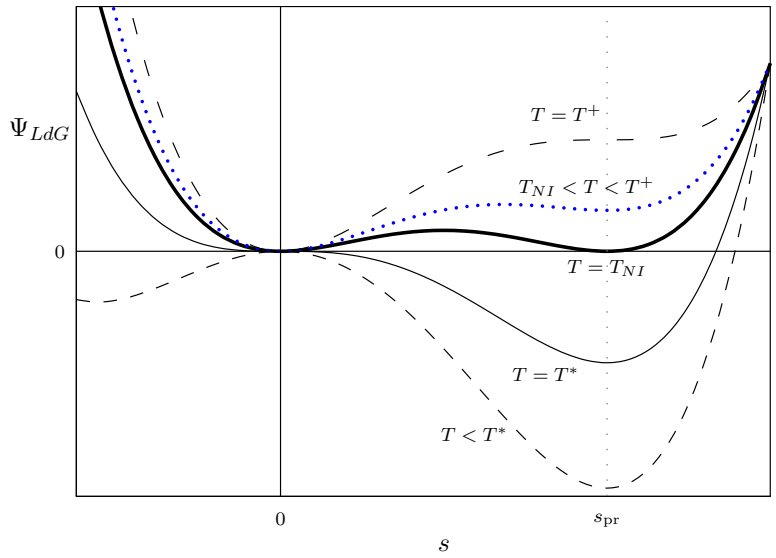

Figure 1.5: Landau-de Gennes potential as function of the temperature T.

- ⋆ $A = \frac{B^2}{12C}$ $\left(\text{i.e. } T = T^* + \frac{B^2}{12aC} = T_{NI}\right)$: the two minima at $s = 0$ and $s = s_+$ have the same value. This temperature marks the transition to the isotropic phase.
- ⋆ $\frac{B^2}{12C} < A < \frac{3B^2}{32C}$ $\left(\text{i.e. } T_{NI} < T < T^* + \frac{3B^2}{32aC} = T^+\right)$: the phase with $s = s_+$ becomes metastable, while the isotropic phase is stable.
- ⋆ $A = \frac{3B^2}{32C}$ $\left(\text{i.e. } T = T^* + \frac{3B^2}{32aC} = T^+\right)$: $\Psi_{\rm LdG}$ possesses the absolute minimum in $s = 0$ and an inflection point in $s = s_+$: the nematic phase ceases to exist. T^+ is the *superheating temperature*.
- ⋆ $A > \frac{3B^2}{32C}$ (i.e. $T > T^+$): the phase is isotropic.

When the tensor order parameter $\mathbf{Q}$ is biaxial and therefore expressed as in (1.16), the Landau-de Gennes potential (1.100) is

$$\Psi_{\rm LdG}(s_1, s_2) = \frac{2}{9}\left(Cs_1^4 - Bs_1^3 + 3As_1^2\right) + \frac{2}{9}\left(6Cs_1^2 + 9Bs_1 + 9A\right)s_2^2 + 2Cs_2^4\,. \tag{1.112}$$

The study of critical points of (1.112) shows that the only admissible solutions, where s_1 and s_2 have physical meanings, are $s_1 = 0, s_+$ as in (1.111) and $s_2 = 0$. Therefore, the ground state of the liquid crystal can be either isotropic or uniaxial, depending on temperature [12]. Even if biaxiality is never preferred, biaxial domains do exist and have been observed, as it will be discussed in Chapter 3.

1.4.3 Elastic energy

We now concentrate on the elastic free energy density term $\Psi_{\rm el}$ in (1.99). The potential $\Psi_{\rm el}$ accounts of the deformation of the liquid crystal and it is minimum whenever the molecular distribution is uniform.
The idea is to expand the energy density in terms of $\mathbf{Q}$ and $\nabla\mathbf{Q}$, as it has been done with the Frank's elastic energy (1.33). Physical reasoning imposes that $\Psi_{\rm el}$ be frame-indifferent, i.e. invariant under rigid rotations, therefore all the terms of the expansion must be scalar functions of $\mathbf{Q}$ and $\nabla\mathbf{Q}$, built by contraction of indexes. Note however that due to the constraints $\mathbf{Q} = \mathbf{Q}^T$ and $\operatorname{tr}\mathbf{Q} = 0$, not all possible contractions are independent; identifying a maximum set of independent invariants is indeed a non-trivial task.

Assuming that $\Psi_{\rm el}$ is quadratic in $\nabla\mathbf{Q}$ and at most quadratic in $\mathbf{Q}$, it is shown in [57] that $\Psi_{\rm el}$ can be expressed as

$$\Psi_{\rm el}(\mathbf{Q},\nabla\mathbf{Q}) \;=\; \Psi_2(\nabla\mathbf{Q}) + \Psi_3(\mathbf{Q},\nabla\mathbf{Q}) + \Psi_4(\mathbf{Q},\nabla\mathbf{Q}), \tag{1.113}$$

where Ψ_3 is linear in $\mathbf{Q}$ and Ψ_4 is quadratic in $\mathbf{Q}$.
The function Ψ_2 is usually written [36] as

$$\Psi_2(\nabla\mathbf{Q}) \;=\; \frac{1}{2}L_1|\nabla\mathbf{Q}|^2 + L_2\,(\operatorname{div}\mathbf{Q})^2 + L_3\sum_{i\,j\,k}\mathrm{Q}_{ij,k}\mathrm{Q}_{ik,j}, \tag{1.114}$$

where a comma denotes differentiation with respect to a fixed orthonormal frame. In its original paper [31], de Gennes proposed an expression analogous to Ψ_2 as the whole elastic energy density. Assuming $\Psi_{\rm el} = \Psi_2$ gives simple expressions for the Frank's elastic constants K_i, but it is not able to distinguish between K_1 and K_3 in what it gives

$$K_1 \;=\; K_3 \;=\; 2s_{\rm pr}^2\,(L_1 + L_2 + L_3)\,, \qquad K_2 \;=\; 2s_{\rm pr}^2 L_1 \tag{1.115}$$

where $s_{\rm pr}$ represents the degree of orientation preferred in the bulk, imposed by the minimum of $\Psi_{\rm LdG}$. The temperature dependence of K_i is retrieved by the temperature dependence of $s_{\rm pr}$. This result is unphysical as $K_1 = K_3$ is contradicted by experiments, therefore one needs to consider also the higher order elastic terms Ψ_3 and Ψ_4.
It can be shown that Ψ_3 has 6 additional independent invariants, while Ψ_4 has 13. To simplify our discussion, we will follow the approach found in [20]. The whole $\Psi_{\rm el}$ involving 22 invariants is nearly intractable, so we decide to retain only those terms able to separate K_1 and K_3. Table 4 of [57] collects all contributions to Frank's constants to both Ψ_3 and Ψ_4. Among all the terms, only 9 contribute differently to K_1 than to K_3. To take into account the least possible number of terms, we consider

only those 4 elements that contribute more to K_1 than to K_3 and disregard all the others. Moreover, we assign one and the same value Λ to the four material constants of these terms.

Finally, we have

$$\Psi_3(\mathbf{Q},\nabla\mathbf{Q}) = \frac{\Lambda}{s_{\rm pr}}\Big(\mathbf{Q}\cdot(\operatorname{div}\mathbf{Q}\otimes\operatorname{div}\mathbf{Q}) + \sum_{i\,j\,k\,l} \mathrm{Q}_{ij}\mathrm{Q}_{ik,l}\mathrm{Q}_{jl,k}\Big), \tag{1.116}$$

$$\Psi_4(\mathbf{Q},\nabla\mathbf{Q}) = \frac{\Lambda}{s_{\rm pr}^2}\Big(\mathbf{Q}^2\cdot(\operatorname{div}\mathbf{Q}\otimes\operatorname{div}\mathbf{Q}) + \sum_{i\,j\,k\,l\,m} \mathrm{Q}_{im}\mathrm{Q}_{mj}\mathrm{Q}_{ik,l}\mathrm{Q}_{jl,k}\Big). \tag{1.117}$$

The compatibility with Frank's theory in the case $s = s_{\rm pr} = $constant and $\beta = 0$ thus yields the expressions for the elastic constants K_i

$$K_1 = 2s_{\rm pr}^2\left(L_1 + L_2 + L_3 + \frac{20}{9}\Lambda\right) \tag{1.118}$$

$$K_2 = 2s_{\rm pr}^2 L_1 \tag{1.119}$$

$$K_3 = 2s_{\rm pr}^2\left(L_1 + L_2 + L_3 - \frac{4}{9}\Lambda\right) \tag{1.120}$$

whence it follows that $(K_1 - K_3) = \frac{16}{3}s_{\rm pr}^2\Lambda$.

The **one constant approximation** now amounts to assuming

$$L_1 = L\,, \qquad L_2 = L_3 = 0\,, \qquad \Lambda = 0, \tag{1.121}$$

so that the elastic energy density reads

$$\Psi_{\rm el}(\mathbf{Q},\nabla\mathbf{Q}) = \frac{1}{2}L|\nabla\mathbf{Q}|^2, \tag{1.122}$$

where L is an elastic constant which does not depend on temperature.

In the case of uniaxial phase, the order parameter is of the form (1.14) and explicitly equation (1.122) is

$$\Psi_{\rm el}(s,\nabla s,\nabla\mathbf{n}) = L\left(\frac{1}{3}|\nabla s|^2 + s^2|\nabla\mathbf{n}|^2\right). \tag{1.123}$$

Proof of eqn. (1.123). The easiest way to perform this calculation makes use of the coordinate expression of $|\nabla\mathbf{Q}|^2$. Given a fixed orthonormal frame $\mathbf{e}_i$ $(i = 1,2,3)$, the components of $\mathbf{Q}$ are

$$\mathrm{Q}_{ij} = s\left(\mathrm{n}_i\mathrm{n}_j - \frac{1}{3}\delta_{ij}\right), \tag{1.124}$$

where δ_{ij} is the Kronecker delta. We remind that $\mathbf{n}\cdot\mathbf{n} = 1$ and $(\nabla\mathbf{n})^T\,\mathbf{n} = \mathbf{0}$ so that the following relations hold

$$\sum_i \mathrm{n}_i^2 = 1 \quad \text{and} \quad \sum_i \mathrm{n}_{i,k}\mathrm{n}_i = 0 \quad (k = 1,2,3). \tag{1.125}$$

Using a comma to denote the partial differentiation, we have

$$\begin{aligned}|\nabla\mathbf{Q}|^2 &= \sum_{ijk} \mathrm{Q}_{ij,k}^2 = \sum_{ijk}\left(s_{,k}\mathrm{n}_i\mathrm{n}_j - \frac{1}{3}s_{,k}\delta_{ij} + s\,\mathrm{n}_{i,k}\mathrm{n}_j + s\,\mathrm{n}_i\mathrm{n}_{j,k}\right)^2 \\ &= \sum_{ijk}\left(s_{,k}^2\mathrm{n}_i^2\mathrm{n}_j^2 + \frac{1}{9}s_{,k}^2\delta_{ij} + s^2\mathrm{n}_{i,k}^2\mathrm{n}_j^2 + s^2\mathrm{n}_{j,k}^2\mathrm{n}_i^2 - \frac{2}{3}s_{,k}^2\mathrm{n}_i\mathrm{n}_j\delta_{ij}\right) \\ &= \frac{2}{3}|\nabla s|^2 + 2s^2|\nabla\mathbf{n}|^2. \end{aligned} \tag{1.126}$$

□

1.4.4 Equilibrium equations

$\mathbf{Q}$ is a map from $\mathcal{B}$ to the manifold $\mathcal{M} \subseteq \mathscr{L}\left(\mathbb{R}^3\right)$ of the null-trace symmetric tensors,

$$\mathcal{M} = \left\{A \in \mathscr{L}\left(\mathbb{R}^3\right) : A = A^T,\, \mathrm{tr}(A) = 0\right\}. \tag{1.127}$$

It is easy to show that $\mathcal{M}$ is indeed a 5-dimensional manifold and that the tangent space is at every point isomorphic to $\mathcal{M}$: $\mathrm{T}_{\mathbf{Q}}\mathcal{M} \cong \mathcal{M}$, $\forall\ \mathbf{Q}$, so that in any point $\mathbf{Q} \in \mathcal{M}$ the projection operator $\mathbf{P}_{\mathbf{Q}} : \mathscr{L}\left(\mathbb{R}^3\right) \to \mathrm{T}_{\mathbf{Q}}\mathcal{M}$ onto the tangent space is simply, $\mathbf{A} \in \mathscr{L}\left(\mathbb{R}^3\right)$

$$\mathbf{P}_{\mathbf{Q}}\,\mathbf{A} = \frac{1}{2}(\mathbf{A} + \mathbf{A}^T) - \frac{1}{3}\,\mathrm{tr}(\mathbf{A})\mathbf{I}. \tag{1.128}$$

We want to write the general equilibrium equations for the energy functional

$$\mathcal{F}[\mathbf{Q}, \nabla\mathbf{Q}] = \int_{\mathcal{B}} \Psi(\mathbf{Q}, \nabla\mathbf{Q})\,\mathrm{d}v \tag{1.129}$$

where $\mathbf{Q}$ is constrained to lie in $\mathcal{M}$.

Let us perform a variation $\mathbf{Q} + \varepsilon\mathbf{U}$ of the functional where at the moment $\mathbf{U}$ is assumed to be an arbitrary tensor [4]. We will introduce afterward the fact that $\mathbf{U}$ cannot be completely arbitrary and is indeed an element of $\mathrm{T}_{\mathbf{Q}}\mathcal{M}$ (and therefore must be symmetric and zero trace). The differential is:

$$\begin{aligned}\mathrm{d}_{[\mathbf{Q},\nabla\mathbf{Q}]}\mathcal{F}(\mathbf{U}, \nabla\mathbf{U}) &= \frac{\partial}{\partial\varepsilon}\int_{\mathcal{B}} \Psi(\mathbf{Q} + \varepsilon\mathbf{U}, \nabla\mathbf{Q} + \varepsilon\nabla\mathbf{U})\,\mathrm{d}v\Big|_{\varepsilon=0} \\ &= \int_{\mathcal{B}}\left(\frac{\partial\Psi}{\partial\mathbf{Q}}\cdot\mathbf{U} + \frac{\partial\Psi}{\partial\nabla\mathbf{Q}}\cdot\nabla\mathbf{U}\right)\mathrm{d}v \\ &= \int_{\mathcal{B}}\left(\frac{\partial\Psi}{\partial\mathbf{Q}} - \mathrm{div}\,\frac{\partial\Psi}{\partial\nabla\mathbf{Q}}\right)\cdot\mathbf{U}\,\mathrm{d}v + \int_{\partial\mathcal{B}}\mathbf{b}\cdot\boldsymbol{\nu}\,\mathrm{d}a. \end{aligned} \tag{1.130}$$

[4] To be more precise, we assume that the functional $\mathcal{F}$ admits an extension $\widehat{\mathcal{F}}$ to the ambient space $\mathscr{L}\left(\mathbb{R}^3\right)$ where $\mathcal{M}$ is embedded. The differential (1.130) is meaningful in this space.

where $\mathbf{b}$ is a vector defined, for every constant vector $\mathbf{a}$, by

$$\mathbf{b}\cdot\mathbf{a} = \frac{\partial\Psi}{\partial\nabla\mathbf{Q}}\cdot(\mathbf{U}\otimes\mathbf{a}). \tag{1.131}$$

Remark 1.11. In the above derivation we have implicitly used the representation theorem, in much the same way as it was done in the proof of Lemma 1.7. All the inner products have been denoted by a dot product (as usual in mechanics) even if they actually refer to different spaces. Under this perspective, the expressions above are better understood when expressed by components in an orthonormal fixed frame. In fact, in such a way, all the inner products are simply replaced by a full saturation of indexes.

$$\left(\operatorname{div}\frac{\partial\Psi}{\partial\nabla\mathbf{Q}}\right)_{ij} = \sum_k\left(\frac{\partial\Psi}{\partial \mathrm{Q}_{ij,k}}\right)_{,k}, \qquad \frac{\partial\Psi}{\partial\nabla\mathbf{Q}}\cdot\nabla\mathbf{U} = \sum_{ijk}\frac{\partial\Psi}{\partial \mathrm{Q}_{ij,k}}\mathrm{U}_{ij,k} \tag{1.132}$$

$$\mathrm{b}_k = \frac{\partial\Psi}{\partial\nabla \mathrm{Q}_{ij,k}}\,\mathrm{U}_{ij} \tag{1.133}$$

In deriving expression (1.130) we have used

$$\left(\frac{\partial\Psi}{\partial \mathrm{Q}_{ij,k}}\mathrm{U}_{ij}\right)_{,k} = \left(\frac{\partial\Psi}{\partial \mathrm{Q}_{ij,k}}\right)_{,k}\mathrm{U}_{ij} + \frac{\partial\Psi}{\partial \mathrm{Q}_{ij,k}}\mathrm{U}_{ij,k}. \tag{1.134}$$

For simplicity, we assume Dirichlet conditions at the boundary, so that we can disregard the surface term in (1.130).
We can now introduce the constraint that $\mathbf{U}$ must belong to the tangent space $\mathrm{T}_{\mathbf{Q}}\mathbf{M}$ and write an arbitrary variation $\mathbf{U}=\mathbf{P}_{\mathbf{Q}}\widehat{\mathbf{U}}$ for a suitable tensor $\widehat{\mathbf{U}}\in\mathscr{L}\left(\mathbb{R}^3\right)$. The first variation of the functional becomes

$$\mathrm{d}_{[\mathbf{Q},\nabla\mathbf{Q}]}\mathcal{F}(\mathbf{U},\nabla\mathbf{U}) = \int_{\mathcal{B}}\mathbf{P}_{\mathbf{Q}}\left(\frac{\partial\Psi}{\partial\mathbf{Q}} - \operatorname{div}\frac{\partial\Psi}{\partial\nabla\mathbf{Q}}\right)\cdot\widehat{\mathbf{U}}\,\mathrm{d}v. \tag{1.135}$$

Therefore, by the arbitrariness of $\widehat{\mathbf{U}}$, we obtain the equilibrium equations

$$\mathbf{P}_{\mathbf{Q}}\left(\frac{\partial\Psi}{\partial\mathbf{Q}} - \operatorname{div}\frac{\partial\Psi}{\partial\nabla\mathbf{Q}}\right) = \mathbf{0}. \tag{1.136}$$

As example, we write equation (1.136) explicitly for the one constant approximation [22]. Assume then that the free energy density is

$$\Psi = \frac{1}{2}L|\nabla\mathbf{Q}|^2 + A\,\mathrm{tr}\,\mathbf{Q}^2 - B\,\mathrm{tr}\,\mathbf{Q}^3 + C\left(\mathrm{tr}\,\mathbf{Q}^2\right)^2, \tag{1.137}$$

where we have used the Landau-de Gennes' potential in the form given in Remark

1.10, because in the present case allows easier computations.

$$\frac{\partial \Psi}{\partial \mathbf{Q}} = 2A\mathbf{Q} - 3B\mathbf{Q}^2 + 4C\,\mathrm{tr}(\mathbf{Q}^2)\mathbf{Q} \tag{1.138}$$

$$\mathbf{P}_{\mathbf{Q}}\frac{\partial \Psi}{\partial \mathbf{Q}} = 2A\mathbf{Q} - 3B\mathbf{Q}^2 + 4C\,\mathrm{tr}(\mathbf{Q}^2)\mathbf{Q} + B\,\mathrm{tr}(\mathbf{Q}^2)\mathbf{I} \tag{1.139}$$

$$\mathrm{div}\,\frac{\partial \Psi}{\partial \nabla \mathbf{Q}} = L\,\mathrm{div}\,\nabla \mathbf{Q} = L\Delta \mathbf{Q} \tag{1.140}$$

$$\mathbf{P}_{\mathbf{Q}}\,\mathrm{div}\,\frac{\partial \Psi}{\partial \nabla \mathbf{Q}} = L\Delta \mathbf{Q}. \tag{1.141}$$

Therefore, the equilibrium equations are

$$-L\Delta \mathbf{Q} + 2A\mathbf{Q} - 3B\mathbf{Q}^2 + 4C\,\mathrm{tr}(\mathbf{Q}^2)\mathbf{Q} + B\,\mathrm{tr}(\mathbf{Q}^2)\mathbf{I} = \mathbf{0}. \tag{1.142}$$

1.4.5 Existence and regularity of minimizers

We want to mention two mathematical results regarding the minimization of the functional (1.123) that will be useful in the next chapter. For details, see [2, 3, 4, 41, 83]. Assuming Dirichlet conditions at the smooth boundary $\partial\mathcal{B}$, we assign the following fields on $\partial\mathcal{B}$ that we may suppose continuous for our purposes

$$s_0 : \partial\mathcal{B} \to I = \left[-\frac{1}{2}, 1\right], \qquad \mathbf{n}_0 : \partial\mathcal{B}\backslash\mathscr{S}(s_0) \to \mathbb{S}^2. \tag{1.143}$$

Note that $\mathbf{n}_0$ is defined only in those points of $\partial\mathcal{B}$ where $s_0 \neq 0$.
The functional we want to minimize is

$$\int_{\mathcal{B}} \left(\frac{1}{3}L|\nabla s|^2 + L\,s^2|\nabla \mathbf{n}|^2 + f(s)\right) \mathrm{d}v, \tag{1.144}$$

where $f(s)$ is a continuous function of $I = [-\frac{1}{2}, 1]$ into $\mathbb{R}$ and plays the role of the Landau-de Gennes potential (1.110).
We define the admissible pairs $(s, \mathbf{n})$ for our functional as follows

$$\mathscr{A}(s_0, \mathbf{n}_0) = \{(s, \mathbf{n}) : \mathcal{B} \to I \times \mathbb{S}^2 \,:\, s \in \mathrm{H}^1(\mathcal{B}, I),\, s\mathbf{n} \in \mathrm{H}^1(\mathcal{B}, \mathbb{R}^3),\ s_0 \text{ and } \mathbf{n}_0 \text{ are the traces of s and } \mathbf{n} \text{ on } \partial\mathcal{B}\}.$$

Then, the following existence theorem holds

Theorem 1.12. Given s_0, $\mathbf{n}_0$ and $f(s)$ as stated above, the problem

$$\min\left\{\int_{\mathcal{B}} \left(\frac{1}{3}L|\nabla s|^2 + L\,s^2|\nabla \mathbf{n}|^2 + f(s)\right) \mathrm{d}v \,:\, (s, \mathbf{n}) \in \mathscr{A}(s_0, \mathbf{n}_0)\right\} \tag{1.145}$$

has at least one solution.

With a slight heavier assumption on f, the following theorem dealing with the regularity of the minimizers can be proved

Theorem 1.13. Let f be of class C^2. If $(\hat{s}, \widehat{\mathbf{n}}) \in \mathscr{A}(s_0, \mathbf{n}_0)$ is a pair that minimize (1.144), then both $\hat{s}$ and $\widehat{\mathbf{u}} = \hat{s}\,\widehat{\mathbf{n}}$ are Lipschitz continuous in any compact subset $\mathscr{K} \subseteq \mathcal{B}$.

2

Boundary-roughness effects

As already discussed in Chapter 1, nematic liquid crystals are fluid aggregates of elongated molecules. When the nematic rods interact with an external surface, the elastic strain energy induces them to align parallel to the unit normal, even if the surface is not perfectly flat [11]. Recent experimental observations confirm that the surface alignment of the nematic director is completely determined by the roughness-induced surface anisotropy [54]. Further analytical calculations, performed within the classical Frank model with unequal elastic constants, have detected the bulk effects induced by a periodically moulded external boundary [9, 34].

A crucial effect, still related to surface roughness, escapes the framework of Frank theory, where the only order parameter is the director. Indeed, it is physically intuitive that nematic molecules will disorder if we force them to follow a rapidly varying boundary condition. This *surface melting* was first experimentally detected in [40, 6]. Recent experimental observations have also measured a boundary-layer structure in the degree of orientation [84]. The surface melting has been confirmed by approximated analytical solutions [7], numerical calculations [76, 61], and molecular Monte Carlo simulations [27].

The combined effect of a rapidly varying director anchoring and surface melting gives rise to an effective weak-anchoring effect that was first observed in [73]. The problem of relating the effective anchoring extrapolation length to the microscopic roughness parameters has been studied in several theoretical papers, all framed within the Frank theory [37, 38, 1, 42]. This observation is of basic significance, since weak anchoring potentials have proven to influence deeply all nematic phenomena, beginning with Freedericksz transitions [81, 83, 63]. Indeed, several theoretical studies have already determined the influence on anchoring energies of the presence of permanent surface dipoles [67] or diluted surface potentials [78, 79].

In this Chapter we analyze in analytical detail the boundary-layer structure induced by a rough surface which bounds a nematic liquid crystal. We set ourselves within the Landau-de Gennes order-tensor theory, to be able to detect the effects on both the director and the degree of orientation. Our results confirm the surface melting already obtained in [7] but allow us to detect new phenomena. First, the nematic

director steepens close to the boundary, so giving rise to an effective weak anchoring potential, which turns out to be deeply related to the surface-melting effect, and thus can be correctly handled only within the order-tensor theory. Furthermore, the boundary layers display a strong dependence on the type of boundary conditions imposed on the degree of orientation. Indeed, the orders of magnitude of all the expected effects depend on whether the boundary conditions are Neumann- or Dirichlet-like. We discuss how these effects may help in ascertaining in experiments how the mesoscopic parameter, which measures the degree of order, interacts with an external surface.

The Chapter is organized as follows. In §2.1 we present the model, we set the geometry of a roughly bounded sample, and derive the Euler-Lagrange partial differential equations that determine the equilibrium configurations. In §2.2 we perform the perturbative two-scale analysis that provides all the analytical details of the boundary-layer structure. In §2.3 we solve an effective problem, in which the rough surface is replaced by a weak-anchoring potential. As a result, we show that a weak-anchoring potential may be given a microscopic interpretation, and we relate the surface extrapolation length to the microscopic roughness parameters. In §2.4 and §2.5 we briefly extend the study to the case of strong roughness and discuss the accuracy of the approximations we have done in modeling the boundary. In §2.6 we draw our conclusions and discuss the validity of our geometric approximations.

2.1 Equilibrium configurations

The degree of order decrease has been recognized by many authors as a crucial effect of surface roughness [7, 61]. We thus describe nematic configurations in the framework of the Landau-de Gennes $\mathbf{Q}$-tensor theory (see Chapter 1).

In order to keep computations simple, we adopt the one-constant approximation for the elastic part of the free-energy functional. We stress, however, that it is straightforward to generalize all what follows to take into account unequal material elastic constants.

The free-energy functional will be (see Chapter 1)

$$\Psi(\mathbf{Q}, \nabla\mathbf{Q}) = \frac{1}{2}L|\nabla\mathbf{Q}|^2 + A\,\mathrm{tr}\,\mathbf{Q}^2 - B\,\mathrm{tr}\,\mathbf{Q}^3 + C\,\mathrm{tr}\,\mathbf{Q}^4\,. \tag{2.1}$$

The potential (2.1) strongly favors uniaxial phases, in which at least two of the three eigenvalues of $\mathbf{Q}$ coincide. In fact, $\mathbf{Q}$ is expected to abandon uniaxiality mainly close to director singularities [74, 16, 18]. We will not deal with any defect structure. Thus, though the uniaxiality constraint is not essential for our purposes, we follow the attitude of avoiding unnecessary complications and restrict our attention to

uniaxial states

$$\mathbf{Q}(\mathbf{r}) = s(\mathbf{r}) \left(\mathbf{n}(\mathbf{r}) \otimes \mathbf{n}(\mathbf{r}) - \frac{1}{3} \mathbf{I} \right) . \tag{2.2}$$

We stress that we are not claiming that biaxiality effects are absent close to an external surface, since indeed the converse holds [14, 15, 17]. However, our results show that, even in the absence of biaxiality, a surface melting exists and an effective weak anchoring arises. A detailed treatment of the complete order-tensor theory would yield more precise quantitative estimates of the effects we will determine anyhow.

The scalar $s \in \left[-\frac{1}{2}, 1\right]$ and the unit vector $\mathbf{n}$ in (2.2) are, respectively, the *degree of orientation* and the *director*. With the aid of (2.2), the potential (2.1) can be written as

$$f_{\rm el}[s, \mathbf{n}] = L \left(s^2 |\nabla \mathbf{n}|^2 + \tfrac{1}{3} |\nabla s|^2 \right) \quad \text{and} \quad f_{\rm LdG}(s) = \tfrac{2}{3} A\, s^2 - \tfrac{2}{9} B\, s^3 + \tfrac{2}{9} C\, s^4 . \tag{2.3}$$

When $A \leq B^2/(12C)$, the absolute minimum of the function $f_{\rm LdG}(s)$ occurs at the *preferred degree of orientation*

$$s_{\rm pr} := \frac{3B + \sqrt{9B^2 - 96AC}}{8C} > 0 . \tag{2.4}$$

In order to gain physical interpretation of the results, we also introduce the *nematic coherence length* ξ and the dimensionless (positive) parameter ω, defined as

$$\xi^2 := \frac{9L}{C} \qquad \text{and} \qquad \omega^2 := \frac{6}{C} \left(s_{\rm pr} B - 4A \right) . \tag{2.5}$$

The nematic coherence length compares the strength of the elastic and thermodynamic contributions to the free-energy functional. It characterizes the size of the domains where the degree of orientation may abandon its preferred value $s_{\rm pr}$. The number ω depends on the depth of the potential well associated with $s_{\rm pr}$. Indeed, it is defined in such a way that $f''_{\rm LdG}(s_{\rm pr}) = L\omega^2/\xi^2$.

By using (2.4),(2.5) we write the bulk free-energy density $f_{\rm b} := f_{\rm el} + f_{\rm LdG}$ as

$$\frac{f_{\rm b}[s, \mathbf{n}]}{L} = s^2 |\nabla \mathbf{n}|^2 + \frac{1}{3} |\nabla s|^2 + \frac{1}{2\xi^2} \left(s^4 - \frac{4}{3} s^3 \left(2 s_{\rm pr} - \frac{\omega^2}{s_{\rm pr}} \right) + 2 s^2 (s_{\rm pr}^2 - \omega^2) \right) . \tag{2.6}$$

2.1.1 Modeling a rough surface

We aim at analyzing the effects that a rough boundary induces in a nematic liquid crystal. Once again, we try to keep our analysis as simple as possible, while still catching the essential features. We thus follow, *e.g.*, [37] in modeling roughness

by imposing a sinusoidally perturbed homeotropic anchoring condition on a flat surface (see Figure 2.1.1). The amplitude and the wavelength characterizing the perturbation will be the crucial parameters in our results.

There are two nontrivial simplifications in our geometric setting. First, we are assuming that the boundary is perfectly sinusoidal, while a physical surface will clearly exhibit a whole roughness spectrum. Second, we are replacing an undulating boundary by an undulating boundary condition on a flat surface. We postpone until Section §2.5 a more detailed discussion on the validity of these simplifying assumptions. We anticipate, however, that none of them introduces qualitative errors. More precisely, the latter amounts to performing an expansion in the roughness amplitude and keeping the leading order in the expansion. As for the treatment of the whole roughness spectrum, it turns out that at the same order of approximation one is allowed to treat a single wavelength at a time and eventually add up all the contributions.

We focus attention on a thin boundary layer, attached to the external surface. Consequently, we disregard the detailed structure of the bulk equilibrium configuration, which will enter our results only as asymptotic *outer* solution for the surface boundary layer. We introduce a Cartesian frame of reference $\{\mathbf{e}_x, \mathbf{e}_y, \mathbf{e}_z\}$ and assume that the nematic spreads in the whole half-space $\mathcal{B} = \{z \geq 0\}$. We further simplify the geometry by assuming that $\mathbf{n}(\mathbf{r}) = \sin\theta(\mathbf{r})\,\mathbf{e}_x + \cos\theta(\mathbf{r})\,\mathbf{e}_z$ and that the asymptotic bulk configuration depends only on z:

$$\theta(\mathbf{r}) \approx \theta_{\rm b}(z) \qquad \text{as} \quad z \to +\infty\,. \tag{2.7}$$

A crucial role in the developments below is played by $\mathrm{m} := \theta_{\rm b}'(0)$, the derivative of the asymptotic solution at $z = 0$, which has the physical dimensions of an inverse length. It represents the effect of any tilted bulk field that competes with the surface anchoring and may well be an electric or magnetic coherence length. Throughout our calculations we will assume that m^{-1} is much greater than both the nematic coherence length and the roughness wavelength. In the presence of an external field so strong that m^{-1} becomes of the order of, or even smaller than, the microscopic lengths above, the following asymptotic expansions fail. In particular, in this extreme regime the surface roughness effects may invade the whole bulk and cannot be replaced by an effective weak-anchoring potential.

In the presence of strong homeotropic anchoring on a flat surface, the boundary condition to be imposed on the director would be $\theta^{(\rm flat)}(x, y, 0) = 0$. On the contrary, we will require

$$\theta(x, y, 0) = \Delta \cos\frac{x}{\eta}\,. \tag{2.8}$$

The boundary condition (2.8) mimics the coarseness of the external surface by introducing two new parameters: the (dimensionless) roughness amplitude Δ and the

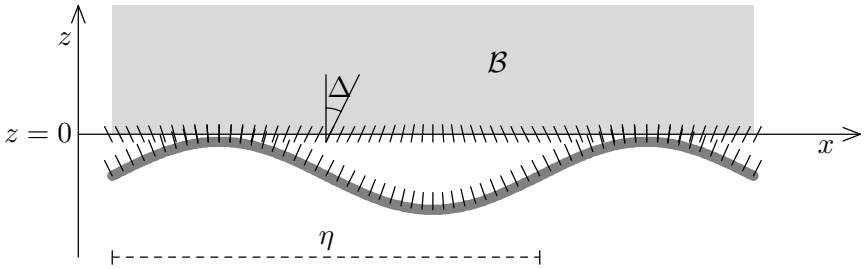

Figure 2.1: Geometric modeling of a rough surface. The physical surface oscillates with a characteristic wavelength η. The homeotropic anchoring at the oscillating boundary induces an oscillation of amplitude Δ in the boundary director. The bulk volume $\mathcal{B}$ is the grey region. Besides the microscopic roughness wavelength η, the two-scale analysis performed below is governed as well by the microscopic nematic coherence length ξ, introduced in (2.5).

roughness wavelength η (see Figure 2.1.1). We remark that the oscillation rate increases as $\eta \to 0^+$, while all roughness effects are expected to vanish in the limit $\Delta \to 0^+$. The requirements (2.7),(2.8) imply that the free-energy minimizer will not exhibit any dependence on the transverse y-coordinate, so that we will henceforth restrict our attention to the dependence on the coordinates (x, z).

It is more complex to ascertain the correct type of boundary conditions which are to be imposed on the degree of orientation s. From the mathematical point of view, it would be natural to imitate the (Dirichlet) strong anchoring imposed on the director and thus set $s(x, y, 0)$ to be equal to some fixed boundary value $\tilde{s}$. Nevertheless, while it is well established that we can induce an easy axis for the director on an external boundary, it is questionable whether we may fix the value of a mesoscopic parameter, which measures the degree of order in a distribution. From the physical point of view, stress-free (Neumann) boundary conditions on the degree of orientation deserve attention as well. In this latter case, we simply leave to the thermodynamic potential (2.1) the assignment of inducing the preferred value $s_{\rm pr}$ in the bulk ($z \to \infty$), while we perform no boundary action on the degree of orientation. To be safe, both possibilities (Dirichlet and Neumann) will be analyzed in §2.2.

2.1.2 Euler-Lagrange equations

Once we consider that $|\nabla \mathbf{n}|^2 = |\nabla \theta|^2$, it is easy to derive the Euler-Lagrange partial differential equations associated with the functional (2.6). They read

$$s^2 \Delta\theta + 2\, s\, \nabla s \cdot \nabla\theta = 0 \qquad \text{and} \qquad \Delta s - 3\, s\, |\nabla\theta|^2 - 3\, \frac{\sigma(s)}{\xi^2} = 0\,, \tag{2.9}$$

where

$$\sigma(s) := s(s - s_{\rm pr})\left(s - s_{\rm pr} + \frac{\omega^2}{s_{\rm pr}}\right) . \tag{2.10}$$

Since the boundary conditions (2.8) are x-periodic, with a period of $2\pi\eta$, we look for solutions of (2.9) in $C^2_{2\pi\eta}$ (the space of C^2-functions, $2\pi\eta$-periodic in the x-direction). To complete the differential system (2.8), in §2.2.2 we will require

$$\begin{cases} \theta(x,0) = \Delta\cos\dfrac{x}{\eta} \\ \dfrac{\partial s}{\partial z}(x,0) = 0 \end{cases} \quad \text{and} \quad \begin{cases} \theta(x,z) \approx \theta_{\rm b}(z) \\ s(x,z) \approx s_{\rm pr} \end{cases} \quad \text{as } z \to \infty \tag{2.11}$$

while in §2.2.3 we will choose

$$\begin{cases} \theta(x,0) = \Delta\cos\dfrac{x}{\eta} \\ s(x,0) = \tilde{s} \end{cases} \quad \text{and} \quad \begin{cases} \theta(x,z) \approx \theta_{\rm b}(z) \\ s(x,z) \approx s_{\rm pr} \end{cases} \quad \text{as } z \to \infty \tag{2.12}$$

2.2 Two-scale analysis

Before proceeding with the perturbation analysis of the differential equations, we state them in dimensionless form. It will turn out that the correct scaling is obtained by measuring lengths in η-units, so that we introduce the new dimensionless coordinates $\bar{x} = x/\eta$, $\bar{z} = z/\eta$ and define the dimensionless parameter $\varepsilon = \xi/\eta$. Equations (2.9) thus become

$$s^2\Delta\theta + 2s\,\nabla s\cdot\nabla\theta = 0 \qquad \text{and} \qquad \varepsilon^2\Delta s - 3\varepsilon^2 s\,|\nabla\theta|^2 - 3\sigma(s) = 0\,, \tag{2.13}$$

where both the gradient and the Laplacian are now to be intended with respect to the scaled variables. The nematic coherence length is usually much smaller than all other characteristic lengths. Consequently, we will look for uniformly asymptotic solutions to (2.13), by treating ε as a small parameter. In this limit, $(2.13)_2$ is singular, so that a regular asymptotic expansion would not provide a uniform approximation of the solution. Indeed, the small parameter ε multiplies the highest derivative, so that we may expect the solution to have a steep behavior in a layer of thickness δ (to be determined), close to the boundary $z = 0$. We refer the reader to the books [50, 10, 62, 77] for the details of the singular perturbation theory we will apply henceforth and, in particular, for the technique of the two-scale method which directly yields a uniform approximation of the solution.

A standard dominant balance argument (that requires us to introduce a stretched variable $Z = \bar{z}/\delta$) allows us to recognize that the boundary layer thickness is $\delta = \varepsilon$.

We then introduce the *fast* variable $Z = \bar{z}/\varepsilon$. The two-scale chain rule requires us to replace $\partial_{\bar{z}}$ by $\left(\partial_{\bar{z}} + \varepsilon^{-1}\partial_Z\right)$, and equations (2.13) take the form (when $s \neq 0$)

$$s\left(\varepsilon^2\theta_{,\bar{x}\bar{x}} + \varepsilon^2\theta_{,\bar{z}\bar{z}} + 2\varepsilon\theta_{,\bar{z}Z} + \theta_{,ZZ}\right) + 2\varepsilon^2 s_{,\bar{x}}\theta_{,\bar{x}} + 2(\varepsilon s_{,\bar{z}} + s_{,Z})(\varepsilon\theta_{,\bar{z}} + \theta_{,Z}) = 0 \tag{2.14}$$

$$\varepsilon^2 s_{,\bar{x}\bar{x}} + \varepsilon^2 s_{,\bar{z}\bar{z}} + 2\varepsilon s_{,\bar{z}Z} + s_{,ZZ} - 3s\left[\varepsilon^2(\theta_{,\bar{x}})^2 + (\varepsilon\theta_{,\bar{z}} + \theta_{,Z})^2\right] - 3\sigma(s) = 0 \tag{2.15}$$

where a comma denotes differentiation with respect to the shown variable. In agreement with the two-scale method, θ and s are now to be intended as $\theta(\bar{x}, \bar{z}, Z)$ and $s(\bar{x}, \bar{z}, Z)$. In other words, θ and s are functions of $\bar{x}$, $\bar{z}$, and Z, which are to be regarded as *independent* variables. It will be only at the very end of our calculations that we will recast the connection between $\bar{z}$ and Z: $Z = \bar{z}/\varepsilon$. We seek solutions which may be given the formal expansions

$$\theta(\bar{x}, \bar{z}, Z) = \theta_0(\bar{x}, \bar{z}, Z) + \varepsilon\theta_1(\bar{x}, \bar{z}, Z) + \varepsilon^2\theta_2(\bar{x}, \bar{z}, Z) + O(\varepsilon^3) \tag{2.16}$$

$$s(\bar{x}, \bar{z}, Z) = s_0(\bar{x}, \bar{z}, Z) + \varepsilon s_1(\bar{x}, \bar{z}, Z) + \varepsilon^2 s_2(\bar{x}, \bar{z}, Z) + O(\varepsilon^3)\ . \tag{2.17}$$

If we insert (2.16)-(2.17) into (2.14)-(2.15), we obtain the following differential equations to $\mathcal{O}(1)$, $\mathcal{O}(\varepsilon)$, and $\mathcal{O}(\varepsilon^2)$:

$$\begin{cases} \frac{1}{s_0}\left(s_0^2\theta_{0,Z}\right)_{,Z} = 0 \\ s_{0,ZZ} - 3s_0(\theta_{0,Z})^2 - 3\sigma(s_0) = 0 \end{cases} \tag{2.18}$$

$$\begin{cases} \frac{1}{s_0}\left(s_0^2\theta_{1,Z}\right)_{,Z} + \frac{1}{s_1}\left(s_1^2\theta_{0,Z}\right)_{,Z} = -2\left(s_0\theta_{0,Z}\right)_{,\bar{z}} - 2s_{0,Z}\theta_{0,\bar{z}} \\ s_{1,ZZ} - 6s_0\theta_{0,Z}\theta_{1,Z} - 3s_1\left(\sigma'(s_0) + (\theta_{0,Z})^2\right) = 6s_0\theta_{0,Z}\theta_{0,\bar{z}} - 2s_{0,\bar{z}Z} \end{cases} \tag{2.19}$$

$$\begin{cases} \frac{1}{s_0}(s_0^2\theta_{2,Z})_{,Z} + \frac{1}{s_2}(s_2^2\theta_{0,Z})_{,Z} = -\frac{1}{s_1}(s_1^2\theta_{1,Z})_{,Z} - \frac{1}{s_0}(s_0^2\theta_{0,\bar{z}})_{,\bar{z}} - \frac{1}{s_0}(s_0^2\theta_{0,\bar{x}})_{,\bar{x}} \\ \qquad\qquad - 2\left(s_0\theta_{1,Z}\right)_{,\bar{z}} - 2\left(s_1\theta_{0,Z}\right)_{,\bar{z}} - 2s_{1,Z}\theta_{0,\bar{z}} - 2s_{0,Z}\theta_{1,\bar{z}} \\ s_{2,ZZ} - 3s_2\left[\sigma'(s_0) + (\theta_{0,Z})^2\right] - 6s_0\theta_{0,Z}\theta_{2,Z} = \frac{3}{2}s_1^2\sigma''(s_0) \\ \qquad + 3s_0\left[(\theta_{0,\bar{z}} + \theta_{1,Z})^2 + (\theta_{0,x})^2\right] \\ \qquad + 6\theta_{0,Z}\left(s_1\theta_{1,Z} + s_1\theta_{0,\bar{z}} + s_0\theta_{1,\bar{z}}\right) - 2s_{1,\bar{z}Z} - s_{0,\bar{z}\bar{z}} - s_{0,xx}\ . \end{cases} \tag{2.20}$$

Analogous equations can be easily derived at any desired order. For any $n \geq 1$, the differential system obtained at $\mathcal{O}(\varepsilon^n)$ is linear in the unknowns θ_n,s_n and may be solved analytically. By virtue of the multiscale method, we find the correct dependence on $\bar{z}, Z$ by requiring that all s_n, θ_n are uniformly bounded as $\varepsilon \to 0^+$ for expanding intervals of the type $0 \leq Z \leq Z^*/\varepsilon$, for a suitable positive constant Z^*. In most practical cases this requirement is equivalent to asking for the removal of secular terms (*i.e.*, terms that diverge as $Z \to +\infty$).

2.2.1 Preliminary remarks about the method

If $y(x;\varepsilon)$ is the continuous *exact* solution of a differential equation that contains a small parameter ε, and

$$\hat{y}^{(k)}(x;\varepsilon) \;=\; y_0(x) + \varepsilon y_1(x) + \cdots + \varepsilon^k y_k(x) \tag{2.21}$$

is the regular expansion of $y(x;\varepsilon)$ up to the kth-order, we define the error as

$$R_k(x;\varepsilon) \;=\; y(x;\varepsilon) - \hat{y}^{(k)}(x;\varepsilon). \tag{2.22}$$

A natural requirement for an asymptotic solution to be satisfactory at the order n in an interval $x \in [a,b]$ is that for any $k \leq n$ and for sufficiently small ε, there exists a constant M_k, independent of ε, such that

$$\sup_{x\in[a,b]} |R_k(x;\varepsilon)| \leq \varepsilon^{k+1} M_k \tag{2.23}$$

and we say that the error is *uniformly* of order at least $k+1$ as $\varepsilon \to 0$. A necessary condition for this is that every $y_k(x)$, $k>0$, be *bounded* in $x \in [a,b]$, in fact

$$\begin{aligned} |\varepsilon^k\, y_k(x)| &= |\hat{y}^{(k)}(x;\varepsilon) - \hat{y}^{(k-1)}(x;\varepsilon)| \leq |\hat{y}^{(k)}(x;\varepsilon) - y(x;\varepsilon)| + |y(x;\varepsilon) - \hat{y}^{(k-1)}(x;\varepsilon)| \\ &= |R_k(x;\varepsilon)| + |R_{k-1}(x;\varepsilon)| \leq \varepsilon^k\, (M_{k-1} + \varepsilon M_k)\,. \end{aligned}$$

In other words, it is expected that the $(k+1)$-term of the expansion provides the principal part of the error $R_k(x;\varepsilon)$. This is exactly the condition that we try to fulfill when using the two-scale method. It is not guaranteed in advance that this will produce a valid asymptotic solution, but the plan we are adopting is the most likely to lead to the desired result.

When the problem is singular like in our case, two (or more) length scales must be introduced, one is the *fast variable* Z (inner variable in the terminology of boundary layer theory) and the other is the *slow variable* $\bar{z}$ (outer variable in boundary layer theory); the two are linked by the stretching relation $Z = \bar{z}/\varepsilon$ in our case. The fast variable describes the rapid variations of the solution and therefore is the one that varies in the boundary layer, while the slow variable varies only outside the boundary layer, in the so called outer region. Of the two only Z can grow indefinitely as $\varepsilon \to 0$ since the boundary layer solution has to match the solution valid in the outer region and therefore must reach values for which $\bar{z} = \varepsilon\, Z$ is finite as $\varepsilon \to 0$. The condition on the boundedness of the expansion terms then tells us that $\theta_k(\bar{x},\bar{z},Z)$ and $s_k(\bar{x},\bar{z},Z)$ must be uniformly bounded in Z for *expanding intervals* $[0, Z^*/\varepsilon]$, where Z^* is a constant. The right dependence of the solution on the slow variable $\bar{z}$ is then retrieved by the use of this condition.

In practice, there is not a unique way to satisfy the above procedure, so we will

adopt the more restrictive rule [50]: the arbitrary functions of $\bar{z}$ are determined by trying to reduce the contribution of the next terms in the expansion, so we require the term $|y_{k+1}(\bar{z}, Z)|$ to be as small as we can over the length scales we are using. Otherwise stated, we choose the arbitrary functions of the slow variable $\bar{z}$ in such a way that the C^0-norm of the term y_k (supposed continuous)

$$\|y_k\|_{C^0} \;=\; \sup\left\{|y_k(\varepsilon Z, Z)| \;:\; Z \in [0, Z^*/\varepsilon]\right\} \tag{2.24}$$

is the smallest possible. In particular this means that we are trying to avoid situations where $\varepsilon^k\, y_k(\bar{z}, \bar{z}/\varepsilon)$ is of order ε^{k-1} since in such a case the perturbation procedure fails. For instance, a term $\varepsilon^k\, y_k(\bar{z}, Z) \;= \varepsilon^k\, A(\bar{z})\, Z\, \mathrm{e}^{-Z}$ is bounded, but replacing the stretching relation $Z = \bar{z}/\varepsilon$ yields $\varepsilon^k\, y_k(\bar{z}, \bar{z}/\varepsilon) \;= \varepsilon^{k-1}\, A(\bar{z})\, \bar{z}\, \mathrm{e}^{-\bar{z}/\varepsilon}$ which is of $\mathcal{O}\left(\varepsilon^{k-1}\right)$. If the asymptotic expansion is working properly, the error at the step k is ruled by the term y_{k+1} and the above criterion can be rephrased informally as "try to minimize the error in the approximation". Of course, there is no a-priori evidence that this rule can always be applied, nonetheless it allows in most practical cases to resolve the arbitrariness in $\bar{z}$ even when no secular terms are given.

2.2.2 Free surface degree of orientation

In terms of the scaled variables, the boundary conditions (2.11) require

$$\begin{cases} \theta(\bar{x}, 0) = \Delta \cos \bar{x} \\ s_{,\bar{z}}(x, 0) = 0 \end{cases} \qquad \text{and} \qquad \begin{cases} \theta(\bar{x}, \bar{z}) \approx \theta_{\mathrm{b}}(\eta \bar{z}) \\ s(\bar{x}, \bar{z}) \approx s_{\mathrm{pr}} \end{cases} \qquad \text{when } \bar{z} \gg 1\,. \tag{2.25}$$

The leading solutions in expansions (2.16),(2.17) are

$$s_0(x, z) = s_{\mathrm{pr}} \qquad \text{and} \qquad \theta_0(x, z) = \mathrm{m}\, z + \Delta \mathrm{e}^{-z/\eta} \cos \frac{x}{\eta}\,, \tag{2.26}$$

where $\mathrm{m} := \theta_{\mathrm{b}}'(0)$. Higher-order asymptotic solutions are gathered by means of laborious but straightforward calculations. After recasting the solutions in terms of the dimensional variables $x = \eta\, \bar{x}$ and $z = \eta\, \bar{z}$, we find

$$\begin{aligned} s(x, z) = s_{\mathrm{pr}} &- \frac{s_{\mathrm{pr}} \xi^2}{\omega^2} \left(\mathrm{m}^2 - \frac{2\,\mathrm{m}\,\Delta}{\eta}\, \mathrm{e}^{-z/\eta} \cos \frac{x}{\eta} + \frac{\Delta^2}{\eta^2}\, \mathrm{e}^{-2z/\eta} \right) \\ &+ \frac{2 s_{\mathrm{pr}}\, \xi^3}{\sqrt{3}\, \omega^3}\, \mathrm{e}^{-\sqrt{3}\omega z/\xi} \left(\frac{\Delta^2}{\eta^3} - \frac{\mathrm{m}\,\Delta}{\eta^2} \cos \frac{x}{\eta} \right) + \mathcal{O}\left(\varepsilon^4\right)\,, \end{aligned} \tag{2.27}$$

$$\begin{aligned} \theta(x, z) = \mathrm{m}\, z + \Delta\, \mathrm{e}^{-z/\eta} \cos \frac{x}{\eta} &+ \frac{\xi^2}{\omega^2} \left(\frac{2\,\mathrm{m}\,\Delta^2}{\eta} \left(1 - \mathrm{e}^{-2z/\eta}\right) \right. \\ &\left. - \frac{\Delta^3}{2\,\eta^2} \left(\mathrm{e}^{-z/\eta} - \mathrm{e}^{-3z/\eta} \right) \cos \frac{x}{\eta} - \frac{2\,\mathrm{m}^2\,\Delta}{\eta}\, z\, \mathrm{e}^{-z/\eta} \cos \frac{x}{\eta} \right) + \mathcal{O}\left(\varepsilon^4\right)\,. \end{aligned} \tag{2.28}$$

The above expansions have been carried out up to the first nontrivial correction of the 0th-order approximation. Indeed, all calculations must be pushed to $\mathcal{O}\left(\varepsilon^3\right)$, since an internal ξ-layer is necessary to satisfy the boundary condition (2.11) in $z=0$. This layer is of $\mathcal{O}\left(\varepsilon^3\right)$ because in the Neumann case the boundary condition (2.11) concerns the first derivative of s, instead of the degree of orientation itself. We remark that the solutions (2.27)-(2.28) are coherently ordered for every fixed value of $\eta \neq 0$. However, they are not uniformly ordered when $\eta \in (0, \bar{\eta}]$; namely we do not have a uniform solution if η is allowed to become of order ξ or, still worse, tend to zero. In other words, the above solutions remain valid as $\eta \to 0^+$ if and only if $\xi = o(\eta)$. The main properties of the equilibrium configurations in the mathematically appealing but physically uncommon case in which η is of the order of, or even smaller than, ξ will be presented in a following Section §2.4.

Two-scale calculations

Zeroth-order solution. It is easily seen that the following zeroth-order solutions satisfy the leading equations in expansions (2.16),(2.17), when Neumann condition for s is assumed at the surface $\bar{z}=0$.

$$s_0(\bar{x},\bar{z},Z) = s_{\rm pr} \qquad \text{and} \qquad \theta_0(\bar{x},\bar{z},Z) = A_0(\bar{x},\bar{z}). \tag{2.29}$$

Here $A_0(\bar{x},\bar{z})$ is unknown and will be determined hereafter.

First-order solution. The $\mathcal{O}(\varepsilon)$ equations then reads

$$\theta_{1,ZZ} = 0, \qquad s_{1,ZZ} - 3\omega^2 s_1 = 0 \tag{2.30}$$

whose general solutions are

$$\theta_1(\bar{x},\bar{z},Z) = A_1(\bar{x},\bar{z}) + B_1(\bar{x},\bar{z})\, Z, \tag{2.31}$$

$$s_1(\bar{x},\bar{z},Z) = C_1(\bar{x},\bar{z})\, \mathrm{e}^{-\sqrt{3}\,\omega Z} + D_1(\bar{x},\bar{z})\, \mathrm{e}^{\sqrt{3}\,\omega Z}. \tag{2.32}$$

We need now to remove secular terms, so that we must impose $D_1(\bar{x},\bar{z}) \equiv 0$ and $B_1(\bar{x},\bar{z}) \equiv 0$. Boundary conditions on s_1 further require $C_1(\bar{x},\bar{z}) \equiv 0$. Therefore we have

$$\theta_1(\bar{x},\bar{z},Z) = A_1(\bar{x},\bar{z}) \qquad \text{and} \qquad s_1(\bar{x},\bar{z},Z) = 0. \tag{2.33}$$

Second-order solution. The $\mathcal{O}\left(\varepsilon^2\right)$ equations are

$$\theta_{2,ZZ} + \Delta_2 A_0 = 0 \tag{2.34}$$

$$s_{2,ZZ} - 3\omega^2 s_2 - 3 s_{\rm pr} |\nabla_2 A_0|^2 = 0 \tag{2.35}$$

where Δ_2 and ∇_2 are respectively the laplacian and the gradient with respect to the variables $(\bar{x},\bar{z})$: $\Delta_2 A_0 = A_{0,\bar{x}\bar{x}} + A_{0,\bar{z}\bar{z}}$ and $\nabla_2 A_0 = (A_{0,\bar{x}}, A_{0,\bar{z}})$.

The general solution of (2.34) is

$$\theta_2(\bar{x},\bar{z},Z) \;=\; A_2(\bar{x},\bar{z}) + B_2(\bar{x},\bar{z})\,Z - \frac{1}{2}\Delta_2 A_0(\bar{x},\bar{z})\,Z^2. \tag{2.36}$$

The removal of secular terms thus yields $B_2(\bar{x},\bar{z}) \equiv 0$ and the equation for $A_0(\bar{x},\bar{z})$: $\Delta_2 A_0 = 0$. The expression of $A_0(\bar{x},\bar{z})$ (and θ_2) is then found by considering the boundary conditions that θ_0 must satisfy. We find:

$$A_0(\bar{x},\bar{z}) \;=\; \mathrm{m}\bar{z} + \Delta \mathrm{e}^{-\bar{z}}\cos\bar{x} \qquad \text{and} \qquad \theta_2(\bar{x},\bar{z},Z) \;=\; A_2(\bar{x},\bar{z}). \tag{2.37}$$

Equation (2.35) can now be solved to give

$$s_2(\bar{x},\bar{z},Z) \;=\; C_2(\bar{x},\bar{z})\,\mathrm{e}^{-\sqrt{3}\omega Z} - \frac{s_{\mathrm{pr}}}{\omega^2}\left(\mathrm{m}^2 + \Delta^2\,\mathrm{e}^{-2\bar{z}} + 2\mathrm{m}\,\Delta\,\mathrm{e}^{-\bar{z}}\cos\bar{x}\right), \tag{2.38}$$

where we have already removed secular terms.
We now want to impose boundary conditions on s. The Neumann condition at $\bar{z} = 0$ requires a little of attention, we examine the procedure in detail.
In the framework of the two-scale analysis, the condition $\dfrac{\partial s(\bar{x},\bar{z})}{\partial \bar{z}} = 0$ on $\bar{z} = 0$, becomes

$$\frac{\partial}{\partial \bar{z}} s(\bar{x},\bar{z},Z) + \frac{1}{\varepsilon}\frac{\partial}{\partial Z} s(\bar{x},\bar{z},Z) \;=\; 0 \quad \text{on} \quad \bar{z} = Z = 0 \tag{2.39}$$

and therefore involves different orders of approximation. If we insert (2.16)-(2.17) in the previous equation, we obtain the following conditions on the boundary $\bar{z} = Z = 0$, $k \geq 0$:

$$\begin{aligned}
&\frac{\partial s_0}{\partial Z} \;=\; 0\\
&\frac{\partial s_0}{\partial \bar{z}} + \frac{\partial s_1}{\partial Z} \;=\; 0\\
&\frac{\partial s_1}{\partial \bar{z}} + \frac{\partial s_2}{\partial Z} \;=\; 0\\
&\cdots\\
&\frac{\partial s_k}{\partial \bar{z}} + \frac{\partial s_{k+1}}{\partial Z} \;=\; 0.
\end{aligned}$$

The first two conditions are already fulfilled by the expressions of s_0 and s_1, while the third provides the condition

$$C_2(\bar{x},0) \;=\; 0 \tag{2.40}$$

that will be later used.

Third-order solution. The $\mathcal{O}\left(\varepsilon^3\right)$ equations are

$$\theta_{3,ZZ} + \Delta_2 A_1 - \frac{2\sqrt{3}\,\omega}{s_{\rm pr}}\,\mathrm{e}^{-\sqrt{3}\omega Z}\,C_2\left(\mathrm{m} - \Delta\,\mathrm{e}^{-\bar{z}}\cos\bar{x}\right) = 0 \tag{2.41}$$

$$s_{3,ZZ} - 3\omega^2 s_3 - 2\sqrt{3}\,\omega\,\mathrm{e}^{-\sqrt{3}\omega Z} C_{2,\bar{z}} - 6 s_{\rm pr}\nabla_2 A_1\cdot\nabla_2 A_0 = 0. \tag{2.42}$$

The general solution of (2.41) is

$$\theta_3(\bar{x},\bar{z},Z) = A_3(\bar{x},\bar{z}) + B_3(\bar{x},\bar{z})\,Z + \frac{2\,\mathrm{e}^{-\sqrt{3}\omega Z}}{\sqrt{3}\,\omega s_{\rm pr}}\,C_2(\bar{x},\bar{z})\left(\mathrm{m} - \Delta\,\mathrm{e}^{-\bar{z}}\cos\bar{x}\right) - \frac{1}{2}\Delta_2 A_1(\bar{x},\bar{z})\,Z^2. \tag{2.43}$$

Again, to avoid infinite terms as $Z\to+\infty$ we set $B_3(\bar{x},\bar{z})\equiv 0$ and $\Delta_2 A_1 = 0$, which in turn gives $A_1(\bar{x},\bar{z})\equiv 0$ since A_1 has to verify homogeneous boundary conditions. We have,

$$\theta_3(\bar{x},\bar{z},Z) = A_3(\bar{x},\bar{z}) + \frac{2\,\mathrm{e}^{-\sqrt{3}\omega Z}}{\sqrt{3}\,\omega s_{\rm pr}}\,C_2(\bar{x},\bar{z})\,\left(\mathrm{m} - \Delta\mathrm{e}^{-\bar{z}}\cos\bar{x}\right). \tag{2.44}$$

The general solution of (2.42) now is

$$s_3(\bar{x},\bar{z},Z) = C_3(\bar{x},\bar{z})\,\mathrm{e}^{-\sqrt{3}\omega Z} - \frac{\mathrm{e}^{-\sqrt{3}\omega Z}}{2\sqrt{3}\omega}\frac{\partial C_2(\bar{x},\bar{z})}{\partial\bar{z}} - Z\,\mathrm{e}^{-\sqrt{3}\omega Z}\frac{\partial C_2(\bar{x},\bar{z})}{\partial\bar{z}}. \tag{2.45}$$

According to the two-scale method, we chose $C_2(\bar{x},\bar{z})$ in order to minimize $|s_3(\bar{x},\bar{z},Z)|$ uniformly in Z (see Section 2.2.1). This implies that $\frac{\partial C_2(\bar{x},\bar{z})}{\partial\bar{z}} = 0$ and therefore C_2 is a function only of $\bar{x}$: $C_2(\bar{x},\bar{z}) = C_2(\bar{x})$. The condition (2.40) then enable us to conclude $C_2(\bar{x},\bar{z})\equiv 0$ and it is easily obtained

$$\theta_3(\bar{x},\bar{z},Z) = A_3(\bar{x},\bar{z}) \qquad \text{and} \qquad s_3(\bar{x},\bar{z},Z) = C_3(\bar{x},\bar{z})\,\mathrm{e}^{-\sqrt{3}\omega Z}. \tag{2.46}$$

Fourth-order solution. To determine the function $A_2(\bar{x},\bar{z})$ which is of interests for us, we need to push the perturbation expansion up to the fourth order. We do not enter here into the full details, since calculations are lengthy and tedious, but straightforward.
The $\mathcal{O}\left(\varepsilon^4\right)$ equation for θ is

$$\theta_{4,ZZ} + \Delta_2 A_2 - \frac{2\sqrt{3}\,\omega}{s_{\rm pr}}\,\mathrm{e}^{-\sqrt{3}\omega Z} C_3\left(\mathrm{m} - \Delta\,\mathrm{e}^{-\bar{z}}\cos\bar{x}\right) - \frac{4\Delta}{\omega^2}\,\mathrm{e}^{-\bar{z}}\Big(\left(\mathrm{m}^2 + \Delta^2\mathrm{e}^{-2\bar{z}}\right)\cos\bar{x} - 2\mathrm{m}\Delta\mathrm{e}^{-\bar{z}}\Big) = 0 \tag{2.47}$$

whose general solution is

$$\theta_4(\bar{x},\bar{z},Z) \;=\; A_4(\bar{x},\bar{z}) + B_4(\bar{x},\bar{z})\,Z + \frac{2\,\mathrm{e}^{-\sqrt{3}\,\omega Z}}{\sqrt{3}\,\omega s_{\mathrm{pr}}}\,C_3(\bar{x},\bar{z})\left(\mathrm{m} - \Delta\,\mathrm{e}^{-\bar{z}}\cos\bar{x}\right) - \left(\frac{1}{2}\Delta_2 A_2(\bar{x},\bar{z}) - \frac{2\Delta}{\omega^2}\mathrm{e}^{-\bar{z}}\Big(\left(\mathrm{m}^2 + \Delta^2\mathrm{e}^{-2\bar{z}}\right)\cos\bar{x} - 2\mathrm{m}\Delta\mathrm{e}^{-\bar{z}}\Big)\right) Z^2. \tag{2.48}$$

Therefore we must choose $B_4(\bar{x},\bar{z}) \equiv 0$ and A_2 satisfies the equation

$$\Delta_2 A_2(\bar{x},\bar{z}) \;=\; \frac{4\Delta}{\omega^2}\mathrm{e}^{-\bar{z}}\Big(\left(\mathrm{m}^2 + \Delta^2\mathrm{e}^{-2\bar{z}}\right)\cos\bar{x} - 2\mathrm{m}\Delta\mathrm{e}^{-\bar{z}}\Big) \tag{2.49}$$

that can be solved by using standard methods (see remark 2.1) to yield

$$\begin{aligned} A_2(\bar{x},\bar{z}) \;&= A_{20} + A_{21}\mathrm{e}^{-\bar{z}}\cos\bar{x} \\ &\quad - \frac{2\mathrm{m}\Delta^2}{\omega^2}\mathrm{e}^{-2\bar{z}} + \frac{\Delta}{\omega^2}\mathrm{e}^{-\bar{z}}\left(\mathrm{e}^{-2\bar{z}}\frac{\Delta^2}{2} - 2\mathrm{m}^2\,\bar{z}\right)\cos\bar{x}. \end{aligned} \tag{2.50}$$

The constants A_{20} and A_{21} are then determined imposing the boundary condition $\theta_2(\bar{x},0,0) = 0$. This yield

$$A_{20} \;=\; \frac{2\mathrm{m}\Delta^2}{\omega^2} \qquad \text{and} \qquad A_{22} \;=\; -\frac{\Delta^3}{2\omega^2}. \tag{2.51}$$

Calculations for $s_4(\bar{x},\bar{z},Z)$, similar to those performed in the discussion of equation (2.42), show that $C_3(\bar{x},\bar{z})$ needs to be function of $\bar{x}$ only: $C_3(\bar{x},\bar{z}) \;=\; C_3(\bar{x})$. The boundary conditions then requires that at $\bar{z} = Z = 0$ it must be

$$\frac{\partial s_2}{\partial \bar{z}} + \frac{\partial s_3}{\partial Z} \;=\; 0 \tag{2.52}$$

from which the expression of $C_3(\bar{x})$ is gathered

$$C_3(\bar{x}) \;=\; \frac{2s_{\mathrm{pr}}\Delta}{\sqrt{3}\,\omega^3}\left(\Delta - \mathrm{m}\cos\bar{x}\right). \tag{2.53}$$

Remark 2.1. Equation (2.49) is of the type

$$u_{,yy} + u_{,xx} \;=\; \left(\alpha\,\mathrm{e}^{-y} + \beta\,\mathrm{e}^{-3y}\right)\cos x + \gamma\,\mathrm{e}^{-2y}. \tag{2.54}$$

We look for regular solutions which are 2π-periodic along the x-axis and satisfy the conditions

$$\text{(a)}\quad u(x,0) \;=\; 0 \qquad \text{and} \qquad \text{(b)}\quad \lim_{y\to+\infty} u(x,y) \;=\; 0. \tag{2.55}$$

Regularity theorems for elliptic equations (see [39]), assure that the solution is analytic, so that it can be expanded in Fourier series in the x variable and no question on the convergence

of the series arises. Moreover, the series can be differentiated term by term. Therefore, we seek a solution of the type

$$u(x,y) \;=\; a_0(y) + \sum_{k=1}^{+\infty} a_k(y)\cos kx, \tag{2.56}$$

where only cosine terms have been considered due to symmetry reasons. In fact, the boundary conditions, the domain and equation (2.54) are invariant under the change of variable $x \to -x$. Therefore, the solution is expected to share the same symmetry, i.e., it has to be even. Insertion of (2.56) into (2.54) yields

$$a_0''(y) + \sum_{k=1}^{+\infty} \left(a_k''(y) - k^2 a_k(y)\right)\cos kx \;=\; \left(\alpha\,\mathrm{e}^{-y} + \beta\,\mathrm{e}^{-3y}\right)\cos x + \gamma\,\mathrm{e}^{-2y}. \tag{2.57}$$

Taking each contribution separately, we get the equations

$$a_0''(y) \;=\; \gamma\,\mathrm{e}^{-2y} \tag{2.58}$$

$$a_1''(y) - a_1(y) \;=\; \alpha\,\mathrm{e}^{-y} + \beta\,\mathrm{e}^{-3y} \tag{2.59}$$

$$a_k''(y) - k^2 a_k(y) \;=\; 0, \qquad k \geq 2, \tag{2.60}$$

whose solutions, satisfying the boundary condition (2.55b), are

$$a_0(y) \;=\; C_0 + \frac{\gamma}{4}\,\mathrm{e}^{-2y} \tag{2.61}$$

$$a_1(y) \;=\; C_1\,\mathrm{e}^{-y} - \frac{\alpha}{4}\,\mathrm{e}^{-y}(1+2y) + \frac{\beta}{8}\,\mathrm{e}^{-3y} \tag{2.62}$$

$$a_k(y) \;=\; C_k\,\mathrm{e}^{-ky}, \qquad k \geq 2. \tag{2.63}$$

The constants C_k can be determined using the boundary condition (2.55a), in particular $C_k = 0$ for $k \geq 2$.

Surface melting

We can highlight three different contributions in the degree of orientation (2.27). First, we notice a uniform decrease in the degree of order, equal to $-s_{\mathrm{pr}}\mathrm{m}^2\xi^2/\omega^2$. This disordering effect is triggered by the θ-derivative m and was certainly to be expected. In fact, a glance to the free-energy functional (2.6) suffices to show that a reduction in s decreases the free energy whenever the gradient of the director is not null. We then find two boundary layers. The former, of thickness η and $\mathcal{O}\left(\varepsilon^2\right)$, is a further reduction of the degree of orientation due to the boundary roughness, which induces a director variation in the x-direction. An internal boundary layer, of thickness ξ and order $\mathcal{O}\left(\varepsilon^3\right)$, is finally needed in order to cancel the normal derivative of s at the external surface. If we take into account all the contributions, the mean surface degree of orientation, defined as the x-average of $s(x,0)$, turns out to be

$$\langle s(x,0)\rangle_x = s_{\mathrm{pr}}\left[1 - \frac{\mathrm{m}^2\xi^2}{\omega^2} - \frac{\Delta^2\xi^2}{\omega^2\eta^2} + \frac{2\Delta^2\xi^3}{\sqrt{3}\,\omega^3\eta^3}\right] + \mathcal{O}\left(\varepsilon^4\right)\ . \tag{2.64}$$

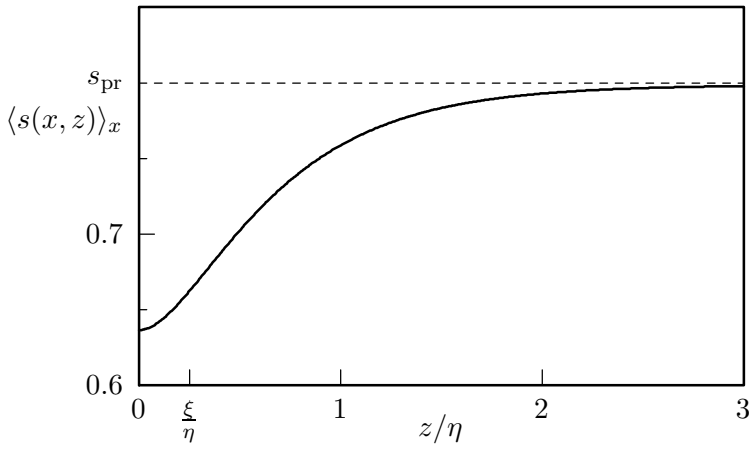

Figure 2.2: Boundary layers in the mean degree of orientation $\langle s(x,z)\rangle_x$ when $\xi = 0.25\eta$, $s_{\rm pr} = 0.8$, $\omega = 0.6$, $\mathrm{m} = 0.1/\eta$, and $\Delta = 1.5$. The plot exhibits the presence of *two* boundary layers, the internal one being required by the free boundary condition applied on s.

Figure 2.2 evidences the reported behaviour of the mean degree of orientation as a function of the distance from the surface.

Effective surface angle

The tilt angle θ exhibits a boundary-layer structure as well. Equation (2.28) shows that such a layer is of $\mathcal{O}\left(\varepsilon^2\right)$ and thickness η. It gives rise to an interesting effective misalignment of the surface director. Indeed, if we allow $z \gg \eta$ in (2.28) we find that

$$\theta(x,z) \approx \theta_{\rm b}(z) = \frac{2\,\mathrm{m}\,\xi^2\Delta^2}{\eta\omega^2} + \mathrm{m}\,z \qquad \text{as} \quad z \gg \eta\,. \tag{2.65}$$

The asymptotic approximation (2.65) shows that an experimental observation, performed sufficiently far from the external plate (with respect to the microscopic scale η), would detect an *effective* tilt angle $\theta_{\rm b}$, whose value at the plate is different from zero, since

$$\theta_{\rm b}(0) = \frac{2\,\mathrm{m}\,\xi^2\Delta^2}{\eta\omega^2}\,. \tag{2.66}$$

Thus, a coarse observation of the nematic configuration measures a surface tilt angle slightly different from the homeotropic prescription $\theta_{\rm surf} = 0$. Figure 2.3 evidences this effect. In the next Section we will analyze in more detail the result (2.66). Then we will show how it matches the predictions of an effective weak-anchoring potential. We remark that the tilt angle does not exhibit any further boundary layer at the smaller scale ξ.

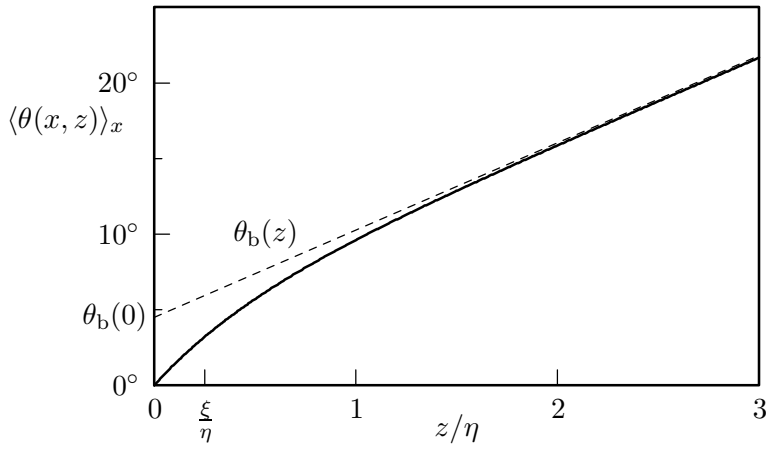

Figure 2.3: Boundary layer in the mean tilt angle $\langle\theta(x,z)\rangle_x$ when $\xi = 0.25\eta$, $s_{\rm pr} = 0.8$, $\omega = 0.6$, $\mathrm{m} = 0.1/\eta$, and $\Delta = 1.5$. The dashed line corresponds to the asymptotic, linear approximation $\theta_{\rm b}(z)$.

2.2.3 Fixed surface degree of orientation

The perturbative analysis of the differential equations (2.9), with the Dirichlet boundary conditions (2.12), would be unnecessarily entangled because of the non-linearity of the thermodynamic potential (2.10). In fact, in this case only implicit solutions for $s_0(x,z,Z)$ can be gathered. In order to pursue our analysis, and still catch the essential features of the solutions, we replace the function σ in (2.9) by its linear approximation $\sigma_1(s) = \omega^2(s - s_{\rm pr})$. This is tantamount to replacing the Landau-de Gennes potential in (2.3) by a tangent quadratic well, still centered in $s_{\rm pr}$. Such an approximation is certainly well justified deep in the nematic phase, when the isotropic state $s = 0$ becomes unstable, and the second well of the Landau-de Gennes potential can be neglected.

The asymptotic properties of the solutions in this case depend critically on the value $\tilde{s}$ forced on the surface. If $\tilde{s} \neq s_{\rm pr}$, the boundary layer induced by the Dirichlet condition dominates over the roughness effect. Indeed, the leading asymptotic solutions are given by

$$\begin{aligned} s(x,z) = s_{\rm pr} &- (s_{\rm pr} - \tilde{s})\ \mathrm{e}^{-\sqrt{3}\omega z/\xi} \\ &- \sqrt{3}\ (s_{\rm pr} - \tilde{s})\ \frac{\xi}{\omega}\,\mathrm{e}^{-\sqrt{3}\omega z/\xi}\left[\frac{\Delta^2}{4\eta}\left(1 - \mathrm{e}^{-2z/\eta}\right) + \frac{3}{2}\,\mathrm{m}^2\, z\right. \\ &\left. - 3\mathrm{m}\Delta\left(1 - \mathrm{e}^{-z/\eta}\right)\cos\frac{x}{\eta} + \frac{\Delta^2}{2\eta}\left(1 - \mathrm{e}^{-2z/\eta}\right)\cos\frac{2x}{\eta}\right] + \mathcal{O}\left(\varepsilon^2\right) \end{aligned} \quad (2.67)$$

$$\theta(x,z) = \mathrm{m}\, z + \Delta \mathrm{e}^{-z/\eta} \cos\frac{x}{\eta} + \frac{\xi}{\sqrt{3}\,\omega}\left[h\left(\frac{z}{\xi}\right) - h(0)\right]\left(\mathrm{m} - \frac{\Delta}{\eta}\mathrm{e}^{-z/\eta}\cos\frac{x}{\eta}\right) + \mathcal{O}\left(\varepsilon^2\right), \qquad (2.68)$$

where

$$h(\zeta) = \log\left[s_{\mathrm{pr}} - (s_{\mathrm{pr}} - \tilde{s})\,\mathrm{e}^{-\sqrt{3}\,\omega\,\zeta}\right] - \frac{(s_{\mathrm{pr}} - \tilde{s})\,\mathrm{e}^{-\sqrt{3}\,\omega\,\zeta}}{s_{\mathrm{pr}} - (s_{\mathrm{pr}} - \tilde{s})\,\mathrm{e}^{-\sqrt{3}\,\omega\,\zeta}} \qquad (2.69)$$

determines the tilt angle variation within the boundary layer. The bulk-asymptotic tilt angle is then given by

$$\theta(x,z) \approx \theta_{\mathrm{b}}(z) = \frac{\mathrm{m}\,\xi}{\sqrt{3}\,\omega}\left(\log\frac{s_{\mathrm{pr}}}{\tilde{s}} + \frac{s_{\mathrm{pr}} - \tilde{s}}{\tilde{s}}\right) + \mathrm{m}\, z \qquad \text{as} \quad z \gg \eta\,. \qquad (2.70)$$

We remark that, when $\tilde{s} \neq s_{\mathrm{pr}}$, the leading contribution to $\theta_{\mathrm{b}}(0)$ is independent of Δ and thus does not depend on the surface roughness. Furthermore, the effective surface tilt angle depends linearly on ξ, which makes it significantly larger than the prediction (2.66), derived with Neumann-like boundary conditions on s, which possesses an extra ξ/η (small) factor. Finally, we remark the fact that $\theta_{\mathrm{b}}(0)$ shares the sign of m if and only if $\tilde{s} < s_{\mathrm{pr}}$. We will return below to the physical origin and implications of this result.

When the induced degree of orientation $\tilde{s}$ does exactly coincide with s_{pr}, all calculations simplify, since $h(\zeta) \equiv \log s_{\mathrm{pr}}$, and all first-order correction in (2.68) vanish. We therefore push our perturbation analysis and obtain

$$s(x,z) = s_{\mathrm{pr}} - \frac{s_{\mathrm{pr}}\xi^2}{\omega^2}\left[\mathrm{m}^2 + \frac{\Delta^2}{\eta^2}\mathrm{e}^{-2z/\eta} - \frac{2\mathrm{m}\,\Delta}{\eta}\mathrm{e}^{-z/\eta}\cos\frac{x}{\eta} - \mathrm{e}^{-\sqrt{3}\,\omega z/\xi}\left(\mathrm{m}^2 + \frac{\Delta^2}{\eta^2} - \frac{2\mathrm{m}\,\Delta}{\eta}\cos\frac{x}{\eta}\right)\right] + \mathcal{O}\left(\varepsilon^3\right) \qquad (2.71)$$

$$\theta(x,z) = \mathrm{m}\, z + \Delta\,\mathrm{e}^{-z/\eta}\cos\frac{x}{\eta} + \frac{\xi^2}{\omega^2}\left(\frac{2\,\mathrm{m}\,\Delta^2}{\eta}\left(1 - \mathrm{e}^{-2z/\eta}\right) - \frac{\Delta^3}{2\,\eta^2}\left(\mathrm{e}^{-z/\eta} - \mathrm{e}^{-3z/\eta}\right)\cos\frac{x}{\eta} - \frac{2\,\mathrm{m}^2\,\Delta}{\eta}\, z\,\mathrm{e}^{-z/\eta}\cos\frac{x}{\eta}\right) + \mathcal{O}\left(\varepsilon^3\right). \qquad (2.72)$$

Equation (2.72) allows us to compute the asymptotic tilt angle θ_{b} when $\tilde{s} = s_{\mathrm{pr}}$. In fact, once we drop all exponentially-decaying terms in (2.72), we arrive at the interesting result that $\theta_{\mathrm{b}}(z)$ does exactly coincide with (2.65), that is, with the expression we derived with a Neumann-like boundary condition on the degree of orientation. In fact, the complete expression (2.72) for the tilt angle $\theta(x,z)$ coincides with (2.28) up to $\mathcal{O}\left(\varepsilon^3\right)$. Thus, any observation on the tilt angle is not able to distinguish among a free and a fixed boundary condition on the degree of orientation,

as long as the imposed value $\tilde{s}$ coincides with the preferred value $s_{\rm pr}$. This similarity between the Neumann and Dirichlet cases can be pursued further. Indeed, we can determine the $\mathcal{O}\left(\varepsilon^2\right)$-contributions in (2.67)-(2.68) also when $\tilde{s} \neq s_{\rm pr}$. If we then use them to compute the $\mathcal{O}\left(\varepsilon^2\right)$-correction to the asymptotic tilt angle (2.70), we arrive at the following expression, valid at $\mathcal{O}\left(\varepsilon^2\right)$ for any value of $\tilde{s}$:

$$\theta(x,z) \approx \theta_{\rm b}(z) = \left[\frac{\mathrm{m}\,\xi}{\sqrt{3}\,\omega}\left(\log\frac{s_{\rm pr}}{\tilde{s}} + \frac{s_{\rm pr}-\tilde{s}}{\tilde{s}}\right) + \frac{2\,\mathrm{m}\,\xi^2\Delta^2}{\eta\omega^2}\right] + \mathrm{m}\,z \quad \text{as } z \gg \eta, \tag{2.73}$$

which yields

$$\theta_{\rm b}(0) = \frac{\mathrm{m}\,\xi}{\sqrt{3}\,\omega}\left(\log\frac{s_{\rm pr}}{\tilde{s}} + \frac{s_{\rm pr}-\tilde{s}}{\tilde{s}}\right) + \frac{2\,\mathrm{m}\,\xi^2\Delta^2}{\eta\omega^2}\,. \tag{2.74}$$

The $\mathcal{O}\left(\varepsilon^2\right)$-contribution to the effective surface angle $\theta_{\rm b}(0)$ is thus fully a roughness effect and does not depend at all on the type of boundary conditions imposed on s. On the other hand, (2.74) confirms that the effective surface angle possesses also an $\mathcal{O}\left(\varepsilon\right)$-term when Dirichlet conditions are imposed on the degree of orientation, and $\tilde{s} \neq s_{\rm pr}$.

Figure 2.4 shows how the degree of orientation varies within the boundary layer as $\tilde{s}$ is fixed above, equal to, or below $s_{\rm pr}$. A double boundary-layer structure emerges. All plots exhibit a decrease of s in a region of characteristic size η: this effect comes from the $\mathcal{O}\left(\varepsilon^2\right)$-contribution. A similar surface melting was already presented and discussed in Figure 2.2. Close to the boundary, the $\mathcal{O}\left(1\right)$-term proportional to $(\tilde{s}-s_{\rm pr})\,\mathrm{e}^{-\sqrt{3}\omega z/\xi}$ settles the desired boundary value of s in a thin boundary layer of characteristic size ξ.

Two-scale calculations

We report here the main steps of the calculations performed under the Dirichlet condition for s at $\bar{z}=0$. We will not describe all the details since they follow the same idea outlined in §2.2.2.

Zeroth-order solution. When Dirichlet condition for s is assumed at the surface $\bar{z}=0$, the zeroth-order solutions for (2.16),(2.17) are

$$s_0(\bar{x},\bar{z},Z) = s_{\rm pr} + B_0(\bar{x},\bar{z})\mathrm{e}^{-\sqrt{3}\omega Z} \qquad \text{and} \qquad \theta_0(\bar{x},\bar{z},Z) = A_0(\bar{x},\bar{z}). \tag{2.75}$$

First order solution. The $\mathcal{O}\left(\varepsilon\right)$ equation for $s(\bar{x},\bar{z},Z)$ then reads

$$s_{1,ZZ} - 3\omega^2 s_1 \;=\; 2\sqrt{3}\,\omega\,\mathrm{e}^{-\sqrt{3}\omega Z}\frac{\partial B_0}{\partial \bar{z}} \tag{2.76}$$

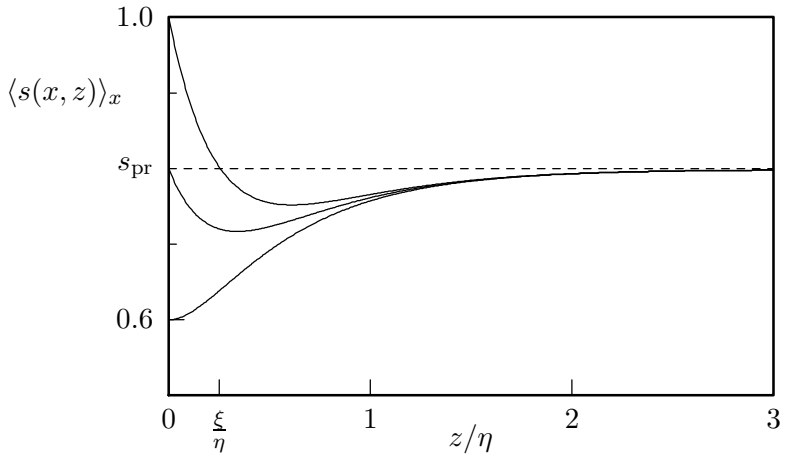

Figure 2.4: Boundary layers in the mean degree of orientation $\langle s(x,z)\rangle_x$, when $\xi = 0.25\eta$, $s_{\rm pr} = 0.8$, $\omega = 0.6$, $\mathrm{m} = 0.1\eta$, and $\Delta = 1.5$, when Dirichlet-like boundary conditions are applied on the degree of orientation. The boundary degree of orientation $\tilde{s}$ is respectively equal to 1 (top), $s_{\rm pr}$ (middle), and 0.6 (bottom).

whose general solution is (neglecting the term $\mathrm{e}^{\sqrt{3}\omega Z}$)

$$s_1(\bar{x},\bar{z},Z) \;=\; B_1(\bar{x},\bar{z})\mathrm{e}^{-\sqrt{3}\omega Z} - \mathrm{e}^{-\sqrt{3}\omega Z}\frac{\partial B_0(\bar{x},\bar{z})}{\partial \bar{z}}\left(Z + \frac{1}{2\sqrt{3}\,\omega}\right). \qquad (2.77)$$

By the use of the non-secularity rule (as expressed in Section 2.2.1) and the boundary condition at $\bar{z} = 0$, we get $B_0(\bar{x},\bar{z}) \;=\; -(s_{\rm pr} - \tilde{s})$.
The correspondent equation for $\theta_1(\bar{x},\bar{z},Z)$ is

$$\left(s_{\rm pr} - (s_{\rm pr} - \tilde{s})\mathrm{e}^{-\sqrt{3}\omega Z}\right)\theta_{1,ZZ} + 2\sqrt{3}\,\omega(s_{\rm pr} - \tilde{s})\,\mathrm{e}^{-\sqrt{3}\omega Z}\,(\theta_{1,Z} + A_{0,\bar{z}}) \;=\; 0 \qquad (2.78)$$

which does not allow the determination of $A_0(\bar{x},\bar{z})$ (so we must proceed to the next order) but can be solved. Finally, we find

$$s_1(\bar{x},\bar{z},Z) \;= B_1(\bar{x},\bar{z})\,\mathrm{e}^{-\sqrt{3}\omega Z} \qquad (2.79)$$

$$\theta_1(\bar{x},\bar{z},Z) \;= A_1(\bar{x},\bar{z}) + \frac{h(Z)}{\sqrt{3}\,\omega}\,\frac{\partial A_0(\bar{x},\bar{z})}{\partial \bar{z}}, \qquad (2.80)$$

where $h(Z) \;=\; \log\left(s_{\rm pr} - (s_{\rm pr} - \tilde{s})\,\mathrm{e}^{-\sqrt{3}\omega Z}\right) - \dfrac{(s_{\rm pr} - \tilde{s})\,\mathrm{e}^{-\sqrt{3}\omega Z}}{s_{\rm pr} - (s_{\rm pr} - \tilde{s})\,\mathrm{e}^{-\sqrt{3}\omega Z}}.$

Second order solution. We will limit ourselves to the evaluation of the terms A_0, A_1 and B_1. We need therefore to go to the $\mathcal{O}\left(\varepsilon^2\right)$ terms of the expansion. Here calculations get much more involved and the philosophy underneath them is very much the same as in the preceding Section, so we will only try to sketch the main

ideas.
The equations are:

$$\begin{aligned}
&\left(s_{\rm pr}-{\rm e}^{-\sqrt{3}\,\omega Z}\,(s_{\rm pr}-\tilde{s})\right)\theta_{2,ZZ}+2\sqrt{3}\,\omega(s_{\rm pr}-\tilde{s})\,{\rm e}^{-\sqrt{3}\,\omega Z}\,\theta_{2,Z}\\
&\quad+\left(s_{\rm pr}-{\rm e}^{-\sqrt{3}\,\omega Z}\,(s_{\rm pr}-\tilde{s})\right)A_{0,\bar{x}\bar{x}}+\left(s_{\rm pr}+3{\rm e}^{-\sqrt{3}\,\omega Z}\,(s_{\rm pr}-\tilde{s})\right)A_{0,\bar{z}\bar{z}}\\
&\quad+2\,{\rm e}^{-\sqrt{3}\,\omega Z}(s_{\rm pr}-\tilde{s})\log\left(s_{\rm pr}-{\rm e}^{-\sqrt{3}\,\omega Z}\,(s_{\rm pr}-\tilde{s})\right)A_{0,\bar{z}\bar{z}}\\
&\quad+2\sqrt{3}\,\omega(s_{\rm pr}-\tilde{s})\,{\rm e}^{-\sqrt{3}\,\omega Z}\,A_{1,\bar{z}}\\
&\quad-\frac{2\sqrt{3}\,\omega s_{\rm pr}^3\,{\rm e}^{-\sqrt{3}\,\omega Z}}{\left(s_{\rm pr}-{\rm e}^{-\sqrt{3}\,\omega Z}\,(s_{\rm pr}-\tilde{s})\right)^3}\,B_1\,A_{0,\bar{z}}\;=\;0
\end{aligned}\tag{2.81}$$

$$\begin{aligned}
&s_{2,ZZ}-3\omega^2 s_2-3\left(s_{\rm pr}-{\rm e}^{-\sqrt{3}\,\omega Z}\,(s_{\rm pr}-\tilde{s})\right)A_{0,\bar{x}}^2\\
&\quad-\frac{3s_{\rm pr}^4}{\left(s_{\rm pr}-{\rm e}^{-\sqrt{3}\,\omega Z}\,(s_{\rm pr}-\tilde{s})\right)^3}\,A_{0,z}^2-2\sqrt{3}\,\omega\,{\rm e}^{-\sqrt{3}\,\omega Z}\,B_{1,\bar{z}}\;=\;0.
\end{aligned}\tag{2.82}$$

Equation (2.81) can be solved and its expression involves the dilogarithm special function

$$\mathrm{Li}_2(\zeta)\;=\;-\int_0^{\zeta}\frac{\log(1-t)}{t}\,{\rm d}t,\tag{2.83}$$

which is real for real argument $\zeta\leq 1$ and complex for $\zeta>1$. If we study the asymptotic behavior of $\theta_2(\bar{x},\bar{z},Z)$ and use the fact that, for $Z\to+\infty$,

$$\mathrm{Li}_2\left(\frac{s_{\rm pr}}{s_{\rm pr}-\tilde{s}}{\rm e}^{\sqrt{3}\,\omega Z}\right)\;\sim\;-\frac{3\omega^2}{2}Z^2-\sqrt{3}\,\omega\,\log\left(-\frac{s_{\rm pr}}{s_{\rm pr}-\tilde{s}}\right)Z\,,\tag{2.84}$$

which follows from the expression [55, 5]

$$\mathrm{Li}_2(\zeta)+\mathrm{Li}_2\left(\frac{1}{\zeta}\right)\;=\;-\frac{\pi^2}{6}-\frac{1}{2}\log^2(-\zeta)\tag{2.85}$$

when we put $\zeta=\frac{s_{\rm pr}}{(s_{\rm pr}-\tilde{s})}{\rm e}^{\sqrt{3}\,\omega Z}$ and consider only the dominant infinite terms as $Z\to+\infty$; we arrive at the equation that $A_0(\bar{x},\bar{z})$ must satisfy to avoid secularity: $\Delta_2 A_0\;=\;0$. Therefore we have

$$A_0(\bar{x},\bar{z})\;=\;{\rm m}\bar{z}+\Delta\,{\rm e}^{-\bar{z}}\cos\bar{x}.\tag{2.86}$$

Note that all the imaginary parts that appear in the above calculations cancel out to yield a pure real final result for $\theta_2(\bar{x},\bar{z},Z)$, as expected.

We can now turn the attention to equation (2.82), find its solution $s_2(\bar{x},\bar{z},Z)$ and then study how $s_2(\bar{x},\bar{z},Z)$ behaves asymptotically at $Z\to+\infty$. It is then found for $B_1(\bar{x},\bar{z})$

$$B_1(\bar{x},\bar{z}) = \frac{\sqrt{3}\,(s_{\rm pr}-\tilde{s})}{\omega}\left(-\frac{3}{2}\mathrm{m}^2\bar{z}-\frac{\Delta^2}{4}(1-\mathrm{e}^{-2\bar{z}})\right.$$
$$\left.+3\mathrm{m}\,\Delta(1-\mathrm{e}^{-\bar{z}})\cos\bar{x}-\frac{\Delta^2}{2}(1-\mathrm{e}^{-2\bar{z}})\cos 2\bar{x}\right). \quad (2.87)$$

Third order solution. We still need to determine the function A_1, so we have to consider also the $\mathcal{O}\left(\varepsilon^3\right)$ equation for θ. As we are not interested in the actual solutions θ_3, but we need only to prevent secular terms in its expression, we can try to study the asymptotic behavior of the solution by means of a direct analysis of the equation. This latest is very intricate, but it is of the form

$$\left(s_{\rm pr}-(s_{\rm pr}-\tilde{s})\mathrm{e}^{-\sqrt{3}\omega Z}\right)\theta_{3,ZZ}(\bar{x},\bar{z},Z) = \alpha(\bar{x},\bar{z})+f(\bar{x},\bar{z},Z), \quad (2.88)$$

where $\alpha(\bar{x},\bar{z})$ and $f(\bar{x},\bar{z},Z)$ are regular functions and $f=\mathcal{O}\left(\mathrm{e}^{-\sqrt{3}\omega Z}\right)$ as $Z\to+\infty$. We can find the term A_1 without solving the equation, if we use the following ad-hoc lemma, where the variable x stands for our fast variable Z.

Lemma 2.2. Given the equation $\left(1+\mathrm{e}^{-x}\right)y''=\alpha+f(x)$ where $f(x)$ is continuous in $[a,+\infty)$, $a\geq 0$ and such that $\lim_{x\to+\infty} f(x)=0$,

(i) if $\alpha\neq 0$, then $y(x)\sim\frac{1}{2}\alpha\,x^2$ for $x\to+\infty$, independently on the given initial conditions

(ii) if $\alpha=0$ and $f(x)=\mathcal{O}\left(\mathrm{e}^{-x}\right)$, then the differential equation admits at least one solution $y(x)$ which is bounded in $[a,+\infty)$.

Proof. (i) Since $\alpha\neq 0$, $\frac{1}{2}\alpha\,x^2$ and its derivative go to infinity as $x\to+\infty$. This allows the use of L'Hôpital's theorem (even if no conditions are imposed on $y(x)$ as $x\to+\infty$, see [71]) to evaluate the limit

$$\lim_{x\to+\infty}\frac{y(x)}{\frac{1}{2}\alpha\,x^2}=\lim_{x\to+\infty}\frac{y'(x)}{\alpha\,x}=\lim_{x\to+\infty}\frac{y''(x)}{\alpha}=\lim_{x\to+\infty}\frac{\alpha+f(x)}{\alpha\,(1+\mathrm{e}^{-x})}=1. \quad (2.89)$$

(ii) Note that $f(x)=\mathcal{O}\left(\mathrm{e}^{-x}\right)$ guarantees that $\int_a^{+\infty}|f(x)|\,\mathrm{d}x<+\infty$.
We can write

$$y'(x)=y'(a)+\int_a^x\frac{f(t)}{1+\mathrm{e}^{-t}}\,\mathrm{d}t. \quad (2.90)$$

Since

$$\left|\int_a^{+\infty}\frac{f(t)}{1+\mathrm{e}^{-t}}\,\mathrm{d}t\right|\leq\int_a^{+\infty}\frac{|f(t)|}{|1+\mathrm{e}^{-t}|}\,\mathrm{d}t\leq\int_a^{+\infty}|f(t)|\,\mathrm{d}t<+\infty, \quad (2.91)$$

it is possible then to choose $y'(a) = -\int_a^{+\infty} \frac{f(t)}{1+\mathrm{e}^{-t}}\,\mathrm{d}t$, so that

$$y'(x) = -\int_x^{+\infty} \frac{f(t)}{1+\mathrm{e}^{-t}}\,\mathrm{d}t, \tag{2.92}$$

from which it follows $\lim_{x\to+\infty} y'(x) = 0$.

Moreover $\int_a^{+\infty} |y'(x)|\,\mathrm{d}x < +\infty$, in fact if we compare the order of infinity of $y'(x)$ with $\frac{1}{x^\gamma}$, $\gamma > 1$, we have (using again L'Hôpital's theorem)

$$\lim_{x\to+\infty} \frac{y'(x)}{\frac{1}{x^\gamma}} = \lim_{x\to+\infty} \frac{y''(x)}{-\gamma\,\frac{1}{x^{\gamma+1}}} = \lim_{x\to+\infty} -\gamma\,x^{\gamma+1}\,\frac{f(x)}{1+\mathrm{e}^{-x}} = 0. \tag{2.93}$$

Due to the continuity of $y(x)$ in $[a,+\infty)$, it enough to show that $y(x)$ has finite limit as $x \to +\infty$, to prove its boundedness.

$$\lim_{x\to+\infty} |y(x)| = \lim_{x\to+\infty} \left| y(a) + \int_a^x y'(t)\,\mathrm{d}t \right| \le |y(a)| + \lim_{x\to+\infty} \int_a^x |y'(t)|\,\mathrm{d}t < +\infty. \tag{2.94}$$

□

Lemma (2.2) says that we necessarily have to impose $\alpha = 0$ to prevent the solution $y(x)$ from being secular. This condition provides the equation that allows the determination of $A_1(\bar{x},\bar{z})$. Again it is found that $\Delta_2 A_1 = 0$. Matching the boundary conditions, we finally have

$$A_1(\bar{x},\bar{z}) = \frac{h(0)}{\sqrt{3}\,\omega}\left(-\mathrm{m} + \Delta\,\mathrm{e}^{-\bar{z}}\,\cos\bar{x}\right). \tag{2.95}$$

2.3 Effective weak anchoring

Once the boundary layer effects fade away, the main macroscopic effect of a rough surface on the director orientation is to allow for an effective surface tilt angle $\theta_\mathrm{b}(0)$, which apparently violates the homeotropic prescription $\theta(0) = 0$ (see (2.66) and (2.74)). It appears then natural to check whether the same macroscopic effect may be modeled through a weak anchoring potential, acting on a smooth surface. In this Section we pursue this similarity and we derive a relation connecting the microscopic roughness parameters with a macroscopic anchoring strength.

To solve the weak-anchoring problem, we consider a nematic liquid crystal which still spreads in the half-space $\mathcal{B} = \{z \ge 0\}$. To better compare our results with classical weak-anchoring models, we settle within Frank's director theory, and thus

look for the equilibrium distribution that minimizes the free-energy functional

$$\mathcal{F}[\mathbf{n}] := L \int_{\mathcal{B}} \left|\nabla \mathbf{n}\right|^2 dv + W \int_{\partial\mathcal{B}} f_{\rm w}[\mathbf{n}]\, da \ . \tag{2.96}$$

The bulk free-energy density in the functional (2.96) can be derived from its order-tensor theory counterpart by setting $s \equiv 1$ in (2.6). The anchoring potential $f_{\rm w}$ is required to attain its minimum at the homeotropic anchoring $\mathbf{n}\big|_{\partial\mathcal{B}} = \mathbf{e}_z$, while W is the *anchoring strength*.

We look again for equilibrium distributions of the type $\mathbf{n}(z) = \sin\theta(z)\,\mathbf{e}_x + \cos\theta(z)\,\mathbf{e}_z$. Thus, the free-energy functional (2.96) per unit transverse area can be written as

$$\mathcal{G}[\theta] := L \int \theta'^2(z)\, dz + W\, f_{\rm w}\big(\theta(0)\big) \ , \tag{2.97}$$

where we assume $f'_{\rm w}(0) = 0$ and $f''_{\rm w}(0) > 0$, in order to guarantee the homeotropic preference. The minimizers of (2.97) satisfy the trivial Euler-Lagrange equation $\theta'' = 0$ and the boundary condition

$$L\theta'(0) - W f'_{\rm w}\big(\theta(0)\big) = 0 \ . \tag{2.98}$$

When the anchoring strength W is large enough, the boundary condition (2.98) requires $\theta(0)$ to be small. When this is the case, a Taylor expansion in (2.98) supplies

$$\theta(0) \approx \frac{L\,\mathrm{m}}{W f''_{\rm w}(0)} = \zeta\,\mathrm{m} \ , \tag{2.99}$$

In (2.99) we have restored the notation $\mathrm{m} = \theta'(0)$, to better compare this estimate with our preceding results, and introduced the *surface extrapolation length*

$$\zeta := \frac{L}{W f''_{\rm w}(0)} \ , \tag{2.100}$$

a quantity that compares the relative strengths of the elastic and anchoring potentials.

The comparison between (2.99) and our results (2.66)-(2.74) relates the surface extrapolation length to the microscopic roughness parameters and/or the surface value of the degree of orientation. To further pursue this similarity we need to consider separately the different anchorings that may be applied to the degree of orientation.

- ⋆ When s is free to choose its boundary value, (2.66) shows that the surface extrapolation length is given by

$$\frac{\zeta}{\xi} = \frac{2\Delta^2}{\omega^2}\,\frac{\xi}{\eta} + \mathcal{O}\left(\frac{\xi^2}{\eta^2}\right) \ . \tag{2.101}$$

Thus, the anchoring strength increases when either the roughness amplitude Δ decreases (towards a smooth surface) or the roughness wavelength increases. An estimate of the order of magnitude of the effective roughness wavelength can be obtained by assuming typical values for the quantities involved in (2.101). Indeed, if we assume $\zeta \approx \xi$, $\Delta \approx 1$, and $\omega \approx \frac{1}{2}$, we arrive at $\eta \approx 10\xi$, which models a roughness wavelength in the hundredths of molecular lengths.

⋆ When the boundary conditions fix the value of the degree of orientation at the surface, (2.74) yields

$$\frac{\zeta}{\xi} = \frac{1}{\sqrt{3}\,\omega}\left(\log\frac{s_{\rm pr}}{\tilde{s}} + \frac{s_{\rm pr}-\tilde{s}}{\tilde{s}}\right) + \frac{2\Delta^2}{\omega^2}\,\frac{\xi}{\eta} + \mathcal{O}\left(\frac{\xi^2}{\eta^2}\right) . \tag{2.102}$$

Equation (2.102) shows that the surface extrapolation length includes two quite different contributions. The former depends on the difference between the boundary and the preferred values of the degree of orientation ($\tilde{s}$ and $s_{\rm pr}$, respectively), while the latter depends on the surface roughness and indeed coincides with (2.101). However, (2.102) may lose sense when $\tilde{s} > s_{\rm pr}$. Indeed, in this case ζ may become negative, so providing an *inverse* weak-anchoring effect. The physical origin of this odd result may be easily understood if we again resort to the $s^2|\nabla\theta|^2$-term in the free-energy density. By virtue of that term, the tilt angle prefers to limit its spatial variations in regions of higher s. If we force in the surface a higher degree of orientation than the bulk value, the tilt angle will flatten close to the surface, thus exhibiting the opposite behaviour with respect to that shown in Figure 2.3. Equation (2.102) shows that this inverse effect may occur whenever

$$\frac{\tilde{s}-s_{\rm pr}}{s_{\rm pr}} \gtrsim \frac{\sqrt{3}\Delta^2}{\omega}\,\frac{\xi}{\eta} + \mathcal{O}\left(\frac{\xi^2}{\eta^2}\right) . \tag{2.103}$$

If we again replace the estimates above for Δ, ω, η, we arrive at the result that a fixed degree of orientation is able to completely hide the roughness-induced effective weak anchoring whenever $\tilde{s}$ exceeds $s_{\rm pr}$ by the 10% of the preferred value $s_{\rm pr}$ itself.

2.4 Strong roughness limit

We now briefly discuss the limit in which the roughness wavelength η is much shorter than the nematic coherence length ξ. We assume therefore that $\varepsilon = \xi/\eta \gg 1$. This limit is unphysical since the coherence length is usually much smaller than all other characteristic lengths, but it is however mathematically appealing.

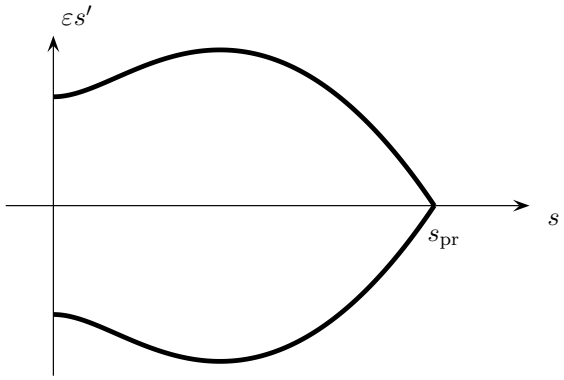

Figure 2.5: Example of the phase portrait of (2.108). In our case the positive branch has physical meaning. In particular the graph shows that when $s = 0$ (at the roughed surface) the derivative s' must be different from zero.

In agreement with the previous discussion, when the limiting surface is strongly grooved, the degree of order decreases near the boundary and we may expect that in our extreme limit the liquid crystal reaches a complete melting to the isotropic phase at $z = 0$. We will therefore assume that $s(x, 0) = 0$. It is then reasonable that the whole director variation will be limited in the region where s is close to zero, in fact in the functional (2.6) no energy cost is associated with the director distortions when $s = 0$. In our strong roughness limit the angle ϑ is allowed to be discontinuous (i.e. $|\nabla\vartheta|$ diverges to infinity) where $s = 0$, so that ϑ reaches its bulk value with a jump right at the surface, while the degree of order grows slowly to the bulk value ($s_{\rm pr}$). We can then neglect the term $s^2|\nabla\mathbf{n}|^2$ in the functional (2.6). In fact, in the region where $|\nabla\mathbf{n}|$ is different from zero, s is close to zero. On the other hand, when $s \neq 0$ the director distribution is nearly uniform. The approximate equilibrium distribution is therefore given by the critical points of

$$\int_0^{+\infty} \left(|\nabla s|^2 + \frac{3\, g(s)}{2\varepsilon^2} \right) \mathrm{d}\bar{z} \tag{2.104}$$

where $g(s)$ is the normalized Landau-de Gennes potential reported here for ease of reference

$$g(s) \;=\; s^4 - \frac{4}{3} s^3 \left(2 s_{\rm pr} - \frac{\omega^2}{s_{\rm pr}} \right) + 2 s^2 (s_{\rm pr}^2 - \omega^2). \tag{2.105}$$

We consider here for simplicity only the expression averaged along the x-direction, i.e. $s(\bar{x}, \bar{z}) = s(\bar{z})$.
It is clear, since the integrand in (2.104) does not explicitly depend on $\bar{z}$, that the following expression is conserved (it is a "constant of motion" in the language of

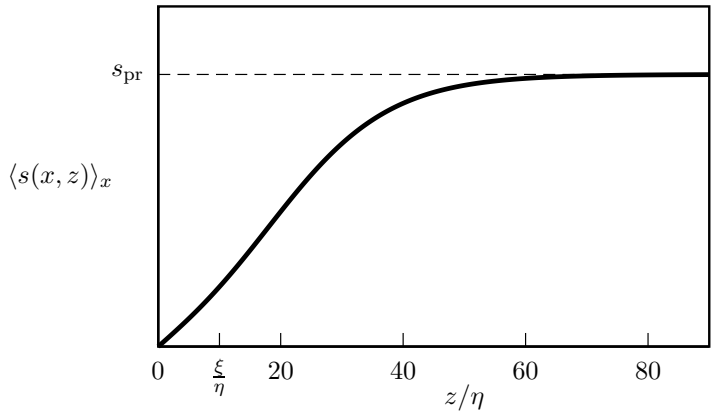

Figure 2.6: Numerical solution of (2.108) with $\varepsilon = 10$, $s_{\rm pr} = 0.8$ and $\omega = 0.6$.

mechanics)

$$\big(\varepsilon\, s'\big)^2 - \frac{3}{2} g(s) \;=\; H_0 \tag{2.106}$$

where the prime denotes differentiation with respect to the z-variable and the constant H_0 can be determined through the boundary conditions. We require

$$\begin{cases} s'(\bar{z}) \approx 0 \\ s(\bar{z}) \approx s_{\rm pr} \end{cases} \qquad \text{as } \bar{z} \to +\infty \tag{2.107}$$

which yields $H_0 = -\frac{3}{2} g(s_{\rm pr})$.
A first integration is therefore given by (see Figure 2.5)

$$\big(\varepsilon\, s'\big)^2 = \frac{3}{2}\big(g(s) - g(s_{\rm pr})\big). \tag{2.108}$$

This equation can be solved numerically, with the additional condition that $s(0) = 0$. The shape of the solution for $\varepsilon = 10$, $s_{\rm pr} = 0.8$ and $\omega = 0.6$ is given in Figure 2.6, to be compared with Figure 2.2.

As expected, since ξ is large, not much energy cost is associated with $s \neq s_{\rm pr}$ over quite long length-scales. Indeed, s reaches the bulk value (in our example) at approximately $z = 60\eta$.

2.5 Approximations in the boundary conditions

In this Section, we want to discuss the validity of two nontrivial simplifications we have introduced in our geometric setting. First, we have assumed that the boundary

is perfectly sinusoidal, while a physical surface will exhibit a whole roughness spectrum. Second, we have replaced an undulating boundary by an undulating boundary condition on a flat surface.

2.5.1 Roughness spectrum

Throughout the Chapter we have studied the bulk effects induced by the presence of a perfectly sinusoidal boundary. In real physical systems, however, the boundary roughness is mostly random, and a whole spectrum of roughness wavelengths is to be expected. In order to estimate whether the effects we have determined may be enforced or hidden by the interference between different wavelengths we briefly report here the results that may be obtained by replacing the boundary condition (2.8) by the more general

$$\theta(x,y,0) = \Delta_1 \cos\frac{x}{\eta_1} + \Delta_2 \cos\left(\frac{x}{\eta_2} + \phi_2\right) , \tag{2.109}$$

with $\eta_1/\eta_2 \notin \{\frac{1}{2}, 1, 2\}$, in order to avoid resonance effects.

We here simply report how the main results are to be modified when stress-free (Neumann) boundary conditions are applied on the degree of orientation. A brief detail of the calculations is reported in the following Subsection.

The first effect we have studied is the surface melting induced by the boundary roughness. Once we average along the x-direction and compute the solutions at the effective boundary $z = 0$, (2.64) is to be replaced by

$$\langle s(x,0)\rangle_x^{(2)} = s_{\rm pr}\left[1 - \frac{\mathrm{m}^2\xi^2}{\omega^2} - \frac{\xi^2}{\omega^2}\left(\frac{\Delta_1^2}{\eta_1^2} + \frac{\Delta_2^2}{\eta_2^2}\right) + \frac{2\xi^3}{\sqrt{3}\,\omega^3}\left(\frac{\Delta_1^2}{\eta_1^3} + \frac{\Delta_2^2}{\eta_2^3}\right)\right] + \mathcal{O}\left(\varepsilon^4\right) . \tag{2.110}$$

Expression (2.66) for the effective surface angle becomes

$$\theta_{\rm b}^{(2)}(0) = \frac{2\,\mathrm{m}\,\xi^2}{\omega^2}\left(\frac{\Delta_1^2}{\eta_1} + \frac{\Delta_2^2}{\eta_2}\right) . \tag{2.111}$$

Equations (2.110)-(2.111) show that the presence of more than one characteristic wavelength does not yield any dramatic result in the averaged quantities that interact with the bulk. In fact, they simply add their contributions, weighted by the roughness amplitudes. The situation is clearly more complex if we aim at computing the exact solutions within the boundary layers. In particular, the x-periodicity is lost as soon as the roughness wavelengths are not commensurable.

Two-scale calculations

Since we need to go to the second order to actually consider the boundary condition (2.109) (boundary conditions are imposed on $A_0(x,z)$, whose equation appears in the $\mathcal{O}\left(\xi^2\right)$ expression), the solutions up to $\mathcal{O}\left(\xi\right)$ are identical to those of §2.2.2 and indeed also the subsequent calculus is very similar. Following the usual technique, we obtain the expressions below, to be compared with those found in §2.2.2.

$$\theta_0(x,z,Z) = \mathrm{m}z + \Delta_1 \mathrm{e}^{-z/\eta_1}\cos\tfrac{x}{\eta_1} + \Delta_2 \mathrm{e}^{-z/\eta_2}\cos\left(\tfrac{x}{\eta_2}+\phi_2\right) \tag{2.112}$$

$$s_0(\bar{x},\bar{z},Z) = s_{\mathrm{pr}} \tag{2.113}$$

$$\theta_1(x,z,Z) = 0 \tag{2.114}$$

$$s_1(\bar{x},\bar{z},Z) = 0 \tag{2.115}$$

$$\theta_2(x,z,Z) = A_2(x,z) \tag{2.116}$$

$$\begin{aligned} s_2(\bar{x},\bar{z},Z) = {} & C_2(x,z)\,\mathrm{e}^{-\sqrt{3}\omega Z} - \tfrac{s_{\mathrm{pr}}}{\omega^2}\Big[\mathrm{m}^2 - 2\mathrm{m}\tfrac{\Delta_1}{\eta_1}\mathrm{e}^{-z/\eta_1}\cos\tfrac{x}{\eta_1} \\ & - 2\mathrm{m}\tfrac{\Delta_2}{\eta_2}\mathrm{e}^{-z/\eta_2}\cos\left(\tfrac{x}{\eta_2}+\phi\right) + \tfrac{\Delta_1^2}{\eta_1^2}\mathrm{e}^{-2\Delta_1^2/\eta_1^2} + \tfrac{\Delta_2^2}{\eta_2^2}\mathrm{e}^{-2\Delta_2^2/\eta_2^2} \\ & + \tfrac{2\Delta_1\Delta_2}{\eta_1\eta_2}\mathrm{e}^{-(z/\eta_1+z/\eta_2)}\cos\left(\tfrac{x}{\eta_2}-\tfrac{x}{\eta_1}+\phi\right)\Big] \end{aligned} \tag{2.117}$$

$$\theta_3(x,z,Z) = A_3(x,z) \tag{2.118}$$

$$s_3(\bar{x},\bar{z},Z) = C_3(x,z)\,\mathrm{e}^{-\sqrt{3}\omega Z}. \tag{2.119}$$

In accordance with the two-scale method, equations at higher orders, not reported here, allow us to determine the conditions that $C_2(x,z)$ and $A_2(x,z)$ must satisfy. Likewise the single wavelength case, it is found $C_2(x,z)=0$, while differences begin to arise when we write the equation for $A_2(x,z)$. Non-secularity condition on $\mathcal{O}\left(\xi^4\right)$ equation requires:

$$\begin{aligned} & \Delta_2 A_2 + \tfrac{8\mathrm{m}}{\omega^2}\left(\tfrac{\Delta_1^2}{\eta_1^3}\mathrm{e}^{-2z/\eta_1} + \tfrac{\Delta_2^2}{\eta_2^3}\mathrm{e}^{-2z/\eta_2}\right) \\ & \quad - \tfrac{4\Delta_1}{\eta_1\omega^2}\mathrm{e}^{-z/\eta_1}\left(\tfrac{\mathrm{m}^2}{\eta_1} + \tfrac{\Delta_1^2}{\eta_1^3}\mathrm{e}^{-2z/\eta_1} + 2\tfrac{\Delta_2^2}{\eta_2^3}\mathrm{e}^{-2z/\eta_2}\right)\cos\tfrac{x}{\eta_1} \\ & \quad - \tfrac{4\Delta_2}{\eta_2\omega^2}\mathrm{e}^{-z/\eta_2}\left(\tfrac{\mathrm{m}^2}{\eta_2} + \tfrac{\Delta_2^2}{\eta_2^3}\mathrm{e}^{-2z/\eta_2} + 2\tfrac{\Delta_1^2}{\eta_1^3}\mathrm{e}^{-2z/\eta_1}\right)\cos\left(\tfrac{x}{\eta_2}+\phi\right) \\ & \quad + \tfrac{8\mathrm{m}\Delta_1\Delta_2}{\eta_1\eta_2\omega^2}\mathrm{e}^{-z/\eta_1-z/\eta_2}\left(\tfrac{1}{\eta_1}+\tfrac{1}{\eta_2}\right)\cos\left(\tfrac{x}{\eta_2}-\tfrac{x}{\eta_1}+\phi\right) \\ & \quad - \tfrac{4\Delta_1^2\Delta_2}{\omega^2\eta_1^2\eta_2^2}\mathrm{e}^{-2z/\eta_1-z/\eta_2}\cos\left(\tfrac{x}{\eta_2}-2\tfrac{x}{\eta_1}+\phi\right) \\ & \quad - \tfrac{4\Delta_1\Delta_2^2}{\omega^2\eta_1^2\eta_2^2}\mathrm{e}^{-z/\eta_1-2z/\eta_2}\cos\left(2\tfrac{x}{\eta_2}-\tfrac{x}{\eta_1}+\phi\right) = 0. \end{aligned} \tag{2.120}$$

A solution to (2.120) is found by direct computation. When boundary conditions are taken into account, one finally has the sought expression for $A_2(x,z)$:

$$\begin{aligned}
A_2(x,z) =& \tfrac{2\mathrm{m}\Delta_1^2}{\omega^2\eta_1}\left(1-\mathrm{e}^{-\frac{2z}{\eta_1}}\right)+\tfrac{2\mathrm{m}\Delta_2^2}{\omega^2\eta_2}\left(1-\mathrm{e}^{-\frac{2z}{\eta_2}}\right)\\
&+\tfrac{\Delta_1}{\omega^2}\mathrm{e}^{-\frac{z}{\eta_1}}\left(-\tfrac{2\mathrm{m}^2\,z}{\eta_1}+\tfrac{2\mathrm{e}^{-\frac{2z}{\eta_2}}\Delta_2^2}{\eta_2(\eta_1+\eta_2)}-\tfrac{2\Delta_2^2}{\eta_2(\eta_1+\eta_2)}+\tfrac{\mathrm{e}^{-\frac{2z}{\eta_1}}\Delta_1^2}{2\eta_1^2}-\tfrac{\Delta_1^2}{2\eta_1^2}\right)\cos\tfrac{x}{\eta_1}\\
&+\tfrac{\Delta_2}{\omega^2}\mathrm{e}^{-\frac{z}{\eta_2}}\left(-\tfrac{2\mathrm{m}^2\,z}{\eta_2}+\tfrac{2\mathrm{e}^{-\frac{2z}{\eta_1}}\Delta_1^2}{\eta_1(\eta_1+\eta_2)}-\tfrac{2\Delta_1^2}{\eta_1(\eta_1+\eta_2)}+\tfrac{\mathrm{e}^{-\frac{2z}{\eta_2}}\Delta_2^2}{2\eta_2^2}-\tfrac{\Delta_2^2}{2\eta_2^2}\right)\cos\left(\tfrac{x}{\eta_2}+\phi\right)\\
&+\tfrac{2\mathrm{m}\Delta_1\Delta_2}{\omega^2}\left(\tfrac{\mathrm{e}^{-\left|\frac{z}{\eta_1}-\frac{z}{\eta_2}\right|}-\mathrm{e}^{-\frac{z}{\eta_1}-\frac{z}{\eta_2}}}{\eta_1}+\tfrac{\mathrm{e}^{-\left|\frac{z}{\eta_1}-\frac{z}{\eta_2}\right|}-\mathrm{e}^{-\frac{z}{\eta_1}-\frac{z}{\eta_2}}}{\eta_2}\right)\cos\left(\tfrac{x}{\eta_2}-\tfrac{x}{\eta_1}+\phi\right)\\
&-\tfrac{\Delta_2\Delta_1^2}{2\omega^2\eta_1\eta_2}\left(\mathrm{e}^{-\left|\frac{2z}{\eta_1}-\frac{z}{\eta_2}\right|}-\mathrm{e}^{-\frac{2z}{\eta_1}-\frac{z}{\eta_2}}\right)\cos\left(\tfrac{x}{\eta_2}-\tfrac{2x}{\eta_1}+\phi\right)\\
&-\tfrac{\Delta_2^2\Delta_1}{2\omega^2\eta_1\eta_2}\left(\mathrm{e}^{-\left|\frac{z}{\eta_1}-\frac{2z}{\eta_2}\right|}-\mathrm{e}^{-\frac{z}{\eta_1}-\frac{2z}{\eta_2}}\right)\cos\left(\tfrac{x}{\eta_1}-\tfrac{2x}{\eta_2}-2\phi\right). \qquad (2.121)
\end{aligned}$$

For generic roughness, we can avoid the particular cases of resonances, i.e., $\eta_1/\eta_2 \notin \{\frac{1}{2},1,2\}$, so that only the first two terms of $A_2(x,z)$ will contribute to the averaged expression along x. It is then readily found the effective surface angle (2.111). Similarly, the $\mathcal{O}\left(\xi^4\right)$ equation for $s_4(x,z,Z)$ yields the condition on $C_3(x,z)$: $\dfrac{\partial C_3}{\partial z}=0$. We can therefore determine C_3, since it is independent of the variable z, simply by imposing the boundary conditions,

$$\begin{aligned}
C_3(x,z) =& \tfrac{2\mathrm{spr}}{\sqrt{3}\omega^3}\left(\tfrac{\Delta_1^2}{\eta_1^3}+\tfrac{\Delta_2^2}{\eta_2^3}-\tfrac{\mathrm{m}\,\Delta_1}{\eta_1^2}\cos\tfrac{x}{\eta_1}-\tfrac{\mathrm{m}\,\Delta_2}{\eta_2^2}\cos\left(\tfrac{x}{\eta_2}+\phi\right)\right.\\
&\left.+\tfrac{\Delta_2\Delta_1\,(\eta_1+\eta_2)}{\eta_1^2\eta_2^2}\cos\left(\tfrac{x}{\eta_2}-\tfrac{x}{\eta_1}+\phi\right)\right). \qquad (2.122)
\end{aligned}$$

The two-scale approximation for the degree of order and its averaged value at the surface (2.110) are then readily obtained.

2.5.2 Modeling an undulating boundary

In §2.1.1 we have modeled a homeotropic boundary condition imposed on an undulating surface through an oscillating boundary condition imposed on a flat surface. In this Section we analyze the validity of such an approximation. In order to avoid unnecessarily lengthy calculations, we perform the present check within the Frank approximation, that is, by assuming that the nematic coherence length ξ is much

smaller than all other lengths involved in the problem. When this is the case, the degree of orientation is constrained to the value $s_{\rm pr}$ that minimizes the Landau-de Gennes potential, the Euler-Lagrange equation $(2.9)_1$ becomes Laplace's equation, and thus the tilt angle θ is harmonic.

We consider the region $\mathcal{A} = \{(x,z) : z \geq \delta\eta \sin x\}$ and look for a x-periodic harmonic function $\theta : \mathcal{A} \to \mathbb{R}$ (with x-period η) that satisfies the boundary conditions

$$\theta(x, \delta\eta \sin \tfrac{x}{\eta}) = \arctan\left(\delta \cos \tfrac{x}{\eta}\right), \qquad \theta(x,z) \approx \tilde{\theta}(z) \quad \text{as } z \to +\infty\,, \tag{2.123}$$

for all values of x. The boundary condition $(2.123)_1$ guarantees that the unit vector $\mathbf{n} = \sin\theta\,\mathbf{e}_x + \cos\theta\,\mathbf{e}_z$ is homeotropically anchored to the physical boundary, while $(2.123)_2$ guarantees that the bulk configuration depends only on the z-coordinate. Let us expand the tilt angle in power series of the amplitude coefficient δ:

$$\theta(x,z) = \sum_{n=0}^{\infty} \theta_n(x,z)\,\delta^n\,. \tag{2.124}$$

We next Fourier-expand all functions θ_n along the periodic direction

$$\theta_n(x,z) = \sum_{k=0}^{\infty} a_{n,k}(z)\,\cos\frac{kx}{\eta} + \sum_{k=1}^{\infty} b_{n,k}(z)\,\sin\frac{kx}{\eta}\,. \tag{2.125}$$

The Laplace equation implies then

$$\theta_n(x,z) = \sum_{k=0}^{\infty} \alpha_{n,k}\,\mathrm{e}^{-kz/\eta}\cos\frac{kx}{\eta} + \sum_{k=1}^{\infty} \beta_{n,k}\mathrm{e}^{-kz/\eta}\,\sin\frac{kx}{\eta}\,, \tag{2.126}$$

where the coefficients $\{\alpha_{n,k}, \beta_{n,k}\}$ can be determined by requiring $(2.123)_1$ to hold. In particular, we expand both sides of $(2.123)_1$ in Taylor series with respect to δ and require that the two expressions match at each order.

Let us now compute the value the tilt angle attains at the (horizontal) height $z = \delta\eta$, which we aim to consider as effective flat boundary (see Figure 2.1.1). We obtain

$$\theta(x,\delta\eta) = \left(\delta - \delta^2\right)\cos\frac{x}{\eta} + \frac{\delta^2}{2}\sin\frac{2x}{\eta} + O(\delta^3)\,. \tag{2.127}$$

In general, it can be shown that the nth coefficient θ_n in expansion (2.124) contains only Fourier components up to $k \leq n$. Thus, the boundary condition (2.8) used in the text is exact up to $O(\delta^2)$. Furthermore, the roughness amplitude Δ simply coincides with δ, the (dimensionless) ratio between the height of the sinusoidal undulations and the roughness wavelength.

2.6 Discussion

We have examined both the boundary layer structure and the bulk effects of a rough surface bounding a nematic liquid crystal. Our main results may be summarized as follows.

- ⋆ The roughness of the surface has been modeled by an oscillating anchoring condition, characterized by an oscillation amplitude Δ and a wavelength η. Figs. 2.2 and 2.4 show that the rough boundary induces a partial melting in a neighborhood (of size η) of the external boundary. When Neumann-like boundary conditions are imposed on the degree of orientation, (2.64) quantifies the mean degree of order at the boundary. By contrast, were s to be forced to a prescribed value $\tilde{s}$ on the surface, (2.67) and (2.71) show that the boundary condition induces a thin boundary layer, determined by the nematic coherence length ξ.

- ⋆ Once the degree of orientation decreases, the spatial variations of the tilt angle become cheaper, and thus θ is keen to steepen close to the external boundary. Figure 2.3 illustrates this effect. As a consequence, the effective boundary tilt angle $\theta_{\rm b}(0)$, extrapolated from the asymptotic outer solution $\theta_{\rm b}(z)$, becomes different from the null homeotropic prescription (see (2.66) and (2.74)). In §2.3 we have shown that a similar effective anchoring breaking takes place when a weak-anchoring potential is assumed on a smooth surface (see (2.100) for the characteristic surface extrapolation length). The comparison between (2.99) and (2.66)-(2.74) allows one to relate the surface extrapolation length to the microscopic roughness parameters and/or the surface value of the degree of orientation (see (2.102) and (2.103)).

- ⋆ When multiple wavelengths are considered in the boundary roughness, the overall effect is the sum of the contributions given by the single wavelengths separately. This fact is described in Section §2.5.

3
Induced biaxiality

Within the Landau-de Gennes theory, the ground state of nematic liquid crystals may be either isotropic or uniaxial, depending on the external temperature. However, biaxial domains have been predicted and observed, especially close to defects and external boundaries. Schopohl and Sluckin [74] analyzed in detail the biaxial core of a $+\frac{1}{2}$ nematic disclination. More recent studies show that a biaxial *cloud* surrounds most nematic defects [16]. Both analytic [70, 18] and numeric [28, 29] asymptotical descriptions of biaxial defect cores have been derived. Other examples of defect-induced biaxiality involve integer-charged disclinations [20, 53, 52] and cylindrical inclusions [59]. The onset of surface biaxiality is closely related to the presence of a symmetry-breaking special direction, which coincides with the surface normal [14]. Indeed, biaxiality has been predicted close to both external boundaries [58, 46] and internal isotropic-nematic interfaces [25, 68].

In this Chapter we show that biaxiality effects are closely related to, but not exclusively confined to, the examples above. In fact, within any spatially-varying director distribution, the director gradient itself breaks uniaxial symmetry about the director. We analyse in detail the structure of the elastic free energy density and come up to the result that, given a director distribution, it is possible to predict the onset of biaxiality, to determine the direction of the secondary optic axis and to estimate the intensity of biaxiality effects. We then apply our general considerations to some specific examples, both within the bulk and close to an external boundary. We remark that we are not dealing with intrinsically biaxial nematic liquid crystals, that is, systems in which the ground state itself becomes biaxial. Such systems, first observed by Yu and Saupe [85], deserve a different treatment [21, 80], since in them uniaxial symmetry is broken already at a molecular level.

This Chapter is organized as follows. In Sections 3.1 and 3.2 we quickly review the order-tensor theory and the free energy density we aim at minimizing. In Section 3.3 we derive and describe our main result, predicting a possible onset of biaxiality whenever the director is not uniform. In the following Section 3.4 we apply the preceding results to some specific examples. Section 3.5 analyzes the case of induced biaxiality close to a limiting surface. In Section 3.6 we collect and discuss our main

results.

3.1 ORDER TENSOR

The present Chapter is devoted to the study of *biaxial* nematics. In this general case, as explained in Chapter 1, the eigenvalues of the order tensor $\mathbf{Q}$ are all different and we can identify the director $\mathbf{n}$ as the eigenvector whose eigenvalue has a different sign with respect to the other two.

This definition may induce an artificial director discontinuity whenever the intermediate eigenvalue crosses 0. In turn, it yields an operative definition that works well when the order tensor is possibly biaxial, but however close to being uniaxial. Once we have introduced the director, once again we define the degree of orientation $s = \frac{3}{2}\mu_{\rm n}$, where $\mu_{\rm n}$ is the eigenvalue associated with $\mathbf{n}$. The other two eigenvalues $\mu_\pm$ can be finally written in terms of the *degree of biaxiality* b: $\lambda_\pm = -\frac{1}{3}\,s \pm b$. As a result we obtain

$$\mathbf{Q}_{\rm bia} = s\left(\mathbf{n}\otimes\mathbf{n} - \frac{1}{3}\,\mathbf{I}\right) + b\,(\mathbf{e}_+\otimes\mathbf{e}_+ - \mathbf{e}_-\otimes\mathbf{e}_-)\,, \tag{3.1}$$

which is analogous to (1.16) of Chapter 1. Here, we have written s and b instead of s_1 and s_2, as we did in (1.16), since in the nearly uniaxial case s and b are more commonly used when one is willing to stress the physical meanings of the coefficients, i.e., s is degree of order and b stands for the degree of biaxiality. Indeed, when $b = 0$, expression (3.1) reduces itself to the uniaxial order tensor.

The sign of b is unessential, since it only involves an exchange between $\mathbf{e}_+$ and $\mathbf{e}_-$. The degree of biaxiality does always satisfy $|b| \le \frac{1}{3}|s|$. Indeed, when $|b| = \frac{1}{3}|s|$ one of the eigenvalues vanishes, and greater biaxiality values would in fact announce an abrupt change in the director (and in the degree of orientation as well).

3.2 FREE ENERGY FUNCTIONAL

Equilibrium states of nematic liquid crystals are identified as extremals of the free-energy functional whose density, in the absence of external fields, comprises two terms

$$\Psi(\mathbf{Q},\nabla\mathbf{Q}) = \Psi_{\rm el}(\mathbf{Q},\nabla\mathbf{Q}) + \Psi_{\rm LdG}(\mathbf{Q})\,. \tag{3.2}$$

Though all the calculations we report could be repeated in a more general framework, we will adopt the 1-constant approximation for the elastic contribution $\Psi_{\rm el}$

$$\Psi_{\rm el}(\mathbf{Q},\nabla\mathbf{Q}) = \frac{L}{2}\,|\nabla\mathbf{Q}|^2\,, \tag{3.3}$$

where L is an average elastic constant.

The Landau-de Gennes potential Ψ_{LdG} (see Section §1.4.2) is a temperature-dependent thermodynamic contribution that takes into account the material tendency to spontaneously arrange in ordered or disordered states:

$$\Psi_{\mathrm{LdG}}(\mathbf{Q}) = A\ \mathrm{tr}\,\mathbf{Q}^2 - B\ \mathrm{tr}\,\mathbf{Q}^3 + C\ \mathrm{tr}\,\mathbf{Q}^4\ . \tag{3.4}$$

The material parameter C must be positive to keep the free-energy functional bounded from below. The potential (3.4) depends only on the eigenvalues of $\mathbf{Q}$, and penalizes biaxial states. Insertion of (3.1) into (3.4) returns

$$\begin{aligned}\Psi_{\mathrm{LdG}}(s,b) = &\frac{2}{9}\left(Cs^4 - Bs^3 + 3As^2\right)\\ &+ \frac{2}{9}\left(6Cs^2 + 9Bs + 9A\right)b^2 + 2Cb^4\ .\end{aligned} \tag{3.5}$$

Let $\alpha = 3A/(Cs_{\mathrm{pr}}^2)$. The absolute minimum of Ψ_{LdG} is located at the uniaxial configuration $(s_{\mathrm{pr}} > 0, b = 0)$, provided

$$\alpha \in [-2, 1] \quad \text{and} \quad B = \tfrac{2}{3}\,Cs_{\mathrm{pr}}(\alpha + 2)\ . \tag{3.6}$$

When looking for minimizers of the free energy functional, we take into account that Landau-de Gennes' contribution usually dominates the elastic one. This approximation holds as long as we do not get too close to a nematic defect. Indeed, experimental observations confirm that neither s nor b depart easily from their preferred values $(s_{\mathrm{pr}}, 0)$.

We then envisage a two-step minimization. In the first step (s, b) are constrained to their optimal values. Minimization proceeds exactly as in Frank's director theory and yields an optimal distribution $\mathbf{n}(\mathbf{r})$. In the second step, we fix the director distribution and determine the perturbative corrections it induces in the optimal values of the scalar order parameters. As a result, we prove that non-uniform director configurations may induce a nonzero degree of biaxiality, and a reduction in the degree of orientation. As a by-product we determine how a non-zero director gradient breaks the local axial symmetry induced by the director, and which direction is chosen by most molecules (among those orthogonal to $\mathbf{n}$).

3.3 Bulk biaxiality

We assume that a specific director distribution $\mathbf{n}(\mathbf{r})$ has been determined by minimizing Frank's free-energy functional, constrained by suitable boundary conditions.

The director distribution may also take into account the effects of any possible external field.

We now prove the following decomposition for the director gradient

$$\begin{aligned}\nabla\mathbf{n} = \lambda_2\,\mathbf{e}_2\otimes\mathbf{e}_2 + \lambda_3\,\mathbf{e}_3\otimes\mathbf{e}_3 + \big(\operatorname{curl}\mathbf{n}\wedge\mathbf{n}\big)\otimes\mathbf{n}\\ + \tfrac{1}{2}\,(\mathbf{n}\cdot\operatorname{curl}\mathbf{n})\,\mathbf{W}(\mathbf{n})\,,\end{aligned} \tag{3.7}$$

where $\mathbf{W}(\mathbf{n})$ denotes the skew tensor associated with $\mathbf{n}$, that is the tensor such that $\mathbf{W}(\mathbf{n})\mathbf{v} = \mathbf{n}\wedge\mathbf{v}$ for any $\mathbf{v}$. We remind that, given two vectors $\mathbf{u}$, $\mathbf{v}$, the tensor product $(\mathbf{u}\otimes\mathbf{v})$ is defined as the second order tensor such that

$$(\mathbf{u}\otimes\mathbf{v})\mathbf{a} = (\mathbf{v}\cdot\mathbf{a})\,\mathbf{u} \quad \text{for any vector } \mathbf{a}\,. \tag{3.8}$$

Furthermore, $\{\lambda_2,\lambda_3\}$, $\{\mathbf{e}_2,\mathbf{e}_3\}$ are respectively the eigenvalues and eigenvectors of the *symmetric part* of $\mathbf{G} = \nabla\mathbf{n} - (\nabla\mathbf{n})\mathbf{n}\otimes\mathbf{n}$, the third eigenvector of $\operatorname{sym}\mathbf{G}$ being $\mathbf{n}$, with null eigenvalue. We remark that

$$\operatorname{div}\mathbf{n} = \operatorname{tr}\nabla\mathbf{n} = \lambda_2+\lambda_3\,. \tag{3.9}$$

PROOF OF (3.7). Let sym and skw be the symmetric and antisymmetric part of a tensor:

$$\operatorname{sym}\mathbf{A} = \tfrac{1}{2}\left(\mathbf{A}+\mathbf{A}^T\right) \tag{3.10}$$

$$\operatorname{skw}\mathbf{A} = \tfrac{1}{2}\left(\mathbf{A}-\mathbf{A}^T\right). \tag{3.11}$$

In order to characterize the tensor $\nabla\mathbf{n}$ we begin by noticing that

$$(\nabla\mathbf{n})^T\mathbf{n} = \tfrac{1}{2}\nabla\big(\mathbf{n}\cdot\mathbf{n}\big) = \mathbf{0}\,, \tag{3.12}$$

since $\mathbf{n}$ is a unit vector. Furthermore, we recall that by definition

$$(\operatorname{skw}\nabla\mathbf{n})\,\mathbf{v} = \tfrac{1}{2}\operatorname{curl}\mathbf{n}\wedge\mathbf{v}. \tag{3.13}$$

Thus,

$$\begin{aligned}(\nabla\mathbf{n})\mathbf{n} &= \big(\operatorname{sym}\nabla\mathbf{n} + \operatorname{skw}\nabla\mathbf{n}\big)\mathbf{n}\\ &= \tfrac{1}{2}\left((\nabla\mathbf{n})+(\nabla\mathbf{n})^T\right)\mathbf{n} + \tfrac{1}{2}\operatorname{curl}\mathbf{n}\wedge\mathbf{n}\\ &= \tfrac{1}{2}\,(\nabla\mathbf{n})\mathbf{n} + \tfrac{1}{2}\operatorname{curl}\mathbf{n}\wedge\mathbf{n}\,,\end{aligned} \tag{3.14}$$

where we have used (3.13) and (3.12). We can finally write

$$(\nabla\mathbf{n})\mathbf{n} = \operatorname{curl}\mathbf{n}\wedge\mathbf{n}. \tag{3.15}$$

If $\mathbf{a}$, $\mathbf{b}$ and $\mathbf{c}$ are three arbitrary vectors, we remind the vector identity

$$(\mathbf{a}\wedge\mathbf{b})\wedge\mathbf{c} = (\mathbf{a}\cdot\mathbf{c})\mathbf{b} - (\mathbf{b}\cdot\mathbf{c})\mathbf{a}, \tag{3.16}$$

which can also be written using the skew tensor $\mathbf{W}(\mathbf{a}\wedge\mathbf{b})$ associated with $\mathbf{a}\wedge\mathbf{b}$,

$$\mathbf{W}(\mathbf{a}\wedge\mathbf{b}) \;=\; \mathbf{b}\otimes\mathbf{a}-\mathbf{a}\otimes\mathbf{b}. \tag{3.17}$$

Let

$$\mathbf{G}=\nabla\mathbf{n}-(\nabla\mathbf{n})\mathbf{n}\otimes\mathbf{n}. \tag{3.18}$$

For any vector $\mathbf{v}$,

$$\begin{aligned}(\operatorname{skw}\mathbf{G})\,\mathbf{v} &= \tfrac{1}{2}(\mathbf{G}-\mathbf{G}^T)\,\mathbf{v}\\ &= \tfrac{1}{2}\Big[\nabla\mathbf{n}-(\nabla\mathbf{n})\mathbf{n}\otimes\mathbf{n}-(\nabla\mathbf{n})^T+\mathbf{n}\otimes(\nabla\mathbf{n})\mathbf{n}\Big]\,\mathbf{v}\\ &= \Big[\operatorname{skw}(\nabla\mathbf{n})+\tfrac{1}{2}\big(\mathbf{n}\otimes(\nabla\mathbf{n})\mathbf{n}-(\nabla\mathbf{n})\mathbf{n}\otimes\mathbf{n}\big)\Big]\,\mathbf{v}\\ &= \tfrac{1}{2}\operatorname{curl}\mathbf{n}\wedge\mathbf{v}+\tfrac{1}{2}\mathbf{W}\big((\nabla\mathbf{n})\mathbf{n}\wedge\mathbf{n}\big)\,\mathbf{v}\\ &= \tfrac{1}{2}\operatorname{curl}\mathbf{n}\wedge\mathbf{v}+\tfrac{1}{2}\left((\nabla\mathbf{n})\mathbf{n}\wedge\mathbf{n}\right)\wedge\mathbf{v}\\ &= \tfrac{1}{2}\big(\operatorname{curl}\mathbf{n}+(\operatorname{curl}\mathbf{n}\wedge\mathbf{n})\wedge\mathbf{n}\big)\wedge\mathbf{v}\\ &= \tfrac{1}{2}\big(\operatorname{curl}\mathbf{n}+(\mathbf{n}\cdot\operatorname{curl}\mathbf{n})\,\mathbf{n}-\operatorname{curl}\mathbf{n}\big)\wedge\mathbf{v}\\ &= \tfrac{1}{2}(\mathbf{n}\cdot\operatorname{curl}\mathbf{n})\,\mathbf{n}\wedge\mathbf{v}\\ &= \tfrac{1}{2}(\mathbf{n}\cdot\operatorname{curl}\mathbf{n})\,\mathbf{W}(\mathbf{n})\,\mathbf{v},\end{aligned} \tag{3.19}$$

where $\mathbf{W}\big((\nabla\mathbf{n})\mathbf{n}\wedge\mathbf{n}\big)$ is the skew tensor associated with the vector $(\nabla\mathbf{n})\mathbf{n}\wedge\mathbf{n}$. Thus,

$$\begin{aligned}\nabla\mathbf{n}=\mathbf{G}+(\nabla\mathbf{n})\mathbf{n}\otimes\mathbf{n} \;&=\; \operatorname{sym}\mathbf{G}+\operatorname{skw}\mathbf{G}+(\nabla\mathbf{n})\mathbf{n}\otimes\mathbf{n}\\ &= \operatorname{sym}\mathbf{G}+\tfrac{1}{2}(\mathbf{n}\cdot\operatorname{curl}\mathbf{n})\,\mathbf{W}(\mathbf{n})+\big(\operatorname{curl}\mathbf{n}\wedge\mathbf{n}\big)\otimes\mathbf{n}\\ &= \lambda_2\mathbf{e}_2\otimes\mathbf{e}_2+\lambda_3\mathbf{e}_3\otimes\mathbf{e}_3+\tfrac{1}{2}(\mathbf{n}\cdot\operatorname{curl}\mathbf{n})\mathbf{W}(\mathbf{n})+\big(\operatorname{curl}\mathbf{n}\wedge\mathbf{n}\big)\otimes\mathbf{n}\,,\end{aligned} \tag{3.20}$$

where $\{\lambda_2,\lambda_3\}$ and $\{\mathbf{e}_2,\mathbf{e}_3\}$ are respectively the eigenvalues and eigenvectors of $\operatorname{sym}\mathbf{G}$. The eigenvectors $\{\mathbf{e}_2,\mathbf{e}_3\}$ are orthogonal to $\mathbf{n}$, since (3.19) implies

$$\begin{aligned}(\operatorname{sym}\mathbf{G})\,\mathbf{n} &= \mathbf{G}\,\mathbf{n}-(\operatorname{skw}\mathbf{G})\,\mathbf{n}\\ &= \big(\nabla\mathbf{n}-(\nabla\mathbf{n})\mathbf{n}\otimes\mathbf{n}\big)\,\mathbf{n}-\tfrac{1}{2}(\mathbf{n}\cdot\operatorname{curl}\mathbf{n})\,\mathbf{W}(\mathbf{n})\,\mathbf{n} \;=\; \mathbf{0}\,.\end{aligned} \tag{3.21}$$

□

Let $\mathbf{S}$ be the symmetric tensor $\mathbf{S}=(\nabla\mathbf{n})\,(\nabla\mathbf{n})^T$. By virtue of (3.12) the director $\mathbf{n}$ is an eigenvector of $\mathbf{S}$ (with null eigenvalue). We can now give one of the main results of this Chapter, stated in form of theorem for clarity.

Theorem 3.1. The elastic free energy density (3.3) may be given the form

$$\begin{aligned}\Psi_{\rm el} = L\Big[&\tfrac{1}{3}\,|\nabla s|^2+|\nabla b|^2+s^2\,|\nabla\mathbf{n}|^2+b^2\Big(|\nabla\mathbf{n}|^2+4|(\nabla\mathbf{e}_+)^T\mathbf{e}_-|^2\Big)\\ &-2sb\Big(\mathbf{e}_+\cdot\mathbf{S}\mathbf{e}_+-\mathbf{e}_-\cdot\mathbf{S}\mathbf{e}_-\Big)\Big]\,.\end{aligned} \tag{3.22}$$

PROOF. Let us differentiate equation (3.1). We obtain

$$\nabla\mathbf{Q} = \left(\mathbf{n}\otimes\mathbf{n} - \tfrac{1}{3}\mathbf{I}\right)\otimes\nabla s + s\left(\nabla\mathbf{n}\odot\mathbf{n} + \mathbf{n}\otimes\nabla\mathbf{n}\right) + \left(\mathbf{e}_+\otimes\mathbf{e}_+ - \mathbf{e}_-\otimes\mathbf{e}_-\right)\otimes\nabla b \\ + b\big(\nabla\mathbf{e}_+\odot\mathbf{e}_+ + \mathbf{e}_+\otimes\nabla\mathbf{e}_+ - \nabla\mathbf{e}_-\odot\mathbf{e}_- - \mathbf{e}_-\otimes\nabla\mathbf{e}_-\big)\,, \tag{3.23}$$

where, given a second-order tensor $\mathbf{L}$ and a vector $\mathbf{u}$, $(\mathbf{L}\odot\mathbf{u})$ is defined as the third-order tensor such that

$$(\mathbf{L}\odot\mathbf{u})\mathbf{a} = \mathbf{L}\mathbf{a}\otimes\mathbf{u} \quad \text{for any vector } \mathbf{a}\,. \tag{3.24}$$

When computing the square norm of $\nabla\mathbf{Q}$, we can make extensive use of the property (3.12) and also take into account that

$$\mathbf{u}\cdot\mathbf{v} = 0 \quad\Longrightarrow\quad (\nabla\mathbf{u})^T\mathbf{v} = -(\nabla\mathbf{v})^T\mathbf{u}\,. \tag{3.25}$$

There are many possible ways to calculate $|\nabla\mathbf{Q}|^2$. Among them, the one we will give here is not the most elegant, but it has the major advantage of being elementary. Indeed, it makes use of the Cartesian components of $\nabla\mathbf{Q}$, in the same spirit of the proof of (1.123).

$$\mathrm{Q}_{ij,k} = \left(\mathrm{n}_i\mathrm{n}_j - \tfrac{1}{3}\delta_{ij}\right)s_{,k} + s\left(\mathrm{n}_{i,k}\mathrm{n}_j + \mathrm{n}_i\mathrm{n}_{j,k}\right) + \left(\mathrm{e}^+_i\mathrm{e}^+_j - \mathrm{e}^-_i\mathrm{e}^-_j\right)b_{,k} \\ + b\left(\mathrm{e}^+_{i,k}\mathrm{e}^+_j + \mathrm{e}^+_i\mathrm{e}^+_{j,k} - \mathrm{e}^-_{i,k}\mathrm{e}^-_j - \mathrm{e}^-_i\mathrm{e}^-_{j,k}\right)\,, \tag{3.26}$$

where, to simplify notation, we have here used a superscript $+$ and $-$ to identify the components of $\mathbf{e}_+$ and $\mathbf{e}_-$, respectively.

The property (3.12) can greatly simplify the calculation of $|\nabla\mathbf{Q}|^2$. For an arbitrary unit vector $\mathbf{v}$, it reads

$$\mathrm{v}_{j,k}\,\mathrm{v}_j \;=\; 0. \tag{3.27}$$

In the following calculation, we suppress the sign of summation for ease of reading and use the convention that *for each term* a summation is to be intended *only* on those indexes explicitly appearing in the term

$$\begin{aligned}
|\nabla\mathbf{Q}|^2 \;&=\; \sum_{ijk}\mathrm{Q}_{ij,k}\,\mathrm{Q}_{ij,k} \\
&= s^2_{,k} - \frac{1}{3}s^2_{,k} - \frac{1}{3}s^2_{,k} + \frac{3}{9}s^2_{,k} - \frac{1}{3}s_{,k}\,b_{,k} + \frac{1}{3}s_{,k}\,b_{,k} \\
&+ s^2\,\mathrm{n}^2_{i,k} + s\,b\,\mathrm{n}_j\,\mathrm{e}^+_{j,k}\,\mathrm{e}^+_i\,\mathrm{n}_{i,k} - s\,b\,\mathrm{n}_j\,\mathrm{e}^-_{j,k}\,\mathrm{e}^-_i\,\mathrm{n}_{i,k} \\
&+ s^2\,\mathrm{n}^2_{j,k} + s\,b\,\mathrm{n}_i\,\mathrm{e}^+_{i,k}\,\mathrm{e}^+_j\,\mathrm{n}_{j,k} - s\,b\,\mathrm{n}_i\,\mathrm{e}^-_{i,k}\,\mathrm{e}^-_j\,\mathrm{n}_{j,k} \\
&- \frac{1}{3}\,s_{,k}\,b_{,k} + b^2_{,k} + \frac{1}{3}\,s_{,k}\,b_{,k} + b^2_{,k} \\
&+ s\,b\,\mathrm{n}_i\,\mathrm{e}^+_{i,k}\,\mathrm{e}^+_j\,\mathrm{n}_{j,k} + b^2\left(\mathrm{e}^+_{i,k}\right)^2 - b^2\,\mathrm{e}^-_i\,\mathrm{e}^+_{i,k}\,\mathrm{e}^+_j\,\mathrm{e}^-_{j,k} \\
&+ s\,b\,\mathrm{n}_j\,\mathrm{e}^+_{j,k}\,\mathrm{e}^+_i\,\mathrm{n}_{i,k} + b^2\left(\mathrm{e}^+_{j,k}\right)^2 - b^2\,\mathrm{e}^+_i\,\mathrm{e}^-_{i,k}\,\mathrm{e}^-_j\,\mathrm{e}^+_{j,k} \\
&- s\,b\,\mathrm{n}_i\,\mathrm{e}^-_{i,k}\,\mathrm{e}^-_j\,\mathrm{n}_{j,k} - b^2\,\mathrm{e}^+_i\,\mathrm{e}^-_{i,k}\,\mathrm{e}^-_j\,\mathrm{e}^+_{j,k} + b^2\left(\mathrm{e}^-_{i,k}\right)^2 \\
&- s\,b\,\mathrm{n}_j\,\mathrm{e}^-_{j,k}\,\mathrm{e}^-_i\,\mathrm{n}_{i,k} - b^2\,\mathrm{e}^-_i\,\mathrm{e}^+_{i,k}\,\mathrm{e}^+_j\,\mathrm{e}^-_{j,k} + b^2\left(\mathrm{e}^-_{j,k}\right)^2\,.
\end{aligned} \tag{3.28}$$

As a consequence, we obtain

$$\begin{aligned}
|\nabla \mathbf{Q}|^2 &= \tfrac{2}{3}\,|\nabla s|^2 + 2\,|\nabla b|^2 + 2s^2\,|\nabla \mathbf{n}|^2 \\
&\quad + 2b^2\Big(|\nabla \mathbf{e}_+|^2 + |\nabla \mathbf{e}_-|^2 - 2(\nabla \mathbf{e}_+)^T\mathbf{e}_- \cdot (\nabla \mathbf{e}_-)^T\mathbf{e}_+\Big) \\
&\quad + 4sb\Big((\nabla \mathbf{e}_+)^T\mathbf{n} \cdot (\nabla \mathbf{n})^T\mathbf{e}_+ - (\nabla \mathbf{e}_-)^T\mathbf{n} \cdot (\nabla \mathbf{n})^T\mathbf{e}_-\Big) \\
&= \tfrac{2}{3}\,|\nabla s|^2 + 2\,|\nabla b|^2 + 2s^2\,|\nabla \mathbf{n}|^2 \\
&\quad + 2b^2\Big(|\nabla \mathbf{e}_+|^2 + |\nabla \mathbf{e}_-|^2 + 2|(\nabla \mathbf{e}_+)^T\mathbf{e}_-|^2\Big) \\
&\quad - 4sb\Big(\mathbf{e}_+ \cdot (\nabla \mathbf{n})(\nabla \mathbf{n})^T\mathbf{e}_+ - \mathbf{e}_- \cdot (\nabla \mathbf{n})(\nabla \mathbf{n})^T\mathbf{e}_-\Big)\,,
\end{aligned} \tag{3.29}$$

where we have used

$$(\nabla \mathbf{e}_-)^T\mathbf{e}_+ \,=\, -(\nabla \mathbf{e}_+)^T\mathbf{e}_-, \qquad\qquad (\nabla \mathbf{e}_\pm)^T\mathbf{n} \,=\, -(\nabla \mathbf{n})^T\mathbf{e}_\pm. \tag{3.30}$$

We can further simplify expression (3.29) if we consider that

$$\begin{aligned}
|\nabla \mathbf{e}_+|^2 + |\nabla \mathbf{e}_-|^2 &= \big|(\nabla \mathbf{e}_+)^T\big|^2 + \big|(\nabla \mathbf{e}_-)^T\big|^2 \\
&= \big|(\nabla \mathbf{e}_+)^T\mathbf{n}\big|^2 + \big|(\nabla \mathbf{e}_+)^T\mathbf{e}_-\big|^2 \\
&\quad + \big|(\nabla \mathbf{e}_-)^T\mathbf{n}\big|^2 + \big|(\nabla \mathbf{e}_-)^T\mathbf{e}_+\big|^2 \\
&= \big|\nabla \mathbf{n}\big|^2 + 2\big|(\nabla \mathbf{e}_+)^T\mathbf{e}_-\big|^2.
\end{aligned} \tag{3.31}$$

Provided we define $\mathbf{S} = (\nabla \mathbf{n})(\nabla \mathbf{n})^T$ and by using (3.31), it is immediate to give (3.29) the expression quoted in (3.22). □

Let us analyze in detail the different terms appearing in (3.22). The first two terms are trivial, since they simply penalize spatial variations of the scalar order parameters. They remind that, even in the presence of spatially-varying preferred values $\big(s_{\rm opt}(\mathbf{r}), b_{\rm opt}(\mathbf{r})\big)$, the equilibrium distribution may not imitate the optimal values. The third term is proportional to $s^2\,|\nabla \mathbf{n}|^2$. This term has been already extensively studied in [36, 19] and in Chapter 2. Its net effect is a decrease in the degree of orientation in places where the director gradient is most rapidly varying. In particular, it strongly pushes the system towards the isotropic state $s = 0$ when the director gradient diverges. The second-last term is proportional to b^2. Since it is positive definite, it simply enhances the character of $b = 0$ as optimal biaxiality value. Thus, were not for the final term we will next consider, biaxiality would never arise naturally in a nematic liquid crystal.

The last term in (3.22) is linear in b. It shifts the optimal biaxiality value away from $b = 0$. In order to minimize the complete free energy density it is worth

to maximize the multiplying factor depending on $\mathbf{S}$. This condition determines the directions $\{\mathbf{e}_+, \mathbf{e}_-\}$ in which the order tensor $\mathbf{Q}$ is pushed to break uniaxial symmetry. Indeed, the term within brackets is maximized when $\{\mathbf{e}_+, \mathbf{e}_-\}$ coincide with the two eigenvectors of $\mathbf{S}$ that are orthogonal to $\mathbf{n}$. If we denote by μ_+, μ_- the correspondent eigenvalues, the linear term becomes simply proportional to $(\mu_+ - \mu_-)$.

Remark 3.2. In fact, let $\mathbf{v}_+$ and $\mathbf{v}_-$ the unit eigenvectors of $\mathbf{S}$ (other than $\mathbf{n}$). If α is the angle between $\mathbf{e}_+$ and $\mathbf{v}_+$, the following decomposition holds

$$\mathbf{e}_+ = \cos\alpha\,\mathbf{v}_+ + \sin\alpha\,\mathbf{v}_- \qquad\qquad \mathbf{e}_- = -\sin\alpha\,\mathbf{v}_+ + \cos\alpha\,\mathbf{v}_-. \tag{3.32}$$

Thus, a little arrangement gives

$$\mathbf{e}_+ \cdot \mathbf{S}\mathbf{e}_+ - \mathbf{e}_- \cdot \mathbf{S}\mathbf{e}_- = (\mu_+ - \mu_-)\cos 2\alpha. \tag{3.33}$$

Extrema of (3.33) are given by $\alpha = \frac{\pi}{2}k$, $k \in \mathbb{Z}$, so that, $\mathbf{e}_+$ and $\mathbf{e}_-$ are indeed along the eigendirections of $\mathbf{S}$.

We thus arrive at the following result.

Natural Biaxiality Rule. *Consider the symmetric tensor* $\mathbf{S} = (\nabla\mathbf{n})\,(\nabla\mathbf{n})^T$. *It always possesses a null eigenvalue (with eigenvector* $\mathbf{n}$*). Whenever its other two eigenvalues do not coincide, biaxiality is naturally induced in the system, and the optimal eigendirections of* $\mathbf{Q}$ *coincide with those of* $\mathbf{S}$.

Since the symmetric tensor $\mathbf{S} = (\nabla\mathbf{n})(\nabla\mathbf{n})^T$ plays a crucial role in inducing biaxiality we now analyze it in more detail. We will need the vector relations reported here below. Let $\mathbf{a}$,$\mathbf{b}$,$\mathbf{c}$ be arbitrary vectors,

$$\mathbf{W}(\mathbf{n})\,(\mathbf{a}\otimes\mathbf{b}) = (\mathbf{n}\wedge\mathbf{a})\otimes\mathbf{b}, \tag{3.34}$$

$$\begin{aligned}(\mathbf{a}\otimes\mathbf{b})\,\mathbf{W}(\mathbf{n}) &= \big(\mathbf{W}(\mathbf{n})^T(\mathbf{a}\otimes\mathbf{b})^T\big)^T = -\big(\mathbf{W}(\mathbf{n})(\mathbf{b}\otimes\mathbf{a})\big)^T \\ &= -\big((\mathbf{n}\wedge\mathbf{b})\otimes\mathbf{a}\big)^T = -\mathbf{a}\otimes(\mathbf{n}\wedge\mathbf{b}),\end{aligned} \tag{3.35}$$

$$\begin{aligned}\mathbf{W}^2(\mathbf{n})\,\mathbf{a} &= \mathbf{W}(\mathbf{n})\,(\mathbf{n}\wedge\mathbf{a}) = \mathbf{n}\wedge(\mathbf{n}\wedge\mathbf{a}) \\ &= (\mathbf{n}\cdot\mathbf{a})\,\mathbf{n} - \mathbf{a} = -\big(\mathbf{I} - \mathbf{n}\otimes\mathbf{n}\big)\mathbf{a}.\end{aligned} \tag{3.36}$$

In particular, we are interested in the following special cases of (3.34) and (3.35)

$$\mathbf{W}(\mathbf{n})\,(\mathbf{e}_2\otimes\mathbf{e}_2) = \mathbf{e}_3\otimes\mathbf{e}_2 \qquad \mathbf{W}(\mathbf{n})\,(\mathbf{e}_3\otimes\mathbf{e}_3) = -\,\mathbf{e}_2\otimes\mathbf{e}_3 \tag{3.37}$$

$$(\mathbf{e}_2\otimes\mathbf{e}_2)\,\mathbf{W}(\mathbf{n}) = -\,\mathbf{e}_2\otimes\mathbf{e}_3 \qquad (\mathbf{e}_3\otimes\mathbf{e}_3)\,\mathbf{W}(\mathbf{n}) = \mathbf{e}_3\otimes\mathbf{e}_2. \tag{3.38}$$

We are now ready to express the tensor $\mathbf{S}$ when (3.7) is used in place of $\nabla\mathbf{n}$.

$$\begin{aligned}\mathbf{S} &= \big[\lambda_2\mathbf{e}_2\otimes\mathbf{e}_2+\lambda_3\mathbf{e}_3\otimes\mathbf{e}_3+\tfrac{1}{2}(\mathbf{n}\cdot\operatorname{curl}\mathbf{n})\mathbf{W}(\mathbf{n})+\big(\operatorname{curl}\mathbf{n}\wedge\mathbf{n}\big)\otimes\mathbf{n}\big]\\ &\quad\cdot\big[\lambda_2\mathbf{e}_2\otimes\mathbf{e}_2+\lambda_3\mathbf{e}_3\otimes\mathbf{e}_3-\tfrac{1}{2}(\mathbf{n}\cdot\operatorname{curl}\mathbf{n})\mathbf{W}(\mathbf{n})+\mathbf{n}\otimes\big(\operatorname{curl}\mathbf{n}\wedge\mathbf{n}\big)\big]\\ &=\lambda_2^2\mathbf{e}_2\otimes\mathbf{e}_2+(\lambda_2-\lambda_3)(\mathbf{n}\cdot\operatorname{curl}\mathbf{n})\operatorname{sym}(\mathbf{e}_2\otimes\mathbf{e}_3)+\lambda_3^2\mathbf{e}_3\otimes\mathbf{e}_3\\ &\quad+\tfrac{1}{4}(\mathbf{n}\cdot\operatorname{curl}\mathbf{n})^2(\mathbf{I}-\mathbf{n}\otimes\mathbf{n})+\big(\operatorname{curl}\mathbf{n}\wedge\mathbf{n}\big)\otimes\big(\operatorname{curl}\mathbf{n}\wedge\mathbf{n}\big)\,.\end{aligned}\tag{3.39}$$

Let $\{0,\mu_+,\mu_-\}$ be the eigenvalues of $\mathbf{S}$. The onset of biaxiality depends whether they latter two are equal or not. Let $\operatorname{curl}\mathbf{n}=c_n\,\mathbf{n}+c_2\,\mathbf{e}_2+c_3\,\mathbf{e}_3$. From (3.39) we obtain

$$(\mu_+-\mu_-)^2\;=\;(c_2^2-c_3^2+\lambda_3^2-\lambda_2^2)^2+4\,c_2^2c_3^2\,.\tag{3.40}$$

Remark 3.3. It is maybe useful to write the matrix form of $\mathbf{S}$, as given by (3.39)

$$\mathbf{S}\;=\;\begin{pmatrix}0 & 0 & 0\\ 0 & c_3^2+\frac{c_n^2}{4}+\lambda_2^2+\frac{1}{2}c_n\,(\lambda_2-\lambda_3) & -c_2c_3\\ 0 & -c_2c_3 & c_2^2+\frac{c_n^2}{4}+\lambda_3^2+\frac{1}{2}c_n\,(\lambda_2-\lambda_3)\end{pmatrix}.\tag{3.41}$$

It is now easier to evaluate the non-zero eigenvalues of $\mathbf{S}$

$$\begin{aligned}\mu_\pm\;&=\frac{1}{4}\Big(c_2^2+2c_3^2+c_n^2+2c_n\,(\lambda_2-\lambda_3)+2\,\big({\lambda_2}^2+{\lambda_3}^2\big)\\ &\quad\pm2\sqrt{\big(c_2^2-c_3^2+\lambda_3^2-\lambda_2^2\big)^2+4\,c_2^2c_3^2}\Big),\end{aligned}\tag{3.42}$$

and then verify (3.40).

In the following Sections we will apply the above results to some practical situations, in order to better interpret their implications.

3.4 Splay, bend and twist biaxiality

3.4.1 Planar fields

We begin by considering a quite common case, that is a situation in which the director is everywhere orthogonal to a fixed direction $\mathbf{e}_z$. When this is the case we can write

$$\mathbf{n}(\mathbf{r})=\cos\vartheta(\mathbf{r})\,\mathbf{e}_x+\sin\vartheta(\mathbf{r})\,\mathbf{e}_y\,,\tag{3.43}$$

where the tilt angle ϑ may depend on all three coordinates. Easy manipulations allow us to write

$$\nabla\mathbf{n}=\mathbf{n}_\perp\otimes\nabla\vartheta\,,\tag{3.44}$$

with $\mathbf{n}_\perp = -\sin\vartheta(\mathbf{r})\,\mathbf{e}_x + \cos\vartheta(\mathbf{r})\,\mathbf{e}_y$. Thus,

$$\mathbf{S} = \big(\mathbf{n}_\perp \otimes \nabla\vartheta\big)\big(\nabla\vartheta \otimes \mathbf{n}_\perp\big) = \big|\nabla\vartheta\big|^2\,\mathbf{n}_\perp \otimes \mathbf{n}_\perp\,. \tag{3.45}$$

The tensor $\mathbf{S}$ is symmetric as expected. Its eigenframe is $\{\mathbf{n}, \mathbf{n}_\perp, \mathbf{e}_z\}$, with eigenvalues $\{0, |\nabla\vartheta|^2, 0\}$. The relevant eigenvalue difference $(\mu_+ - \mu_-) = |\nabla\vartheta|^2$ induces spontaneous biaxiality whenever the tilt angle is not uniform. This result has a simple physical interpretation. Since the director does never lift from the $(\mathbf{e}_x, \mathbf{e}_y)$ plane, nematic molecules are naturally induced to avoid the direction $\mathbf{e}_z$. As a consequence, the order tensor breaks the uniaxial symmetry. It decreases the eigenvalue in the $\mathbf{e}_z$ direction, and consequently increases the planar eigenvalue associated with $\mathbf{n}_\perp$.

Among the many examples of nontrivial planar configurations we next analyze three particularly significant ones.

3.4.2 Pure splay

The splay field is defined as $\mathbf{n}(\mathbf{r}) = \mathbf{e}_r$, where $\mathbf{e}_r$ is the radial unit vector in cylindrical co-ordinates. If we complete an orthonormal basis by introducing the tangential and axial unit vectors $\mathbf{e}_\vartheta, \mathbf{e}_z$, standard calculations allow to prove that

$$\nabla\mathbf{n} = \frac{1}{r}\,\mathbf{e}_\vartheta \otimes \mathbf{e}_\vartheta \quad \text{and} \quad \mathbf{S} = \frac{1}{r^2}\,\mathbf{e}_\vartheta \otimes \mathbf{e}_\vartheta\,. \tag{3.46}$$

Thus, $\mu_+ = r^{-2}$, $\mu_- = 0$, and the elastic free energy density is given by

$$\Psi_{\text{el}} = L\left(\frac{1}{3}\,|\nabla s|^2 + |\nabla b|^2 + \frac{(s-b)^2}{r^2}\right)\,. \tag{3.47}$$

Biaxiality favours the tangential direction with respect to the axial direction. The r^{-2} factor implies that biaxiality (and the degree of orientation decrease as well) is expected to show close to the symmetry axis. Figures 3 and 5 of [20] exactly confirm this result.

3.4.3 Pure bend

We again consider the same cylindrical coordinate frame above, and analyze the bend field $\mathbf{n}(\mathbf{r}) = \mathbf{e}_\vartheta$. We obtain

$$\nabla\mathbf{n} = -\frac{1}{r}\,\mathbf{e}_r \otimes \mathbf{e}_\vartheta \quad \text{and} \quad \mathbf{S} = \frac{1}{r^2}\,\mathbf{e}_r \otimes \mathbf{e}_r\,. \tag{3.48}$$

Again, $\mu_+ = r^{-2}$, $\mu_- = 0$, and the elastic free energy density can be given exactly the same expression (3.47). Biaxiality now favours the radial direction, and again concentrates close to the (disclination) symmetry axis.

3.4.4 Pure twist

In Cartesian coordinates the twist field is defined as $\mathbf{n}(\mathbf{r}) = \cos kz\,\mathbf{e}_x + \sin kz\,\mathbf{e}_y$. If we again introduce the unit vector $\mathbf{n}_\perp(\mathbf{r}) = -\sin kz\,\mathbf{e}_x + \cos kz\,\mathbf{e}_y$, we obtain

$$\nabla\mathbf{n} = k\,\mathbf{n}_\perp \otimes \mathbf{e}_z \quad \text{and} \quad \mathbf{S} = k^2\,\mathbf{n}_\perp \otimes \mathbf{n}_\perp\,. \tag{3.49}$$

We now have $\mu_+ = k^2$, $\mu_- = 0$. Again, biaxiality favours $\mathbf{n}_\perp$, that is, the (x, y) plane, with respect to the transverse direction $\mathbf{e}_z$. The elastic free energy density still coincides with (3.47), with only a k^2 replacing the r^{-2} factor. However, this coincidence must not induce to guess that Ψ_{el} does always depend on s and b only through the combination $(s - b)$, as we will evidence below.

3.4.5 Escape in the third dimension

We now consider a nontrivial three-dimensional example: the escape in the third-dimension. This field was first determined by Cladis and Kléman [30] as an everywhere continuous director field able to fulfill homeotropic boundary conditions on a cylinder of radius R. Let $\mathbf{n}(\mathbf{r}) = \cos\phi(r)\,\mathbf{e}_r + \sin\phi(r)\,\mathbf{e}_z$ be the director field, and let $\mathbf{n}_\perp(\mathbf{r}) = -\sin\phi(r)\,\mathbf{e}_r + \cos\phi(r)\,\mathbf{e}_z$. We obtain

$$\nabla\mathbf{n} = \frac{\cos\phi}{r}\,\mathbf{e}_\vartheta \otimes \mathbf{e}_\vartheta + \phi'\,\mathbf{n}_\perp \otimes \mathbf{e}_r\,, \tag{3.50}$$

$$\mathbf{S} = \frac{\cos^2\phi}{r^2}\,\mathbf{e}_\vartheta \otimes \mathbf{e}_\vartheta + \phi'^2\,\mathbf{n}_\perp \otimes \mathbf{n}_\perp\,. \tag{3.51}$$

Expression (3.51) for $\mathbf{S}$ shows that, within the order tensor $\mathbf{Q}$, either $\mathbf{n}_\perp$ or $\mathbf{e}_\vartheta$ may be preferred, depending on whether ϕ'^2 is greater or smaller than $\cos^2\phi/r^2$. This result turns out to be particularly challenging, if we consider that in Cladis-Kléman's escape in the third dimension the tilt angle ϕ is given by

$$\phi(r) = \frac{\pi}{2} - 2\arctan\frac{r}{R}\,. \tag{3.52}$$

A simple calculation allows us to show that (3.52) implies $\phi'^2 = \cos^2\phi/r^2$. Thus, the third-dimension escape turns out to be one of the few spatially-varying director fields which do not induce any biaxiality. The elastic free-energy density in Cladis-Kleman's third-dimension escape is given by

$$\Psi_{\text{el}} = L\left(\frac{1}{3}\,|\nabla s|^2 + |\nabla b|^2 + \frac{8R^2\,s^2}{(r^2+R^2)^2} + \frac{4(R^4+r^4)\,b^2}{r^2(r^2+R^2)^2}\right)\,. \tag{3.53}$$

3.5 SURFACE BIAXIALITY

In this Section we estimate the degree of biaxiality induced by an external surface on which strong anchoring is enforced. We consider separately the cases of homeotropic and planar anchoring.

3.5.1 Preliminary geometric tools

We first recall some results on differential forms and moving frames that will be useful in the following (see [26, 44, 66] for details). Since we are only interested in two dimensional manifolds *embedded* in $\mathbb{R}^3$, we will always assume that a Riemann structure (i.e., a scalar product) on the surface is induced by $\mathbb{R}^3$. We will denote the dimension of a manifold with a superscript number, i.e., $\mathcal{M}^2$ for a surface.
Let $\{\mathbf{e}_i\}$, $i = 1...n$ be a *frame* for the manifold $\mathcal{M}^n$, that is, each $\mathbf{e}_i$ is a vector field such that at every point of $\mathcal{M}^n$ the $\{\mathbf{e}_i\}$ are n independent tangent vectors.
A connection is then defined by assigning the *vectors* $\nabla_{\mathbf{X}}\mathbf{e}_i$, being $\mathbf{X}$ an arbitrary vector field. The derivative $\nabla_{\mathbf{X}}\mathbf{e}_i$ can be decomposed with respect to the frame $\{\mathbf{e}_i\}$: $\nabla_{\mathbf{X}}\mathbf{e}_i = \mathbf{e}_k\,\omega^k{}_i(\mathbf{X})$. Here, $\omega^k{}_i(\mathbf{X})$ assigns to each vector $\mathbf{X}$ the component of $\nabla_{\mathbf{X}}\mathbf{e}_i$ along $\mathbf{e}_k$.
By the defining properties of connections, the functions $\mathbf{X} \mapsto \omega^k{}_i(\mathbf{X})$ are linear. Therefore $\omega^k{}_i$ are *differential 1-forms* and are called *connection forms*.
By the arbitrariness of $\mathbf{X}$, we can write

$$\nabla\mathbf{e}_i = \mathbf{e}_k \otimes \omega^k{}_i. \tag{3.54}$$

Let us now introduce the *dual frame* of 1-forms, or co-frame, $\{\theta^j\}$, $j = 1...n$. This is the set of 1-forms such that $\theta^j(\mathbf{e}_i) = \delta^j_i$. Since $\{\theta^j\}$ are a base for the space of the 1-forms, the connection forms can be written as a linear combination of the $\{\theta^j\}$. We will denote by ω^k_{ji} the components of the connection forms with respect to θ^j:

$$\omega^k{}_i = \omega^k_{ji}\,\theta^j. \tag{3.55}$$

On Riemannian manifolds, the metric tensor g is by definition symmetric and positive definite. Therefore, we can always find an *orthonormal* frame field such that $\mathbf{e}_i \cdot \mathbf{e}_j = \delta_{ij}$, where the scalar (dot) product is inherited by the euclidean ambient space. Equivalently, we can write the metric tensor using the dual language

$$g = \sum_{i=1}^{n} \theta^i \otimes \theta^i. \tag{3.56}$$

We are now able to state what is the basic theorem for our purposes [26].

Theorem 3.4. Suppose $(\mathcal{M}^n, g)$ is a Riemann manifold and $\{\mathbf{e}_i\}$, $i = 1...n$ is an *orthonormal* frame field (a set of tangent vectors on a neighborhood $U \subset \mathcal{M}$ which is linearly independent everywhere) with dual frame $\{\theta^j\}$, $j = 1...n$.
Then there exists a unique set of n^2 differential *1-forms* $\omega^j{}_k$ on U such that

$$\mathrm{d}\theta^j = \theta^k \wedge \omega^j{}_k \tag{3.57}$$

$$\omega^j{}_k + \omega^k{}_j = 0. \tag{3.58}$$

Here "d" stands for the exterior derivative of forms and "$\wedge$" means the exterior product of forms. Equation (3.58) guarantees that the connection forms are "skew symmetric" and therefore there are only $n(n-1)/2$ independent forms. The connection $\omega^j{}_k$ is completely identified by this theorem and when $\{\mathbf{e}_i\}$ is a *coordinate frame*, it corresponds to the usual Levi-Civita connection (which is metric compatible and torsion free). Equation (3.57) is usually called *first structure equation*.

Remark 3.5. Usually in continuum mechanics the ambient space is $\mathbb{R}^3$ and a slightly different language is used. We write, as usually done in previous Sections, the gradient $\nabla_{\mathbf{X}}\mathbf{e}$ as $(\nabla\mathbf{e})\mathbf{X}$.
Let $\{\mathbf{e}_i\}$, $i = 1, 2, 3$ be an orthonormal moving frame. For every two orthogonal vectors $\mathbf{a}$ and $\mathbf{b}$ we have

$$\nabla(\mathbf{a}\cdot\mathbf{b}) = 0 = (\nabla\mathbf{a})^T\mathbf{b} + (\nabla\mathbf{b})^T\mathbf{a}. \tag{3.59}$$

Moreover, by (3.54), we have $(\nabla\mathbf{e}_i)\mathbf{e}_j = \mathbf{e}_k\,\omega^k{}_i(\mathbf{e}_j)$. Orthonormality then assures that $\omega^k{}_i(\mathbf{e}_j) = \mathbf{e}_k\cdot(\nabla\mathbf{e}_i)\mathbf{e}_j$.
When we employ the dual base and the decomposition (3.55), we also obtain

$$\omega^k_i(\mathbf{e}_j) = \omega^k_{hi}\,\theta^h(\mathbf{e}_j) = \omega^k_{hi}\,\delta^h_j = \omega^k_{ji}. \tag{3.60}$$

It is now easy to show that the skew symmetry of the connection forms, as stated in (3.58), is a consequence of the orthonormality condition

$$\begin{aligned}\omega^k_{ji} &= \mathbf{e}_k\cdot(\nabla\mathbf{e}_i)\mathbf{e}_j = (\nabla\mathbf{e}_i)^T\mathbf{e}_k\cdot\mathbf{e}_j \\ &= -(\nabla\mathbf{e}_k)^T\mathbf{e}_i\cdot\mathbf{e}_j = -\mathbf{e}_i\cdot(\nabla\mathbf{e}_k)\mathbf{e}_j = -\omega^i_{jk}.\end{aligned} \tag{3.61}$$

Parallel surfaces

Let $\mathcal{M}^3$, $p \in \mathcal{M}^3$, be a Riemann manifold with a coordinate chart (u^1, u^2, τ) around p. Take the metric tensor

$$g = g_{11}\mathrm{d}u^1 \otimes \mathrm{d}u^1 + g_{22}\mathrm{d}u^2 \otimes \mathrm{d}u^2 + \mathrm{d}\tau \otimes \mathrm{d}\tau. \tag{3.62}$$

The orthonormal dual frame is therefore

$$\theta^1 = \sqrt{g_{11}}\,\mathrm{d}u^1, \qquad \theta^2 = \sqrt{g_{22}}\,\mathrm{d}u^2, \qquad \theta^3 = \mathrm{d}\tau, \tag{3.63}$$

and the vector frame is

$$\mathbf{e}_1 = \frac{1}{\sqrt{g_{11}}}\frac{\partial}{\partial u^1}, \qquad \mathbf{e}_2 = \frac{1}{\sqrt{g_{22}}}\frac{\partial}{\partial u^2}, \qquad \mathbf{e}_3 = \frac{\partial}{\partial \tau}. \tag{3.64}$$

Taking the exterior derivative of (3.63) we obtain

$$\begin{cases} \mathrm{d}\theta^1 = \frac{g_{11,2}}{2\sqrt{g_{11}}}\,\mathrm{d}u^2\wedge\mathrm{d}u^1 + \frac{g_{11,3}}{2\sqrt{g_{11}}}\,\mathrm{d}\tau\wedge\mathrm{d}u^1 = \frac{\left(\sqrt{g_{11}}\right)_{,2}}{\sqrt{g_{11}g_{22}}}\,\theta^2\wedge\theta^1 + \frac{g_{11,3}}{2g_{11}}\,\theta^3\wedge\theta^1 \\ \mathrm{d}\theta^2 = \frac{g_{22,1}}{2\sqrt{g_{22}}}\,\mathrm{d}u^1\wedge\mathrm{d}u^2 + \frac{g_{22,3}}{2\sqrt{g_{22}}}\,\mathrm{d}\tau\wedge\mathrm{d}u^2 = \frac{\left(\sqrt{g_{22}}\right)_{,1}}{\sqrt{g_{11}g_{22}}}\,\theta^1\wedge\theta^2 + \frac{g_{22,3}}{2g_{22}}\,\theta^3\wedge\theta^2 \\ \mathrm{d}\theta^3 = 0. \end{cases} \tag{3.65}$$

The connection forms can now be calculated simply by comparing (3.65) with the first structure equations $\mathrm{d}\theta^j = \theta^k\wedge\omega^j{}_k$. Explicitly these are

$$\begin{cases} \mathrm{d}\theta^1 = \theta^2\wedge\omega^1{}_2 + \theta^3\wedge\omega^1{}_3 \\ \mathrm{d}\theta^2 = \theta^1\wedge\omega^2{}_1 + \theta^3\wedge\omega^2{}_3 \\ \mathrm{d}\theta^3 = \theta^1\wedge\omega^3{}_1 + \theta^2\wedge\omega^3{}_2. \end{cases} \tag{3.66}$$

After some algebra, we obtain

$$\begin{cases} \omega^1{}_2 = -\omega^2{}_1 = \frac{\left(\sqrt{g_{11}}\right)_{,2}}{\sqrt{g_{11}g_{22}}}\,\theta^1 - \frac{\left(\sqrt{g_{22}}\right)_{,1}}{\sqrt{g_{11}g_{22}}}\,\theta^2 \\ \omega^1{}_3 = -\omega^3{}_1 = \frac{g_{11,3}}{2g_{11}}\,\theta^1 \\ \omega^2{}_3 = -\omega^3{}_2 = \frac{g_{22,3}}{2g_{22}}\,\theta^2. \end{cases} \tag{3.67}$$

In particular, we note that $\nabla\mathbf{e}_3$ have the simple expression

$$\nabla\mathbf{e}_3 = \mathbf{e}_1\otimes\omega^1{}_3 + \mathbf{e}_2\otimes\omega^2{}_3 = \frac{g_{11,3}}{2g_{11}}\,\mathbf{e}_1\otimes\theta^1 + \frac{g_{22,3}}{2g_{22}}\,\mathbf{e}_2\otimes\theta^2. \tag{3.68}$$

Using the vector relation, commonly adopted in continuum mechanics for an orthonormal frame of reference in $\mathbb{R}^3$, $(\mathbf{a}\otimes\mathbf{b})\mathbf{c} = \mathbf{a}(\mathbf{b}\cdot\mathbf{c})$, we can thus write the gradient in the familiar form

$$\nabla\mathbf{e}_3 = \frac{g_{11,3}}{2g_{11}}\,\mathbf{e}_1\otimes\mathbf{e}_1 + \frac{g_{22,3}}{2g_{22}}\,\mathbf{e}_2\otimes\mathbf{e}_2. \tag{3.69}$$

Remark 3.6. One may wonder whether it is possible to introduce new coordinates (v^1, v^2) such that the unit vectors $\mathbf{e}_1$ and $\mathbf{e}_2$ are *coordinate* vectors with respect to the new system. Dually, the requirement is that (v^1, v^2) satisfy $\theta^1 = \mathrm{d}v^1$ and $\theta^2 = \mathrm{d}v^2$. By the property of the exterior derivative $\mathrm{d}^2 = 0$ (i.e., taking the derivative twice yields zero), we

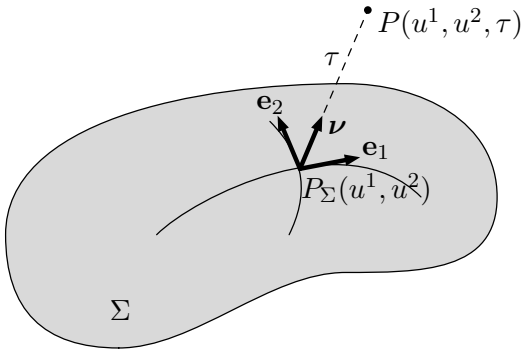

Figure 3.1: Geometric setting for the surface parametrization introduced in the text.

locally have that (v^1, v^2) are the sought coordinates if and only if $\mathrm{d}\theta^1 = 0$ and $\mathrm{d}\theta^2 = 0$. In our case, this translates into

$$\mathrm{d}\theta^1 = (\sqrt{g_{11}})_{,2}\, \mathrm{d}u^2 \wedge \mathrm{d}u^1 = 0 \qquad \Rightarrow \qquad g_{11,2} = 0 \tag{3.70}$$

$$\mathrm{d}\theta^1 = (\sqrt{g_{22}})_{,1}\, \mathrm{d}u^1 \wedge \mathrm{d}u^2 = 0 \qquad \Rightarrow \qquad g_{22,1} = 0. \tag{3.71}$$

Hence, the connection forms in this particular case reduce to

$$\begin{cases} \omega^1{}_2 = -\omega^2{}_1 = 0 \\ \omega^1{}_3 = -\omega^3{}_1 = \frac{g_{11,3}}{2g_{11}}\, \mathrm{d}v^1 \\ \omega^2{}_3 = -\omega^3{}_2 = \frac{g_{22,3}}{2g_{22}}\, \mathrm{d}v^2. \end{cases} \tag{3.72}$$

Let now Σ be the smooth surface (embedded in $\mathbb{R}^3$), which bounds the system we are interested in. Let $\boldsymbol{\nu}$ be the unit normal, everywhere pointing in the direction of the bulk. In a neighbourhood of a point $P_\Sigma \in \Sigma$, with local coordinates (u^1, u^2), we parameterize points in the bulk through a coordinate set (u^1, u^2, τ) such that

$$P(u^1, u^2, \tau) = P_\Sigma(u^1, u^2) + \tau\, \boldsymbol{\nu}(u^1, u^2)\,, \tag{3.73}$$

where P_Σ is the projection of P onto Σ, and τ is the distance of P from the same surface. Of course such a parametrization is in general well-defined only in a neighbourhood of the point P_Σ.

For every fixed value of τ, (3.73) defines a *parallel surface* Σ_τ at a distance τ from Σ. Locally in $\mathbb{R}^3$, these parallel surfaces give a regular change of variable between the Cartesian coordinates (x, y, z) in $\mathbb{R}^3$ and (u^1, u^2, τ). Otherwise stated, when we consider only those points where the transformation is regular, (u^1, u^2, τ) are a local coordinate chart for the manifold $\mathcal{M}^3$ given by the union of the parallel surfaces.

Suppose that the coordinate vectors $\mathbf{r}_1 = \dfrac{\partial P_\Sigma}{\partial u^1}$ and $\mathbf{r}_2 = \dfrac{\partial P_\Sigma}{\partial u^2}$ are such that

$$\mathbf{r}_1 \cdot \mathbf{r}_1 = E, \quad \mathbf{r}_1 \cdot \mathbf{r}_2 = 0, \quad \mathbf{r}_2 \cdot \mathbf{r}_2 = G. \tag{3.74}$$

Furthermore, since the normal vector $\boldsymbol{\nu}$ is a unit vector, we know that

$$0 = \frac{\partial}{\partial u^i}(\boldsymbol{\nu} \cdot \boldsymbol{\nu}) = 2\boldsymbol{\nu} \cdot \frac{\partial \boldsymbol{\nu}}{\partial u^i}, \tag{3.75}$$

so that the derivatives of $\boldsymbol{\nu}$ are *tangent* vectors. Therefore, we can make the further assumption that

$$\frac{\partial \boldsymbol{\nu}}{\partial u^1} = -\kappa_1 \mathbf{r}_1 \qquad \frac{\partial \boldsymbol{\nu}}{\partial u^2} = -\kappa_2 \mathbf{r}_2 \tag{3.76}$$

where κ_1 and κ_2 are the principal curvatures of the surface. Hence, (u^1, u^2) form what is called an *orthogonal* patch *adapted* to the surface, so that the coordinate vectors are along the principal directions.

Remark 3.7. The above conditions are not restrictive. In fact, it is well known that everywhere outside umbilic points the first and second fundamental forms can be diagonalized simultaneously [66] providing the two orthogonal principal directions. Thus choosing the curvature lines as the coordinate lines, one can easily verify that (3.74) and (3.76) hold. There is also an elegant and easy proof of this fact that employs the Frobenius' theorem in its dual form [82, 44]. The easiest way to enunciate it in a form suitable for our purposes is

Theorem 3.8. Let θ^a $(a = 1, \ldots, r)$ a set of 1-forms on an open set $V \in \mathcal{M}^n$ $(r < n)$, linearly independent at every point $p \in V$. The following statements are equivalent:

(i) There exist local coordinates $(V; u^i)$ at every point $p \in V$, such that $\theta^a = A^a_b \, \mathrm{d}u^b$ $(b = 1, \ldots, r)$.

(ii) $\mathrm{d}\theta^a \wedge \theta^1 \wedge \ldots \wedge \theta^r = 0$.

We now want to apply this theorem to find if the frame $\{\mathbf{e}_1, \mathbf{e}_2\}$ define integral curves that can be used as coordinates curves on the surface. Consider the 1-form θ^2, dual of $\mathbf{e}_2$. Condition 3.8(ii) is

$$\mathrm{d}\theta^2 \wedge \theta^2 = 0. \tag{3.77}$$

This is trivially satisfied since all the p-forms with $p > 2$ are null on a 2-dimensional manifold. By Frobenius' theorem, there are local coordinates (u^1, u^2) on the surface and a scalar function A (usually called an *integrating factor*), such that $\theta^2 = A \, \mathrm{d}u^2$. The $1-$dimensional submanifold $\mathscr{N}$ defined by $u^2 = \text{const.}$ has the tangent space spanned by $\frac{\partial}{\partial u^1}$. Since

$$\langle \tfrac{\partial}{\partial u^1}, \theta^2 \rangle = \langle \tfrac{\partial}{\partial u^1}, A \, \mathrm{d}u^2 \rangle = 0 \tag{3.78}$$

and by definition $\langle \mathbf{e}_1, \theta^2 \rangle = 0$, the vector fields $\mathbf{e}_1$ and $\frac{\partial}{\partial u^1}$ are everywhere parallel. Therefore $\mathscr{N}$ is the integral line of the field $\mathbf{e}_1$.
Analogous argument applies when θ^1 is considered, instead of θ^2.

We can now calculate the metric tensor of the 3-dimensional manifold $\mathcal{M}^3$ associated with the change of variable (3.73): $g_{ij} = \frac{\partial P}{\partial u^i} \cdot \frac{\partial P}{\partial u^j}$, i.e.

$$g = (1-\kappa_1\tau)^2\, E\, \mathrm{d}u^1 \otimes \mathrm{d}u^1 + (1-\kappa_2\tau)^2\, G\, \mathrm{d}u^2 \otimes \mathrm{d}u^2 + \mathrm{d}\tau \otimes \mathrm{d}\tau, \tag{3.79}$$

which is of the particular form considered in (3.62).
Let us introduce the orthonormal frame $\{\mathbf{e}_1, \mathbf{e}_2, \boldsymbol{\nu}\} = \{\mathbf{r}_1/\sqrt{g_{11}}, \mathbf{r}_2/\sqrt{g_{22}}, \boldsymbol{\nu}\}$ and the respective dual frame $\{\theta^1, \theta^2, \theta^3\}$. The theory described above in the Section can then applied to this special case. It must be noted that the vector field $\boldsymbol{\nu}$ is now to be interpreted as an *extension* of the unit normal to the surface. Indeed, $\boldsymbol{\nu}$ is no longer to be thought of as defined only on the surface Σ but it is $\boldsymbol{\nu}\big(P(u^1,u^2,\tau)\big) = \boldsymbol{\nu}_\Sigma\big(P_\Sigma(u^1,v^2)\big)$, where $\boldsymbol{\nu}_\Sigma$ has been used here to identify the unit normal to Σ.

We obtain from (3.67)

$$\begin{cases} \omega^1{}_2 = -\omega^2{}_1 = \frac{\left((1-\kappa_1\tau)\sqrt{E}\right)_{,2}\theta^1 - \left((1-\kappa_2\tau)\sqrt{G}\right)_{,1}\theta^2}{(1-\kappa_1\tau)(1-\kappa_2\tau)\sqrt{EG}} \\ \omega^1{}_3 = -\omega^3{}_1 = -\frac{\kappa_1}{1-\kappa_1\tau}\,\theta^1 \\ \omega^2{}_3 = -\omega^3{}_2 = -\frac{\kappa_2}{1-\kappa_2\tau}\,\theta^2. \end{cases} \tag{3.80}$$

Using $\nabla\mathbf{e}_i = \mathbf{e}_k \otimes \omega^k{}_i$, we finally have the gradients

$$\begin{aligned} \nabla\mathbf{e}_1 = &-\frac{\Big((1-\kappa_1\tau)\sqrt{E}\Big)_{,2}\,\mathbf{e}_2\otimes\mathbf{e}_1 - \Big((1-\kappa_2\tau)\sqrt{G}\Big)_{,1}\,\mathbf{e}_2\otimes\mathbf{e}_2}{(1-\kappa_1\tau)(1-\kappa_2\tau)\sqrt{EG}} \\ &+ \frac{\kappa_1}{1-\kappa_1\tau}\,\boldsymbol{\nu}\otimes\mathbf{e}_1 \end{aligned} \tag{3.81}$$

$$\begin{aligned} \nabla\mathbf{e}_2 = &\frac{\Big((1-\kappa_1\tau)\sqrt{E}\Big)_{,2}\,\mathbf{e}_1\otimes\mathbf{e}_1 - \Big((1-\kappa_2\tau)\sqrt{G}\Big)_{,1}\,\mathbf{e}_1\otimes\mathbf{e}_2}{(1-\kappa_1\tau)(1-\kappa_2\tau)\sqrt{EG}} \\ &+ \frac{\kappa_2}{1-\kappa_2\tau}\,\boldsymbol{\nu}\otimes\mathbf{e}_2 \end{aligned} \tag{3.82}$$

$$\nabla\boldsymbol{\nu} = -\frac{\kappa_1}{1-\kappa_1\tau}\,\mathbf{e}_1\otimes\mathbf{e}_1 - \frac{\kappa_2}{1-\kappa_2\tau}\,\mathbf{e}_2\otimes\mathbf{e}_2. \tag{3.83}$$

For completeness, we also report the gradient of a *scalar* function $h(P)$

$$\begin{aligned}\nabla h &= h_{,1}\,\mathrm{d}u^1 + h_{,2}\,\mathrm{d}u^2 + h_{,3}\,\mathrm{d}\tau \\ &= \frac{h_{,1}}{(1-\kappa_1\tau)\sqrt{E}}\,\theta^1 + \frac{h_{,2}}{(1-\kappa_2\tau)\sqrt{G}}\,\theta^2 + h_{,3}\,\theta^3 \\ &= \frac{h_{,1}}{(1-\kappa_1\tau)\sqrt{E}}\,\mathbf{e}_1 + \frac{h_{,2}}{(1-\kappa_2\tau)\sqrt{G}}\,\mathbf{e}_2 + h_{,3}\,\boldsymbol{\nu},\end{aligned} \tag{3.84}$$

where, again, with an abuse of notation, we have identified the orthonormal frame $\{\mathbf{e}_1, \mathbf{e}_2, \boldsymbol{\nu}\}$ with its dual $\{\theta^1, \theta^2, \theta^3\}$.

Remark 3.9. It is perhaps convenient to rewrite (3.81)-(3.84) in matrix form with respect to the basis $\{\mathbf{e}_1, \mathbf{e}_2, \boldsymbol{\nu}\}$. For shortness, define

$$\mathrm{A}_1 = (1-\kappa_1\tau)\sqrt{E} \qquad \mathrm{A}_2 = (1-\kappa_2\tau)\sqrt{G} \tag{3.85}$$

$$\mathrm{B}_1 = \frac{\kappa_1}{1-\kappa_1\tau} \qquad \mathrm{B}_2 = \frac{\kappa_2}{1-\kappa_2\tau}. \tag{3.86}$$

Hence, we have

$$\nabla\mathbf{e}_1 = \begin{pmatrix} 0 & 0 & 0 \\ -\frac{\mathrm{A}_{1,2}}{\mathrm{A}_1\,\mathrm{A}_2} & \frac{\mathrm{A}_{2,1}}{\mathrm{A}_1\,\mathrm{A}_2} & 0 \\ \mathrm{B}_1 & 0 & 0 \end{pmatrix} \qquad \nabla\mathbf{e}_2 = \begin{pmatrix} \frac{\mathrm{A}_{1,2}}{\mathrm{A}_1\,\mathrm{A}_2} & -\frac{\mathrm{A}_{2,1}}{\mathrm{A}_1\,\mathrm{A}_2} & 0 \\ 0 & 0 & 0 \\ 0 & \mathrm{B}_2 & 0 \end{pmatrix} \tag{3.87}$$

$$\nabla\boldsymbol{\nu} = \begin{pmatrix} -\mathrm{B}_1 & 0 & 0 \\ 0 & -\mathrm{B}_2 & 0 \\ 0 & 0 & 0 \end{pmatrix} \qquad \nabla h = \begin{pmatrix} \frac{h_{,1}}{\mathrm{A}_1} & \frac{h_{,2}}{\mathrm{A}_2} & h_{,3} \end{pmatrix}. \tag{3.88}$$

3.5.2 Homeotropic anchoring

In this Section, we assume that the surface director is parallel to the unit normal $\boldsymbol{\nu}$ to a given (smooth) surface Σ. We also assume that the director keeps its normal direction, at least in a thin surface slab. Then, $\nabla\mathbf{n}$ turns out to be closely related to the curvature tensor. Using (3.83), we can write

$$\nabla\mathbf{n} = -\frac{\kappa_1}{1-\kappa_1\tau}\,\mathbf{e}_1\otimes\mathbf{e}_1 - \frac{\kappa_2}{1-\kappa_2\tau}\,\mathbf{e}_2\otimes\mathbf{e}_2\,, \tag{3.89}$$

where $\{\kappa_1, \kappa_2\}$ and $\{\mathbf{e}_1, \mathbf{e}_2\}$ denote respectively the principal curvatures and principal directions at P_Σ.

From (3.89) we obtain $\operatorname{curl}\mathbf{n} = \mathbf{0}$, $\mathbf{G} = \nabla\mathbf{n}$, and

$$\mathbf{S} = \frac{\kappa_1^2}{(1-\kappa_1\tau)^2}\,\mathbf{e}_1\otimes\mathbf{e}_1 + \frac{\kappa_2^2}{(1-\kappa_2\tau)^2}\,\mathbf{e}_2\otimes\mathbf{e}_2\,. \tag{3.90}$$

Equation (3.90) shows that biaxiality arises naturally close to an external surface where homeotropic anchoring is enforced. This effect is triggered by the difference between the principal curvatures. More precisely, the tangent direction preferred by the order tensor is the one along which the surface curves more rapidly. Close to a symmetric saddle, where $\kappa_1 = -\kappa_2$, the denominator of (3.90) induces biaxiality along the direction which is convex towards the side occupied by the liquid crystal.

3.5.3 Planar anchoring

When planar anchoring is enforced on a curved surface, it is natural to assume that the chosen direction coincides with one of the principal directions along Σ. We then keep the same notations as above and assume, for instance, $\mathbf{n}\big(P(u^1,u^2,\tau)\big) = \mathbf{n}\big(P_\Sigma(u^1,u^2)\big) = \mathbf{e}_1(u^1,u^2)$.

When this is the case, by (3.81) we obtain

$$\begin{aligned}\nabla\mathbf{n} \;=\; & -\frac{\Big((1-\kappa_1\tau)\sqrt{E}\Big)_{,2}\;\mathbf{e}_2\otimes\mathbf{e}_1 - \Big((1-\kappa_2\tau)\sqrt{G}\Big)_{,1}\;\mathbf{e}_2\otimes\mathbf{e}_2}{(1-\kappa_1\tau)(1-\kappa_2\tau)\sqrt{EG}} \\ & + \frac{\kappa_1}{1-\kappa_1\tau}\,\boldsymbol{\nu}\otimes\mathbf{e}_1 \end{aligned} \tag{3.91}$$

According to (3.88), the matrix expression of $\mathbf{S} = (\nabla\mathbf{n})(\nabla\mathbf{n})^T$ is

$$\mathbf{S} \;=\; \begin{pmatrix} 0 & 0 & 0 \\ 0 & \frac{(\mathrm{A}_{1,2})^2+(\mathrm{A}_{2,1})^2}{\mathrm{A}_1^2\,\mathrm{A}_2^2} & -\frac{\mathrm{B}_1\mathrm{A}_{1,2}}{\mathrm{A}_1\mathrm{A}_2} \\ 0 & -\frac{\mathrm{B}_1\mathrm{A}_{1,2}}{\mathrm{A}_1\mathrm{A}_2} & \mathrm{B}_1^2 \end{pmatrix}. \tag{3.92}$$

From expression (3.92) it is not immediately clear whether or not biaxiality is induced and under which conditions. We can try to identify the *uniaxial* states, i.e., states where $\mathbf{S}$ has two equal eigenvalues.

The matrix (3.92) is of the form

$$\mathbf{S} \;=\; \begin{pmatrix} 0 & 0 & 0 \\ 0 & a & b \\ 0 & b & c \end{pmatrix}, \tag{3.93}$$

whose non-trivial eigenvalues are

$$\mu_\pm \;=\; \frac{1}{2}\left(a+c\pm\sqrt{4b^2+(a-c)^2}\right). \tag{3.94}$$

Uniaxial phase is given when the condition $\mu_+ = \mu_-$ is fulfilled, i.e., when $4b^2 + (a-c)^2 = 0$. Therefore, we have

$$\text{uniaxial state} \Leftrightarrow \begin{cases} b = 0 \\ a = c \end{cases} \quad \Leftrightarrow \quad \begin{cases} \mathrm{B}_1 \mathrm{A}_{1,2} = 0 \\ (\mathrm{A}_{1,2})^2 + (\mathrm{A}_{2,1})^2 = \mathrm{B}_1^2 \, \mathrm{A}_1^2 \, \mathrm{A}_2^2. \end{cases} \tag{3.95}$$

The only possible solutions are

$$\begin{cases} \mathrm{B}_1 = 0 \\ (\mathrm{A}_{1,2})^2 + (\mathrm{A}_{2,1})^2 = 0 \end{cases}, \qquad \begin{cases} \mathrm{A}_{1,2} = 0 \\ (\mathrm{A}_{2,1})^2 = \mathrm{B}_1^2 \, \mathrm{A}_1^2 \, \mathrm{A}_2^2 \end{cases}. \tag{3.96}$$

Taking into account expressions (3.85-3.86), we have that biaxiality is not naturally induced whenever the geometric parameters of the limiting surface Σ satisfy one of the two systems

$$\begin{cases} \kappa_1 = 0 \\ E_{,2} = 0 \\ \kappa_{2,1} = 0 \\ G_{,1} = 0 \end{cases}, \qquad \begin{cases} \kappa_{1,2} = 0 \\ E_{,2} = 0 \\ \left((1 - \kappa_2 \tau)\sqrt{G}\right)_{,1}^2 = {\kappa_1}^2 (1 - \kappa_2 \, \tau)^2 \, EG \end{cases}. \tag{3.97}$$

A plane or a cylindrical surface are examples of $(3.97)_1$. An example of $(3.97)_2$ is less trivial to produce . It is interesting however to notice that both solutions require that the principal curvature κ_1 is constant along direction 2 and $E_{,2} = 0$. Therefore, in the case $\mathbf{n} \equiv \mathbf{e}_1$, the coefficient $(1,1)$ of the surface metric tensor must be independent of the second variable, i.e., lengths along the direction $\mathbf{e}_1$ are measured in the same way when we move parallel to $\mathbf{e}_2$. Conditions (3.97) are rather special. Generally speaking, we can say that biaxiality "almost always" arises when a planar anchoring is enforced. In particular, we have biaxiality whenever the curvature along the prescribed direction is different from zero.

Example 3.10. Consider a 2 dimensional sphere in $\mathbb{R}^3$ with radius R. A possible parametrization employing the azimuthal angle $\phi \in [0, 2\pi)$ and polar angle $\vartheta \in [0, \pi]$, is

$$P(\vartheta, \phi) = R \sin\vartheta \cos\phi \, \mathbf{i} + R \sin\vartheta \sin\phi \, \mathbf{j} + R \cos\vartheta \, \mathbf{k}, \tag{3.98}$$

where as usual $\mathbf{i}$, $\mathbf{j}$ and $\mathbf{k}$ are the unit vectors in a Cartesian frame of reference.
The coordinate frame is orthogonal and when the vectors are normalized the following orthonormal moving frame is gathered

$$\begin{cases} \mathbf{e}_1 = \mathbf{e}_\vartheta = \cos\vartheta \, \cos\phi \, \mathbf{i} + \cos\vartheta \, \sin\phi \, \mathbf{j} - \sin\vartheta \, \mathbf{k} \\ \mathbf{e}_2 = \mathbf{e}_\phi = -\sin\vartheta \, \sin\phi \, \mathbf{i} + \sin\vartheta \, \cos\phi \, \mathbf{j} \\ \boldsymbol{\nu} = \sin\vartheta \, \cos\phi \, \mathbf{i} + \sin\vartheta \, \sin\phi \, \mathbf{j} + \cos\vartheta \, \mathbf{k}. \end{cases} \tag{3.99}$$

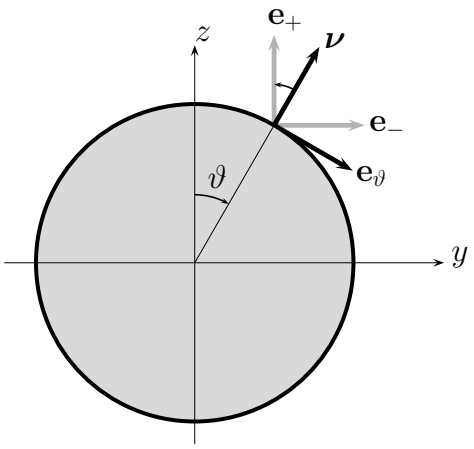

Figure 3.2: Biaxiality axes when the planar anchoring $\mathbf{n} \equiv \mathbf{e}_\varphi$ is enforced.

The metric tensor on the sphere is

$$g \;=\; R^2 \left(\mathrm{d}\vartheta \otimes \mathrm{d}\vartheta + \sin^2 \vartheta \, \mathrm{d}\phi \otimes \mathrm{d}\phi \right). \tag{3.100}$$

Of course, it is not possible to identify two principal directions since every point of the sphere is umbilic. Nevertheless, we identify κ_1 e κ_2 with the normal curvatures along the (orthogonal) coordinate lines ϕ =constant and ϑ =constant and therefore $\kappa_1 \;=\; \kappa_2 \;=\; -1/R$.

A parallel surface at a distance τ from the sphere will be again a sphere with radius $R + \tau$. The formulas for the gradients of the frame basis $(\mathbf{e}_\vartheta, \mathbf{e}_\phi, \nu)$ can be calculated from the well known expressions for spherical coordinates found in vector analysis textbooks. We can as well use (3.81)-(3.83) to get to the same result

$$\nabla \mathbf{e}_\vartheta \;=\; -\,\frac{1}{R+\tau} \left(\boldsymbol{\nu} \otimes \mathbf{e}_\vartheta - \cot\vartheta \, \mathbf{e}_\phi \otimes \mathbf{e}_\phi \right) \tag{3.101}$$

$$\nabla \mathbf{e}_\phi \;=\; -\,\frac{1}{R+\tau} \left(\boldsymbol{\nu} \otimes \mathbf{e}_\phi + \cot\vartheta \, \mathbf{e}_\vartheta \otimes \mathbf{e}_\phi \right). \tag{3.102}$$

Suppose now that a liquid crystal is in contact with the outside of the sphere and a *planar* strong anchoring is enforced such that $\mathbf{n} \equiv \mathbf{e}_\vartheta$. The tensor $\mathbf{S}$ is

$$\mathbf{S} \;=\; (\nabla \mathbf{e}_\vartheta)(\nabla \mathbf{e}_\vartheta)^T \;=\; \frac{1}{(R+\tau)^2} \left(\cot^2\vartheta \, \mathbf{e}_\phi \otimes \mathbf{e}_\phi + \boldsymbol{\nu} \otimes \boldsymbol{\nu} \right). \tag{3.103}$$

So the directions of induced biaxiality are given by the coordinate direction $\mathbf{e}_\phi$ and the normal vector $\boldsymbol{\nu}$. The biaxiality is maximum where the eigenvalues most differ. Since $\cot\vartheta$ diverges at $\vartheta = 0, \pi$ we have the maximum biaxiality at the north and south poles, as it was to be expected since these are defects points.

A more interesting scenario is gained when the planar anchoring is imposed along the parallels of the sphere $\mathbf{n} \equiv \mathbf{e}_\phi$. The tensor $\mathbf{S}$ is

$$\begin{aligned} \mathbf{S} \;&=\; (\nabla \mathbf{e}_\phi)(\nabla \mathbf{e}_\phi)^T \\ &=\; \frac{1}{(R+\tau)^2} \left(\cot^2\vartheta \, \mathbf{e}_\vartheta \otimes \mathbf{e}_\vartheta + \cot\vartheta \left(\mathbf{e}_\vartheta \otimes \boldsymbol{\nu} + \boldsymbol{\nu} \otimes \mathbf{e}_\vartheta \right) + \boldsymbol{\nu} \otimes \boldsymbol{\nu} \right). \end{aligned} \tag{3.104}$$

which is not diagonal and therefore it is not immediately clear along which directions the biaxiality is going to arise. It is a matter of simple computation to find the eigenvectors and the eigenvalues of (3.104)

$$\mathbf{e}_+ = -\sin\vartheta\,\mathbf{e}_\vartheta + \cos\vartheta\,\boldsymbol{\nu} = \mathbf{k} \tag{3.105}$$

$$\mathbf{n} = \mathbf{e}_\phi \tag{3.106}$$

$$\mathbf{e}_- = \cos\vartheta\,\mathbf{e}_\vartheta + \sin\vartheta\,\boldsymbol{\nu}, \tag{3.107}$$

and $\{\mu_+, \mu_-\} = \left\{0, \left((R+\tau)\,\sin\vartheta\right)^{-2}\right\}$.

We want to stress the fact that the vector $\mathbf{e}_+$ is parallel to the fixed unit vector $\mathbf{k}$ and therefore is always parallel to the z-axis. This gives a simple picture of how the biaxiality axes rotates when moving from one pole to the equator along a meridian (see Fig. 3.2). Again, the maximum biaxiality is obtained at the north and south pole since these are defects points and the eigenvalue μ_- is infinite.

When the planar anchoring is not assumed to be along a principal direction, the same decomposition of §3.4.1 can be used

$$\mathbf{n} = \cos\vartheta\,\mathbf{e}_1 + \sin\vartheta\,\mathbf{e}_2\,, \qquad \mathbf{n}_\perp = -\sin\vartheta\,\mathbf{e}_1 + \cos\vartheta\,\mathbf{e}_2, \tag{3.108}$$

where ϑ is the tilt angle between $\mathbf{n}$ and $\mathbf{e}_1$.

We find,

$$\begin{aligned}\nabla\mathbf{n} &= -\sin\vartheta\,\mathbf{e}_1\otimes\nabla\vartheta + \cos\vartheta\,\mathbf{e}_2\otimes\nabla\vartheta + \cos\vartheta\,\nabla\mathbf{e}_1 + \sin\vartheta\,\nabla\mathbf{e}_2\\ &= \mathbf{n}_\perp\otimes\nabla\vartheta + \cos\vartheta\,\nabla\mathbf{e}_1 + \sin\vartheta\,\nabla\mathbf{e}_2,\end{aligned} \tag{3.109}$$

and

$$\begin{aligned}\mathbf{S} &= (\nabla\mathbf{n})(\nabla\mathbf{n})^T\\ &= |\nabla\vartheta|^2\,\mathbf{n}_\perp\otimes\mathbf{n}_\perp + \cos^2\vartheta\,(\nabla\mathbf{e}_1)(\nabla\mathbf{e}_1)^T + \sin^2\vartheta\,(\nabla\mathbf{e}_2)(\nabla\mathbf{e}_2)^T.\end{aligned} \tag{3.110}$$

to be compared with (3.44) and (3.45). A direct dependence on geometric parameters can be obtained by using (3.81-3.84).

3.6 DISCUSSION

We have shown that any spatially-varying director distribution may induce the onset in biaxial domains even in nematic liquid crystals whose ground state is strictly uniaxial. In particular, in Section 3.3 we have stressed the crucial role played by $\mathbf{S} = (\nabla\mathbf{n})(\nabla\mathbf{n})^T$. The tensor $\mathbf{S}$, which is symmetric and positive semidefinite by

construction, always possesses one null eigenvalue, with eigenvector $\mathbf{n}$. Equation (3.22) shows that biaxiality arises naturally whenever the other two eigenvalues of $\mathbf{S}$ are different. Then, equation (3.40) shows that such eventuality is closely related to the vector curl $\mathbf{n}$ and the eigenvalues entering in the decomposition (3.7) of the director gradient.

In Section 3.4 we have applied the considerations above to some model cases. As it could be easily predicted the pure splay, bend, and twist fields, being all planar, exhibit some degree of biaxiality which privileges the director plane over the orthogonal direction. A less trivial result is that there are spatially-varying director configurations that do not induce biaxiality at all. Cladis-Kléman's escape in the third dimension yields a unexpected example of this phenomenon. Section 3.5 analyzes the onset of surface biaxiality both in the case of homeotropic and planar alignment. In the former case, biaxiality is ruled by the difference between the principal curvatures along the surface.

To conclude our analysis we want to give a numerical estimate of the magnitude of the biaxiality phenomena we are predicting. In all nontrivial cases, the free-energy density will contain a $O(b)$-term, which triggers the biaxiality onset. To obtain a rough estimate, we can neglect the $O(b^4)$-term in Ψ_{LdG}, and the $O(b^2)$-term in Ψ_{el}, both with respect to the dominant $O(b^2)$-term, appearing in Ψ_{LdG}. When this is the case, the (local) preferred value of b may be obtained by minimizing the function

$$\begin{aligned} g(b) &= \frac{2}{9}\left(6Cs^2+9Bs+9A\right)b^2 - 2Lsb\big(\mu_+-\mu_-\big) \\ &\approx 2(2+\alpha)Cs_{\mathrm{pr}}^2b^2 - 2Ls_{\mathrm{pr}}b\big(\mu_+-\mu_-\big) \\ &= \frac{2Ls_{\mathrm{pr}}}{\xi_{\mathrm{n}}^2}\Big(b^2-\xi_{\mathrm{n}}^2\big(\mu_+-\mu_-\big)b\Big)\,, \end{aligned} \tag{3.111}$$

where we have replaced $s \approx s_{\mathrm{pr}}$ and introduced the *nematic coherence length*

$$\xi_{\mathrm{n}}^2 = \frac{L}{Cs_{\mathrm{pr}}(2+\alpha)}\,. \tag{3.112}$$

The (local) optimal value of the degree of biaxiality is then

$$b_{\mathrm{opt}} \approx \tfrac{1}{2}\,\xi_{\mathrm{n}}^2\left(\mu_+-\mu_-\right). \tag{3.113}$$

Though b_{opt} may vary from point to point, we have to keep in mind that in general the equilibrium configuration will not coincide with b_{opt} because of the $|\nabla b|^2$-term, and the boundary conditions. To make an explicit example, let us consider a nematic cylindric capillary of radius R, with homeotropic conditions enforced at the surface. Then, the difference between the eigenvalues of $\mathbf{S}$ at the surface is R^{-2} and the surface biaxiality is of the order of $(\xi_{\mathrm{n}}/R)^2$. Since the nematic coherence length

hardly exceeds the tenths of a μm, we obtain $b_{\rm opt} \lesssim 10^{-2}$ for a μm-capillary. The scenario changes completely close to a nematic defect, where at least one of the eigenvalues of $\mathbf{S}$ diverges. Both the pure-splay and the pure-bend examples above yield $(\mu_+ - \mu_-) = r^{-2}$, which implies $b_{\rm opt} \approx (\xi_{\rm n}/r)^2$. The biaxiality *cloud* cannot be neglected if we come too close to the defect.

A

Equilibrium configurations close to a bifurcation point

We want to study the extrema of a functional $\mathscr{F}$, depending on a real function $u(x)$, its first derivative $u'(x)$ and a positive real parameter λ,

$$\mathscr{F}[u,u'|\lambda] = \int_a^b \mathscr{L}(u,u'|\lambda)\,\mathrm{d}x + W^+ f\left(u(a)\right) + W^- f(u(b)), \tag{A.1}$$

where $W^\pm$ are two positive constants and f is a smooth even function of u with a local minimum for u identically zero and strictly convex around this point. Furthermore, let the integrand be of the form

$$\mathscr{L}(u,u'|\lambda) \;=\; \frac{1}{2}g(u){u'}^2 - \lambda\, h(u), \tag{A.2}$$

where g and h are smooth even functions of u; g is strictly positive and h is strictly convex around $u \equiv 0$. The functional (A.1) is the prototype of many energy functionals encountered in physics.

In order to obtain the Euler-Lagrange equation for (A.1), we introduce the first variation, defined as

$$\mathrm{d}\mathscr{F}[u,u'|\lambda]\varphi \;=\; \frac{\partial}{\partial\epsilon}\mathscr{F}[u+\epsilon\varphi, u'+\epsilon\varphi'|\lambda]\bigg|_{\epsilon=0}, \tag{A.3}$$

whence

$$\begin{aligned}\mathrm{d}\mathscr{F}[u,u'|\lambda]\varphi \;=& \int_a^b \left(\frac{\partial\mathscr{L}}{\partial u} - \frac{\mathrm{d}}{\mathrm{d}x}\frac{\partial\mathscr{L}}{\partial u'}\right)\varphi\,\mathrm{d}x + \left[\left(\frac{\partial\mathscr{L}}{\partial u'} + W^+\frac{\partial f}{\partial u}\right)\varphi\right]_{x=b} \\ &- \left[\left(\frac{\partial\mathscr{L}}{\partial u'} - W^-\frac{\partial f}{\partial u}\right)\varphi\right]_{x=a}.\end{aligned} \tag{A.4}$$

Without loss of generality we suppose $x \in [-1/2, 1/2]$. Furthermore, we introduce the following notation: plus and/or minus superscripts denote function values in $x = 1/2$ and/or $x = -1/2$. From (A.4) and by the arbitrariness of φ, the equilibrium equation

$$g\,u'' + \frac{1}{2}g_u\,{u'}^2 + \lambda\,h_u = 0 \qquad x \in (-1/2, 1/2) \tag{A.5}$$

follows together with the related boundary conditions

$$\pm g^{\pm} u'^{\pm} + W^{\pm} f_u^{\pm} = 0 \qquad x = \pm 1/2. \tag{A.6}$$

We remark that Dirichlet ($u^{\pm} = 0$) or Neumann ($(u')^{\pm} = 0$) boundary conditions can be reached in the limiting cases $g^{\pm}/W^{\pm} \to 0$ or $W^{\pm}/g^{\pm} \to 0$, respectively.

By construction, the equilibrium equation (A.5) together with the boundary conditions (A.6), admits the trivial solution $u = 0$. We consider a slightly perturbed solution, with respect to $u = 0$. Assume the perturbation expansion

$$u(x) = \varepsilon u_1(x) + o(\varepsilon). \tag{A.7}$$

The parameter ε is defined by $\varepsilon = \sqrt{\lambda/\lambda_0 - 1} \ll 1$, whence it follows easily

$$\lambda \; = \; \lambda_0(1 + \varepsilon^2), \tag{A.8}$$

where the parameter λ_0 will be determined within the linear analysis. By replacing (A.7) and (A.8) into (A.5) and (A.6) we obtain, up to first order,

$$g^0 \, u_1'' + \lambda_0 h_{uu}^0 u_1 \; = \; 0, \qquad x \in (-1/2, 1/2), \tag{A.9}$$

$$\pm g^0 \, u_1'^{\pm} + W^{\pm} f_{uu}^0 u_1^{\pm} \; = \; 0, \qquad x = \pm 1/2, \tag{A.10}$$

where the superscript zero denotes functions evaluated in $u = 0$. The general solution of (A.9) is

$$u_1(x) \; = \; A_1 \cos(\Omega \, x) + B_1 \sin(\Omega \, x), \tag{A.11}$$

where $\Omega^2 = \lambda_0 h_{uu}^0 / g^0$ and A_1 and B_1 are constants to be determined. Boundary conditions (A.10) yield a linear homogeneous system in the unknowns A_1 and B_1

$$\begin{pmatrix} -\Omega g^0 \sin\frac{\Omega}{2} + W^- f_{uu}^0 \cos\frac{\Omega}{2} & -\Omega g^0 \cos\frac{\Omega}{2} - W^- f_{uu}^0 \sin\frac{\Omega}{2} \\ -\Omega g^0 \sin\frac{\Omega}{2} + W^+ f_{uu}^0 \cos\frac{\Omega}{2} & \Omega g^0 \cos\frac{\Omega}{2} + W^+ f_{uu}^0 \sin\frac{\Omega}{2} \end{pmatrix} \begin{pmatrix} A_1 \\ B_1 \end{pmatrix} = \begin{pmatrix} 0 \\ 0 \end{pmatrix} \tag{A.12}$$

whose solution is trivial unless the two equations are linearly dependent. Let $\mathbb{M}$ be the 2×2 matrix at left side member of (A.12). Existence of nontrivial solutions above the bifurcation point, impose $\det(\mathbb{M}) = 0$ which gives an implicit equation for Ω (and therefore for λ_0)

$$(W^- + W^+) \, \Omega \, g^0 \, f_{uu}^0 \, \cos\Omega + \left(W^- W^+ \, \left(f_{uu}^0\right)^2 - \Omega^2 \left(g^0\right)^2 \right) \sin\Omega = 0 \tag{A.13}$$

and allows to calculate the ratio between the constants B_1 and A_1

$$K = \frac{B_1}{A_1} = \frac{-\Omega\, g^0\, \sin\frac{\Omega}{2} + W^-\, f^0_{uu}\, \cos\frac{\Omega}{2}}{\Omega\, g^0\, \cos\frac{\Omega}{2} + W^-\, f^0_{uu}\, \sin\frac{\Omega}{2}}. \tag{A.14}$$

Note that (A.13) admits a countable infinity of solutions. The solution in the interval $[-\pi, \pi]$ determines the critical parameter Ω_{cr} and correspondingly λ_{cr} and K_{cr}. Finally, we can put the linear solution in the form

$$u_1(x) \;=\; A_1\big(\cos(\Omega_{cr}\, x) + K_{cr}\sin(\Omega_{cr}\, x)\big). \tag{A.15}$$

It is easy to check that $K \neq 0$ only in the case of asymmetric boundary conditions, $W^+ \neq W^-$.

The amplitude A_1 still remains undetermined. This indetermination given by the first approximation can be rendered definite by using compatibility conditions at higher orders in ε.

Let us expand the solution as power series of ε

$$u = \varepsilon u_1 + \varepsilon^2 u_2 + \varepsilon^3 u_3 + ... \tag{A.16}$$

By replacing this expression into (A.5) and (A.6) and keeping the ε^2 terms we arrive at

$$g^0\, u_2'' + \lambda_{cr} h^0_{uu} u_2 \;=\; 0$$

and the boundary conditions

$$\pm g^0\, \left(u_1'\right)^{\pm} + W^{\pm} f^0_{uu} u_1^{\pm} \;=\; 0.$$

The equation for u_2 as well as its boundary conditions, are identical to the ones obtained for u_1. As before, they do not allow the evaluation of the amplitude A_1.

Pushing the perturbation algorithm to $\mathcal{O}\left(\varepsilon^3\right)$ we obtain the equation for u_3

$$g^0\, u_3'' + \lambda_{cr} h^0_{uu} u_3 = -\frac{1}{2} g^0_{uu}\left(u_1^2 u_1'' \;+\; u_1 {u_1'}^2\right) - \lambda_{cr} u_1 \left(h^0_{uu} + \frac{1}{6} u_1^2 h^0_{uuuu}\right), \tag{A.17}$$

and the associated boundary conditions

$$\pm g^0\, u_3'^{\pm} + W^{\pm} f^0_{uu} u_3^{\pm} = \mp \frac{1}{2} g^0_{uu}\left(u_1^{\pm}\right)^2 u_1'^{\pm} - \frac{1}{6} W^{\pm} f^0_{uuuu}\left(u_1^{\pm}\right)^3. \tag{A.18}$$

Equation (A.17) can be solved taking into account (A.15). Its general solution is of the form

$$u_3(x) \;=\; A_3\cos(\Omega_{cr}\, x) + B_3\sin(\Omega_{cr}\, x) + u_3^p(x), \tag{A.19}$$

where $u_3^p(x)$ is a particular solution. After some algebra, it can be shown that

$$u_3^p(x) \;=\; \alpha\, u_1(x)^3 + \left(\frac{1}{2} + \beta\, A_1^2\right) x\, u_1'(x), \tag{A.20}$$

where

$$\alpha \;=\; \frac{h^0_{uuuu}}{48\, h^0_{uu}} - \frac{g^0_{uu}}{8\, g^0} \qquad\qquad \beta \;=\; \left(1 + K_{cr}^2\right)\left(\frac{h^0_{uuuu}}{16\, h^0_{uu}} - \frac{g^0_{uu}}{8\, g^0}\right).$$

Substitution in the boundary conditions (A.18), gives a linear system in the unknown A_3 and B_3 of the form $\mathbb{M}\,\mathbf{x} \;=\; \mathbf{b}$ where $\mathbf{x} = (A_3, B_3)^T$, $\mathbf{b} = (b^-, b^+)^T$ with

$$b^{\pm} \;=\; \mp g^0\, u_3^{p\,\prime\pm} - W^{\pm} f^0_{uu} u_3^{p\,\pm} \mp \frac{1}{2} g^0_{uu} \left(u_1^{\pm}\right)^2 u_1'^{\pm} - \frac{1}{6} W^{\pm} f^0_{uuuu} \left(u_1^{\pm}\right)^3.$$

Let $\mathbf{m}_1$ and $\mathbf{m}_2$ be the column vectors composing $\mathbb{M}$. In order to solve this system we must have $\mathbf{b} \in \mathrm{span}\{\mathbf{m}_1, \mathbf{m}_2\} = \mathrm{span}\{\mathbf{m}_1\} = \mathrm{span}\{\mathbf{m}_2\}$ since $\mathbf{m}_1$ and $\mathbf{m}_2$ are linearly dependent ($\det(\mathbb{M}) \;=\; 0$). Therefore, we gather a *third order* algebraic equation in A_1 from one of the two determinants $\det(\mathbf{m}_1|\mathbf{b}) = 0$ or $\det(\mathbf{m}_2|\mathbf{b}) = 0$. By introducing the notations $v^{\pm} = u^{\pm}/A_1$, $\gamma^{\pm} \;=\; \sqrt{\Omega_{cr}^2 (g^0)^2 + (W^{\pm})^2\, (f^0_{uu})^2}$,

$$\varpi \;=\; \gamma^+ u_1^- \left[(\gamma^-)^2 + 2W^- g^0 f^0_{uu}\right] + \gamma^- u_1^+ \left[(\gamma^+)^2 + 2W^+ g^0 f^0_{uu}\right], \tag{A.21}$$

$$\eta \;=\; 12\alpha\, g^0\, f^0_{uu} + 3 f^0_{uu}\, g^0_{uu} - g^0\, f^0_{uuuu}, \tag{A.22}$$

a tedious but easy computation yields the equation for the amplitude

$$A_1^3 \left[6\,\beta\,\varpi + 2\left(W^- \gamma^+ (u_1^-)^3 + W^+ \gamma^- (u_1^+)^3\right)\,\eta\right] + 3\, A_1\, \varpi = 0. \tag{A.23}$$

Equation (A.23) admits the trivial solution $A_1 \;=\; 0$ and other two real opposite solution. The former corresponds to the trivial solution which can be showed to be unstable. Due to the symmetry of the problem the other two represent the amplitude of nontrivial solutions with the same energy.

The procedure described above is fairly standard but rather involved. We now give an easier way to gather the first order expansion and then resolve its amplitude degeneracy. Consider a direct expansion of the functional (A.1) in power of ε, under the assumptions $u(x) = \varepsilon u_1(x)$, $x \in [-1/2, 1/2]$ and $\lambda \;=\; \lambda_0(1+\varepsilon^2)$. We remark the fact that we are only considering the first order expansion of the solution. On the contrary, we expand the functional up to any desired order. Thus, up to the second order we obtain

$$\mathscr{F}[\varepsilon u_1, \varepsilon u_1' | \lambda] = f^0\left(W^- + W^+\right) - \lambda_0 h^0 + \varepsilon^2 \int_a^b \left(\frac{1}{2} g^0 u_1'^2 - \frac{1}{2}\lambda_0 h^0_{uu} u_1^2 - \lambda_0 h^0\right) \mathrm{d}x$$
$$+ \varepsilon^2 \frac{1}{2} f^0_{uu}\left(W^-\left(u_1^-\right)^2 + W^+\left(u_1^+\right)^2\right). \tag{A.24}$$

It is easy to check that the $\mathcal{O}(1)$ term of the functional is constant, while the $\mathcal{O}\left(\varepsilon^2\right)$ is minimized by the linear problem (A.9)-(A.10). Therefore, u_1 is still of the form (A.15).

To remove the amplitude indetermination we push the expansion of $\mathscr{F}$ to higher orders. The $\mathcal{O}\left(\varepsilon^4\right)$ term of the functional expansion is the first non-trivial term. It reads

$$\varepsilon^4 \int_a^b \left(\frac{1}{4} g^0_{uu} u_1^2 u_1'^2 - \frac{1}{2}\lambda_{cr} h^0_{uu} u_1^2 - \frac{1}{24}\lambda_{cr} h^0_{uuuu} u_1^4\right) \mathrm{d}x$$
$$+ \varepsilon^4 \frac{1}{24} f^0_{uuuu}\left(W^-\left(u_1^-\right)^4 + W^+\left(u_1^+\right)^4\right). \tag{A.25}$$

Once again, we stress the fact that in (A.25), only the $\mathcal{O}(\varepsilon)$ term of solution expansion has been taken into account. Note that the form of u_1 is now known and a direct integration of (A.25) can be performed, to yield a polynomial expression in the amplitude A_1 only. Therefore, minimization of the functional (A.25) reduces to calculate the minima of a polynomial function.

By using the identity ${u_1'}^2 + \Omega_{cr}^2 u_1^2 = A_1^2\left(1 + K_{cr}^2\right)\Omega_{cr}^2$ and integrating by parts, the following representations of the integrals involved in (A.25) are obtained

$$\int_{-\frac{1}{2}}^{\frac{1}{2}} u_1^2 \,\mathrm{d}x = \frac{1}{2}\left[A_1^2(1 + K_{cr}^2)\, x - \frac{1}{\Omega_{cr}^2} u_1\, u_1'\right]_{-\frac{1}{2}}^{\frac{1}{2}},$$

$$\int_{-\frac{1}{2}}^{\frac{1}{2}} u_1^4 \,\mathrm{d}x = \frac{3}{4} A_1^2(1 + K_{cr}^2) \int_{-\frac{1}{2}}^{\frac{1}{2}} u_1^2 \,\mathrm{d}x - \left[\frac{1}{4\Omega_{cr}^2} u_1^3\, u_1'\right]_{-\frac{1}{2}}^{\frac{1}{2}}.$$

By the use of the boundary conditions for u_1 and differentiating with respect to the amplitude, we finally gather the equation for A_1

$$A_1^3\left[12\, g^0_{uu}\, h^0_{uu}\left(1 + K_{cr}^2\right)\Theta + g^0\left(4\, h^0_{uu}\, f^0_{uuuu} - h^0_{uuuu}\, f^0_{uu}\right)\Gamma_4\right] \tag{A.26}$$
$$-6\, A_1\, h^0_{uu}\left(2g^0 + g^0_{uu}\right)\Theta = 0,$$

where we have set

$$\Gamma_2 = W^-\left(u_1^-\right)^2 + W^+\left(u_1^+\right)^2, \qquad \Gamma_4 = W^-\left(u_1^-\right)^4 + W^+\left(u_1^+\right)^4,$$

$$\Theta = (1 + K_{cr}^2)\Omega_{cr}^2 g^0 + f_{uu}^0 \Gamma_2.$$

If A_1 has to realize the minimum, the derivative of this expression must be zero. In this way, we arrive at an algebraic equation in A_1 and A_1^3 which gives the same results of equation (A.23).

A quick check of the usefulness of these techniques may be the buckling of Euler's beam clamped at one end under an external axial load. In this case it can be shown that the functional takes the form

$$\mathscr{F}[\vartheta', \vartheta|\lambda] = \int_{-1/2}^{1/2} \left(\frac{1}{2}(\vartheta')^2 + \lambda \cos\vartheta \right) \mathrm{d}x, \tag{A.27}$$

which has to be minimized with the boundary conditions $\vartheta(-1/2) = 0$ and $\vartheta'(1/2) = 0$. The first order approximation is the well known

$$\vartheta_1(x) = \pm 2 \left[\cos\left(\frac{\pi}{2}x\right) + \sin\left(\frac{\pi}{2}x\right) \right]. \tag{A.28}$$

Bibliography

[1] A. L. Alexe-Ionescu, R. Barberi, G. Barbero, and M. Giocondo, *Anchoring energy for nematic liquid crystals: Contribution from the spatial variation of the elastic constants*, Phys. Rev. E, 49 (1994), p. 5378.

[2] L. Ambrosio, *Existence of minimal energy configurations of nematic liquid crystals with variable degree of orientation*, Manuscripta Math., 68 (1990), pp. 215–228.

[3] ——, *Regularity of solutions of a degenerate elliptic variational problem*, Manuscripta Math., 68 (1990), pp. 309–326.

[4] L. Ambrosio and E. G. Virga, *A boundary-value problem for nematic liquid crystals with variable degree of orientation*, Arch. Rational Mech. Anal., 114 (1991), pp. 335–347.

[5] G. Andrews, R. Askey, and R. Roy, *Special Functions*, Cambridge University Press, Cambridge, 1999.

[6] R. Barberi and G. Durand, *Order parameter of a nematic liquid crystal on a rough surface*, Phys. Rev. A, 41 (1990), p. 2207.

[7] G. Barbero and G. Durand, *Curvature induced quasi-melting from rough surfaces in nematic liquid crystals*, J. Phys. II, 1 (1991), p. 651.

[8] ——, *Splay-bend curvature and temperature-induced surface transitions in nematic liquid crystals*, Phys. Rev. E, 48 (1993), pp. 1942–1947.

[9] F. Batalioto, I. H. Bechtold, E. A. Oliveira, and L. R. Evangelista, *Effect of microtextured substrates on the molecular orientation of a nematic liquid-crystal sample*, Phys. Rev. E, 72 (2005).

[10] C. M. Bender and S. A. Orszag, *Advanced Mathematical Methods for Scientists and Engineers*, Springer-Verlag, New York, 1999.

[11] D. W. Berreman, *Solid surface shape and the alignment of an adjacent nematic liquid crystal*, Phys. Rev. Lett., 28 (1972), p. 1683.

[12] P. Biscari and G. Capriz, *Optical and statistical anisotropy in nematics*, Rend. Mat. Acc. Lincei, 4 (1993), pp. 307–313.

[13] P. Biscari, G. Capriz, and E. G. Virga, *Biaxial nematic liquid crystals* (in: C. Baiocchi and J. L. Lions *Boundary-value problems for partial differential equations and applications*), Masson, Paris, 1993.

[14] ——, *On surface biaxiality*, Liq. Cryst., 16 (1994), pp. 479–489.

[15] P. Biscari and G. Guidone Peroli, *A hierarchy of defects in biaxial nematics*, Comm. Math. Phys., 186 (1997), pp. 381–392.

[16] P. Biscari, G. Guidone Peroli, and T. J. Sluckin, *The topological microstructure of defects in nematic liquid crystals*, Mol. Cryst. Liq. Cryst., 292 (1997), pp. 91–101.

[17] P. Biscari, G. Napoli, and S. Turzi, *Bulk and surface biaxiality in nematic liquid crystals*, Phys. Rev. E, 74, 031708 (2006), pp. 1–7.

[18] P. Biscari and T. J. Sluckin, *Expulsion of disclinations in nematic liquid crystals*, Euro. J. Appl. Math., 14 (2003), pp. 39–59.

[19] P. Biscari and S. Turzi, *Boundary-roughness effects in nematic liquid crystals*, SIAM J. Appl. Math., 67 (2007), pp. 447–463.

[20] P. Biscari and E. G. Virga, *A surface-induced transition in polymeric nematics*, Liq. Cryst., 22 (1997), pp. 419–425.

[21] F. Biscarini, C. Chiccoli, P. Pasini, F. Semeria, and C. Zannoni, *Phase diagram and orientational order in a biaxial lattice model: a monte carlo study*, Phys. Rev. Lett., 75 (1995), pp. 1803–1806.

[22] F. Bisi, E. C. Gartland Jr., R. Rosso, and E. G. Virga, *Order reconstruction in frustrated nematic twist cells*, Phys. Rev. E, 68 (2003), p. 021707.

[23] M. Born and E. Wolf, *Principles of Optics: Electromagnetic Theory of Propagation, Interference and Diffraction of Light*, Cambridge University Press, Cambridge, 7 ed., 1999.

[24] P. Chaudhari, J. Lacey, and J. Doyle et al., *Atomic-beam alignment of inorganic materials for liquid-crystal displays*, Nature, 411 (2001), p. 56.

[25] Z. Y. Chen, *Biaxial effect at an isotropic-nematic interface*, Phys. Rev. E, 47 (1993), pp. 3765–3767.

[26] S.-S. Chern, W. H. Chen, and K. S. Lam, *Lectures on Differential Geometry*, World Scientific Pub. Co. Inc., Singapore, 1999.

[27] D. L. Cheung and F. Schmid, *Monte Carlo simulations of liquid crystals near rough walls*, J. Chem. Phys., 122 (2005).

[28] C. Chiccoli, I. Feruli, O. D. Lavrentovich, P. Pasini, S. V. Shiyanovskii, and C. Zannoni, *Topological defects in schlieren textures of biaxial and uniaxial nematics*, Phys. Rev. E, 66 (2002), p. 030701.

[29] C. Chiccoli, P. Pasini, I. Feruli, and C. Zannoni, *Biaxial nematic droplets and their optical textures: a lattice model computer simulation study*, Mol. Cryst. 441 (2005), p. 319.

[30] P. Cladis and M. Kléman, *Non-singular disclinations of strength $S = +1$ in nematics*, J. Physique, 33 (1972), pp. 591–598.

[31] P. G. de Gennes, *Short range order in the isotropic phase of nematic*, Molec. Cryst. Liq. Cryst., 12 (1971), p. 193.

[32] P. G. de Gennes and J. Prost, *The Physics of Liquid Crystals*, Oxford University Press, Oxford, 1995.

[33] H. J. Deuling, *Deformation of nematic liquid crystals in an electric field*, Mol. Cryst. Liq. Cryst., 19 (1972), p. 123.

[34] J. Elgeti and F. Schmid, *Nematic liquid crystals at rough and fluctuating interfaces*, Eur. Phys. J. E, 18 (2005), pp. 407–415.

[35] J. L. Ericksen, *Inequalities in liquid crystals theory*, Phys. Fluids, 9 (1966), pp. 1205–1207.

[36] J. L. Ericksen, *Liquid crystals with variable degree of orientation*, Arch. Rational Mech. Anal., 113 (1991), pp. 97–120.

[37] L. R. Evangelista and G. Barbero, *Theoretical analysis of actual surfaces: The effect on the nematic orientation*, Phys. Rev. E, 48 (1993), p. 1163.

[38] ——, *Walls of orientation induced in nematic-liquid-crystal samples by inhomogeneous surfaces*, Phys. Rev. E, 50 (1994), p. 2120.

[39] L. C. Evans, *Partial Differential Equations*, American Mathematical Society, 1998.

[40] S. Faetti, M. Gatti, V. Palleschi, and T. J. Sluckin, *Almost critical behavior of the anchoring energy at the interface between a nematic liquid crystal and a SiO substrate*, Phys. Rev. Lett., 55 (1985), pp. 1681–1684.

[41] H. L. Fang, *On nematic liquid crystals with variable degree of orientation*, Comm. Pure Appl. Math., 44 (1991), pp. 453–468.

[42] J. B. Fournier and P. Galatola, *Effective anchoring and scaling in nematic liquid crystals*, Eur. Phys. J. E, 2 (2000), pp. 59–65.

[43] F. C. Frank, *On the theory of liquid crystals*, Discuss. Faraday Soc., 25 (1958), pp. 19–28.

[44] T. Frankel, *The Geometry of Physics: An Introduction*, Cambridge University Press, Cambridge, 2003.

[45] W. M. Gibbons, P. J. Shannon, S.-T. Sun, and B. J. Swetlin, *Surface-mediated alignment of nematic liquid crystals with polarized laser light*, Nature, 351 (1991), p. 49.

[46] B. Groh and S. Dietrich, *Fluids of rodlike particles near curved surfaces*, Phys. Rev. E, 59 (1999), pp. 4216–4228.

[47] B. D. Guenther, *Modern Optics*, Wiley, Cambridge, 1990.

[48] R. Hardt, D. Kinderlehrer, and F.-H. Lin, *Existence and partial regularity of static liquid crystal configurations*, Comm. Math. Phys., 105 (1986), pp. 547–570.

[49] ——, *Stable defects of minimizers of constrained variational principles*, Ann. Inst. Henri Poincaré Nonlin. Anal., 5 (1988), pp. 297–322.

[50] M. H. Holmes, *Introduction to Perturbation Methods*, Springer-Verlag, New York, 1995.

[51] P. Kaiser, W. Wiese, and S. Hess, *Stability and instability of an uniaxial alignment against biaxial distortions in the isotropic and nematic phases of liquid-crystals*, J. Non-Equilib. Thermodyn., 17 (1992), p. 153.

[52] S. Kralj and E. G. Virga, *Core hysteresis in nematic defects*, Phys. Rev. E, 66 (2002), p. 021703.

[53] S. Kralj, E. G. Virga, and S. Žumer, *Biaxial torus around nematic point defects*, Phys. Rev. E, 60 (1999), pp. 1858–1866.

[54] S. Kumar, J. H. Kim, and Y. Shi, *What aligns liquid crystals on solid substrates? the role of surface roughness anisotropy*, Phys. Rev. Lett., 94 (2005).

[55] L. Lewin, *Polylogarithms and Associated Functions*, Elsevier North Holland, New York, 1981.

[56] E. M. Lifshitz and L. D. Landau, *Statistical Physics (Course of Theoretical Physics, Volume 5)*, Butterworth-Heinemann, 1984.

[57] L. Longa, D. Monselesan, and H.-R. Trebin, *An extension of the Landau-Ginzburg-de Gennes theory of liquid crystals*, Liq. Cryst., 2 (1987), pp. 769–796.

[58] E. Martín del Río, M. M. Telo da Gama, and E. de Miguel, *Surface-induced alignment at model nematic interfaces*, Phys. Rev. E, 52 (1995), pp. 5028–5039.

[59] G. McKay and E. G. Virga, *Mechanical actions on nanocylinders in nematic liquid crystals*, Phys. Rev. E, 71 (2005), p. 041702.

[60] N. D. Mermin, *The topological theory of defects in ordered media*, Rev. Mod. Phys., 51 (1979), pp. 591–648.

[61] V. Mocella, C. Ferrero, M. Iovane, and R. Barberi, *Numerical investigation of surface distortion and order parameter variation in nematics*, Liq. Cryst., 26 (1999), p. 1345.

[62] J. A. Murdock, *Perturbations. Theory and Methods*, Wiley-Interscience, New York, 1991.

[63] G. Napoli, *Weak anchoring effects in electrically driven Freedericksz transitions*, J. Phys. A: Math. Gen., 39 (2006), pp. 11–31.

[64] G. Napoli and S. Turzi, *On the determination of nontrivial equilibrium configurations close to a bifurcation point*, Computers and Mathematics with Applications, to appear.

[65] M. Nobili and G. Durand, *Disorientation-induced disordering at a nematic-liquid-crystal solid interface*, Phys. Rev. A, 46 (1992), pp. R6174–R6177.

[66] B. O'Neill, *Elementary Differential Geometry*, Academic Press, San Diego, 1997.

[67] M. A. Osipov, T. J. Sluckin, and S. J. Cox, *Influence of permanent molecular dipoles on surface anchoring of nematic liquid crystals*, Phys. Rev. E, 55 (1997), pp. 464–476.

[68] V. Popa-Nita, T. J. Sluckin, and A. A. Wheeler, *Statics and kinetics at the nematic-isotropic interface: effects of biaxiality*, J. Physique II, 7 (1997), pp. 1225–1243.

[69] A. Rapini and M. Papoular, *Distortion d'une lamelle nématique sous champ magnétique. conditions d'angrage aux paroix*, J. Phys. Colloque C4, 54 (1969).

[70] R. Rosso and M. C. P. Brunelli, *Forces on nematic disclinations with optimal core*, Continuum Mech. Thermodyn., 13 (2001), p. 383.

[71] W. Rudin, *Principles of Mathematical Analysis*, McGraw-Hill Publishing Co., 3 ed., 1976.

[72] M. Ruetschi, P. Grutter, J. Funfschilling, and H. J. Guntherodt, *Creation of liquid-crystal wave-guides with scanning force microscopy*, Science, 265 (1994), p. 512.

[73] Y. Sato, K. Sato, and T. Uchida, *Relationship between rubbing strength and surface anchoring of nematic liquid-crystal*, Jap. J. Appl. Phys. Lett., 31 (1992), pp. L579–L581.

[74] N. Schopohl and T. J. Sluckin, *Defect core structure in nematic liquid crystals*, Phys. Rev. Lett., 59 (1987), pp. 2582–2584.

[75] R. H. Self, C. P. Please, and T. J. Sluckin, *Deformation of nematic liquid crystals in an electric field*, Euro. J. of Applied Mathematics, 13 (2002), pp. 1–23.

[76] G. Skačej, A. L. Alexe-Ionescu, G. Barbero, and S. Žumer, *Surface-induced nematic order variation: Intrinsic anchoring and subsurface director deformations*, Phys. Rev. E, 57 (1998), p. 1780.

[77] D. R. Smith, *Singular-perturbation theory. An introduction with applications*, Cambridge University Press, Cambridge, 1985.

[78] A. M. Sonnet and E. G. Virga, *Dilution of nematic surface potentials: Statics*, Phys. Rev. E, 61 (2000), pp. 5401–5406.

[79] A. M. Sonnet, E. G. Virga, and G. E. Durand, *Dilution of nematic surface potentials: Relaxation dynamics*, Phys. Rev. E, 62 (2000), pp. 3694–3701.

[80] A. M. Sonnet, E. G. Virga, and G. E. Durand, *Dielectric shape dispersion and biaxial transitions in nematic liquid crystals*, Phys. Rev. E, 67 (2003), p. 061701.

[81] A. Strigazzi, *Surface elasticity and Freedericksz threshold in a nematic cell weakly anchored*, Nuovo Cim. D, 10 (1988), pp. 1335–1344.

[82] P. Szekeres, *A Course in Modern Mathematical Physics: Groups, Hilbert Space and Differential Geometry*, Cambridge University Press, 2005.

[83] E. G. Virga, *Variational Theories for Liquid Crystals*, Chapman & Hall, 1995.

[84] L. Xuan, T. Tohyama, T. Miyashita, and T. Uchida, *Order parameters of the liquid crystal interface layer at a rubbed polymer surface*, J. Appl. Phys., 96 (2004), pp. 1953–1958.

[85] L. J. Yu and A. Saupe, *Observation of a biaxial nematic phase in potassium laurate-1-decanol-water mixtures*, Phys. Rev. Lett., 45 (1980), p. 1000.